Thermal Performance of High-Volume Fly Ash and Steel Slag Fine Aggregate Based Sustainable Cementitious Composites

THESIS

Submitted in partial fulfillment

of the requirements for the degree of

DOCTOR OF PHILOSOPHY

By

ANIRUDDHA TANGIRALA

ID No. 2019PHXF0017P

Under the supervision of

Dr. MUKUND LAHOTI

Assistant Professor, Department of Civil Engineering

BIRLA INSTITUTE OF TECHNOLOGY & SCIENCE

PILANI-333031 (RAJASTHAN), INDIA

2024

BIRLA INSTITUTE OF TECHNOLOGY & SCIENCE,

PILANI (RAJASTHAN)

CERTIFICATE

This is to certify that the thesis titled **"Thermal Performance of High-Volume Fly Ash and Steel Slag Fine Aggregate Based Sustainable Cementitious Composites"** submitted by Mr. **Aniruddha Tangirala** ID No **2019PHXF0017P** for award of Ph.D. of the Institute, embodies original work done by him under my supervision.

Date:

Signature in full of the Supervisor

Name: Dr. MUKUND LAHOTI

Designation: Assistant Professor

2024

Acknowledgements

A Ph.D. is not just a path for scientific exploration but also a significant journey for personal growth. This challenging and rewarding process depends on the support, patience, and goodwill of many individuals, from mentors and peers to family and friends.

Foremost, my gratitude goes to my supervisor, Dr. Mukund Lahoti, whose guidance was pivotal in acquainting me with the fundamentals of research. His instruction on how to effectively write and present, coupled with his boundless patience, were invaluable. Dr. Lahoti's knack for simplification, making complex situations readily solvable, truly stands out. His support extended beyond advice, as evidenced by his generous funding for achieving research goals, which greatly encouraged my endeavours.

I extend my thanks to Prof. Anupam Singhal, a key member of my Doctoral Advisory Committee, whose support and guidance were instrumental throughout this process. Likewise, Prof. G. Muthukumar's guidance and support were indispensable, completing an advisory team that could not have been better.

Mr. Jaspal Singh, the Senior Technician at the Concrete Laboratory, played a pivotal role in my Ph.D. I thank him for his constant advice on how to conduct experiments, customizing available instruments for my study and for going above and beyond in helping me through this journey.

A special acknowledgment goes to Mr. Sushil Kumar, whose expertise was crucial in all my castings and planning. His extensive on-field experience and manufacturing capabilities were essential; without them, many of my PhD objectives would have been unattainable.

The leadership at BITS Pilani, including Honourable Vice Chancellor Prof. V Ramgopal Rao and Honourable Director Prof. Sudhir Kumar Barai, has fostered a culture that emphasizes the freedom of scientific expression and innovation.

I extend my deepest gratitude to my parents, Mr. TVSS Avadhanulu and Mrs. Pratibha Harwalkar. For the past 25 years, they have placed my education at the forefront of their priorities. It is my sincere hope that the completion of my Ph.D. fills them with both joy and pride. I must also thank my brother Koustubh who provided me with advice during crucial times. I extend my heartfelt gratitude to my brother Sanket, who has been the most significant figure in my life. I dedicate my life to living by the principles that we learned together and shared over the years.

I must express my profound gratitude to my uncles and aunty, Mr. Anjani Kumar, Mr. Prasanna, Mr. Krishnamurthy, and Mrs. Ambuja, for their unwavering support. Being away from my parents for more than a decade, they provided the assistance that was crucial during this time. Their kindness and support were instrumental in enabling me to complete my Ph.D.

I would like to extend my heartfelt gratitude to Mr. Prashant Tede of MasterRheobuild for supplying the essential superplasticizer. His invaluable support was crucial in achieving my research objectives and successfully completing my PhD.

Additionally, I owe a great deal of gratitude to the friends I made during my Ph.D. tenure. Mr. Dhruv, Mr. Pradeep, Mr. Vivek and Mr. Harsh. They have significantly eased my journey, sharing in both laughter and challenges.

This thesis stands as a testament not just to my efforts but to the collective support and guidance of these individuals. My heartfelt thanks to all.

-Aniruddha Tangirala

Abstract

This doctoral thesis advances the field of sustainable construction materials through the development of fibre reinforced cementitious composites that exhibit exceptional thermal stability and durability. By strategically incorporating high-volume fly ash, fine steel slag aggregates and basalt-polypropylene hybrid fibres, this research overcomes conventional limitations in fire resistance and strength retention at elevated temperatures.

The study begins with the formulation of mixes that utilize high-volume fly ash (up to 60% by weight replacement of cement) and a hybrid fibre reinforcement to significantly enhance the material's resistance to thermal-induced damage and spalling. One of the mixes designed maintained a relative residual compressive strength of 93, 117, 102 and 38% after exposure to 200, 400, 600 and 800°C respectively, demonstrating a notable improvement in thermal performance. Furthermore, significant reductions in mass loss were observed in the mix. This initial finding was supported by detailed microstructural analyses, revealing the critical role of fly ash in enhancing the hydration products within the composite system.

Building upon this foundation, the inclusion of steel slag aggregates further improved the thermal endurance of the cementitious composite. The mix featuring a combination of high-volume fly ash and 100% steel slag aggregates, achieved remarkable strength retention, with residual compressive strength percentages of 101, 115, 113 and 55% at temperatures at 200, 400, 600 and 800°C respectively. The higher strength retention was attributed to synergistic effect of pozzolanic reactions, tobermorite formation and improvement in interfacial transition zone. Also, incorporation of basalt and polypropylene fibres improved the resistance against cracking and spalling.

A long-term durability investigation was conducted in parallel, which revealed high resistance to chloride ion penetration and significant improvements in compressive strength over time.

Notably, mixes with steel slag aggregates demonstrated no volumetric instability, challenging previous concerns about the long-term performance of such materials.

The research further explored the composites resistance to environmental thermal fatigue, identifying that these mixes show enhanced compressive and flexural strengths under cyclic temperature fluctuations generally observed in the environment. The mix with 100% steel slag aggregates in particular demonstrated a continual increase in strength whereas the mixes with ordinary river sand demonstrated a decline in strength post 180 thermal cycles.

The study also considered the special case of airfield pavements and examined the impact of combined environmental thermal fatigue and exposure to aircraft operating fluids. The developed composite succeeded to delay the deterioration of the composite from aircraft fluids by utilizing higher temperatures of the environmental thermal fatigue.

In summary, this thesis contributes to the development of eco-friendly, durable, and thermally stable construction materials and presents a comprehensive understanding of the mechanisms underlying their performance. The findings emphasize the potential of using high-volume fly ash, fine steel slag aggregates, and hybrid fibres to create sustainable solutions for modern construction challenges.

Table of Contents

List of Tables

List of Figures

List of abbreviations

Abbreviation	Description
1V-BF	Mix with 1% basalt fibre instead 2%
2PP	Mix with twice the volume of polypropylene fibre w.r.t control mix
12BF18	Mix with both 12 and 18mm Basalt fibre
30SS	Mix with 30% replacement of river sand
50FA	Mix with 50% fly ash
60FA	Mix with 60% fly ash
100SS	Mix with 100% replacement of river sand
BF	Basalt fibre
BF1	Mix with 1% basalt fibre
C	Calcium carbonate
C_2S	Belite
C_3S	Alite
CCs	Combined cycles of environmental thermal fatigue and aircraft fluids
CH	Portlandite
CSH	Calcium-Silicate-Hydrate
CTE	Coefficient of thermal expansion
DSC	Differential Scanning Calorimetry
E	Ettringite
ETF	Environmental thermal fatigue
F-SS	100% substitution of river sand with steel slag fine aggregates
FA	Fly ash
FOD	Foreign object debris
FR-FRCC	Fire resistant fibre reinforced cementitious composites
FRCC	Fibre reinforced cementitious composites

HBF	Mix with both 12 and 18mm Basalt fibre
HL-BF	Hybrid length Basalt fibre: Mix containing both 12 and 18mm
HVFA	High volume fly ash
ITZ	Interfacial transition zone
M	Mullite
MIP	Mercury intrusion porosimetry
OPC	Ordinary Portland cement
P	Portlandite
P-SS	Partial substitution of river sand with 30% steel slag fine aggregates
PP	Polypropylene
Q	Quartz
R60FA	Mix with 60% fly ash and reduced silica fume
RS	River sand
SCM	Supplementary cementitious material
SEM	Scanning electron microscope
SF	Silica fume
SP	Superplasticizer
SS	Steel slag
SS100	100% substitution of river sand with steel slag fine aggregates
SS30	30% substitution of river sand with steel slag fine aggregates
T	Tobermorite
TGA	Thermogravimetric analysis
XRD	X-Ray diffraction
XRF	X-Ray fluorescence

Chapter 1
Introduction

1.1 Background

The production of ordinary Portland cement (OPC), a common ingredient in fibre-reinforced cementitious composites (FRCC), is highly energy and resource-intensive and responsible for approximately 7-10% of global CO_2 emissions [1,2]. It is estimated that the production of a single ton of cement requires a massive 3000-4300 MJ of fuel, 120-160 kWh of electricity, and 1.5-1.6 tons of raw materials [3,4]. This concern is especially pressing as the high cement content in FRCC mixes renders them highly unsustainable which is not in line with the United Nations sustainable development goals.

Traditional concrete in addition to being highly unsustainable is prone to damage when exposed to elevated temperatures [5–7]. Incorporation of wastes generated in allied industries as substitutes for clinker and aggregates can ameliorate both sustainability aspect and thermal endurance of concrete [8]. Fly ash (FA) has emerged as a primary supplementary cementitious material (SCM) because of its widespread availability and resulting improvement in fresh state, mechanical, and durability properties of the composite [9–12]. Matos et al. [13] found that FA replacement by 60% has the potential to reduce the CO_2 emissions of concrete by 30%. Regardless of its abundance, sustainability, and resulting improvement in properties, only a small proportion of the total available FA is being utilized [14]. Under exceptional cases, a FA replacement of 30-35% is allowed in the current construction industry and several researchers have demonstrated that increasing the FA content beyond 30% leads to slower strength gain as evidenced by widespread availability of unhydrated or partially hydrated FA particles in the microstructure [15–17]. At ambient temperatures, the lower rate of strength development is the primary deterrent to its utilization in high volumes in cementitious composites. However,

researchers have recently observed that these unhydrated FA particles may lead to improvement in the rate of pozzolanic reaction at elevated temperature because of internal autoclaving [18]. Therefore, replacing cement with high volume fly ash (HVFA) may be beneficial in higher strength retention at elevated temperatures.

In addition to the selection of right SCM, sustainability and thermal performance can further be improved by use of alternative fine aggregates. Construction-grade River sand (RS) is becoming increasingly scarce and is likely to be exhausted by the year 2050 [19]. As construction industry is the primary consumer of natural river sand, potential alternatives in the form of wastes generated must be explored [20]. Steel slag (SS) generated from the production of steel using electric arc furnace is one such alternative which has demonstrated great potential to improve sustainability, and in some cases strength. Researchers have demonstrated the positive impact of utilization of SS aggregates in cement and concrete composites in terms of improved sustainability, and fire durability performance [21,22]. Additionally, use of SS aggregates may also lead to significant improvement in interfacial transition zone (ITZ). However, it is important to note that existing literature points out some drawbacks of SS aggregates, particularly concerning volume instability and reduced durability [23]. Moreover, while the potential of SS in improving the fire performance of FRCC is recognized, there is a scarcity of studies in this area. More research is essential to confirm the effects of SS under thermal conditions and to assess its volume stability and durability. Consequently, given the potential for fire performance improvement, the use of HVFA and steel slag aggregates in cementitious composites appears to be highly advantageous. Nevertheless, the slow reactivity of fly ash that causes significant changes to the microstructure with time and possible volume instability of steel slag aggregates necessitates a long-term study to assess their suitability.

It should further be noted that the elevated temperature performance is equally measured by the capacity of the material to resist spalling. Spalling in concrete refers to the breaking off layers or pieces from the surface of the concrete which significantly affects the load carrying capacity of load carrying members. Therefore, spalling resistance also needs to be considered along with a higher strength retention during the material development. Traditionally, steel, and polypropylene (PP) fibres have been incorporated into the cementitious composites to enhance the building fire safety. This hybrid combination has been effective in mitigating the excessive cracking, explosive spalling, and improving the ambient and post-fire performance of the cementitious composites [24,25]. Though the effectiveness of steel fibres under fire exposure has already been well recognized, there is a critical need to find similar alternatives considering its impact on the environment. Industries producing iron and steel cause 71 % of the environmental impact that originate from total metal production. Moreover, steel being a high-density material also increases the structural dead load. Basalt fibres (BF), on the other hand, are inert, requires no additives and generates no solid waste during manufacturing and hence, are popularly known to be 21st century's non-polluting green material [26,27]. With all the sustainability benefits, the end product is also corrosion resistant, has high melting point, and excellent mechanical properties of high tensile strength and elastic modulus [28,29]. BF have also been observed to significantly improve the fire resistance of concrete [30]. This enhancement was attributed to the exceptional thermal stability of these fibres, which preserves the structural integrity of the concrete under high temperatures. Additionally, the inherent crack-bridging properties of BF contribute to maintaining the durability of the material when exposed to fire. Furthermore, the residual strength and spalling resistance was found to be further improved with the hybridization with BF and PP fibres.

In addition to the structural fires which represent high-intensity events with low probability of occurrence, cyclic environmental temperature fluctuations must be considered as they are

highly frequent. The repeated expansions and contractions associated with these fluctuations may cumulatively contribute to a decline in concrete properties. Environmental thermal fatigue (ETF) of concrete refers to the deterioration that occurs in concrete due to the repeated variation in temperature over an extended duration [31]. Typically, the temperature of structural elements during daytime can increase to 60-70°C when the ambient atmospheric temperatures is around 30°C [32]. This temperature may significantly drop during night or during rains, leading to thermal shock. This issue is critical for concrete as different constituents may expand and contract at different rates when subjected to temperature changes. Over time, this differential thermal expansion and contraction can cause microcracks to form and propagate within the concrete, leading to a reduction in its structural integrity and durability.

This problem is more serious in case of the airfield pavements that cost significantly higher than the ordinary pavements. Airfield pavements face distinct challenges due to their vast size, heavy loads, and exposure to fluids leaked from aircraft and severe weather [33]. They must endure wear, impacts, and chemical attacks that can weaken the concrete, causing damage and reducing lifespan. This results in hazardous debris accumulation on the pavement, compromising aircraft safety and increasing maintenance costs. Therefore, creating advanced materials that can withstand these stresses is vital for efficient and safe airfield management.

Overall, research on the behaviour of HVFA-based composites at elevated temperatures is scarce, with no studies addressing the effects of cyclic temperature variation and aircraft fluids on HVFA-SS based FRCC, despite the potential shown by the basic constituents. Existing studies on HVFA have primarily focused on enhancement of sustainability of cementitious composites. Therefore, this study is novel from the perspective of its approach towards enhancement in properties by utilization of a new combination of matrix and fibres. Additionally, a novel incentive that prioritizes the thermal performance enhancement using

HVFA over traditional sustainability measures has been proposed. Sustainability and thermal performance are further enhanced with the incorporation of SS. The traditional method of utilization of fibres with large differences in melting point (BF-PP) has also been considered to enhance spalling resistance. A novel holistic approach of preservation of the composite at elevated temperatures from enhancements in matrix, aggregate, ITZ and spalling protection has been demonstrated. Also, a long-term study investigating the mechanical performance and durability has been conducted to ensure that the basic criteria of a construction material are satisfied. Subsequently, the developed mixes were tested against repeated thermal exposure. A special case study was conducted to assess the suitability of HVFA-SS and BF-PP based cementitious composites for airfield pavements that are frequently exposed to thermal fluctuations and chemical attacks from leaked aircraft fluids.

1.2 Research objectives

The primary objective of this study was to develop a sustainable FRCC with high thermal endurance and subsequently, study its behaviour under sub-elevated temperatures and durability conditions. The main objectives of the study can be outlined as below.

1. To develop a high-temperature-resistant HVFA and BF-PP based cementitious composite, capable of withstanding temperatures up to 800°C.
2. To enhance the thermal resistance of the developed mix using SS aggregates and variations to the fibre length and content.
3. To investigate the long-term mechanical and durability properties of the developed composite.
4. To assess the suitability of the developed mix under ETF conditions.
5. To assess the suitability of the developed mix under airfield exposure conditions for pavement application.

1.3 Scope of the study

This study focuses on developing an environmentally friendly and durable FRCC capable of withstanding high as well as sub-elevated temperatures and chemical attacks. This was achieved by incorporating HVFA and SS aggregates as primary constituents, contributing to improved thermal performance and durability. The addition of hybrid BF-PP fibres is intended to further improve the mechanical properties and structural integrity of the composite under thermal stresses and chemical attacks.

The use of HVFA and SS aggregates, both by-products of industrial processes, aligns with the principles of waste valorisation and circular economy. These materials not only reduce the reliance on traditional cement and aggregates, but also provide a method to enhance thermal stability of cementitious composites. A key aspect is its thermal durability, especially at high temperatures up to 800°C. Upon development of a high temperature resistant material that also satisfies the basic requirements of a construction material, its suitability in applications such as airfield pavements exposed to repeated heating and cooling cycles and chemical attacks was investigated.

1.4 Organisation of thesis

This thesis consists of nine chapters. The details of all the chapters have been explained below

Chapter 1: Introduction

This chapter provides information of the overall problem of sustainability and thermal susceptibility of the concrete and introduces the utilization of HVFA-SS and BF-PP based FRCC as a possible solution. Also, objectives and the scope of the study have been discussed in detail.

Chapter 2: Literature review

A thorough literature survey was conducted to ascertain the properties of FA, SS and BF-PP fibres. The possibility of enhanced thermal performance with this combination has been studied and reported in this chapter. Furthermore, gap-analysis was conducted to plan the chapters ahead.

Chapter 3: Experimental program and methodology

This chapter first highlights the materials used in the study and their characteristics. In addition, it also outlines all the experimental setups and testing procedures employed in subsequent chapters.

Chapter 4: Utilization of HVFA and hybrid basalt-polypropylene fibres for development of thermally enhanced FRCC

The suitability of HVFA and BF-PP have been investigated for the fire resistant FRCC (FR-FRCC). Investigations related to compressive and mass retention were made. A thorough relationship was established between the observed compressive and mass loss results with the scanning electron microscopy (SEM), X-Ray diffraction (XRD), and thermogravimetric analysis (TGA) to uncover the underlying mechanisms of the observed performance. The concept of thermal performance enhancers has been introduced in this chapter.

Chapter 5: Enhancement of the fire performance of developed FRCC with additional utilization of steel slag fine aggregates

Enhancement in properties of the FR-FRCC was attempted with incorporation of SS fine aggregates. The primary focus of the study was the variation in ITZ of the RS and SS aggregates

with increasing temperatures. A mechanism based on synergistic alliance of HVFA, SS and hybrid BF-PP has been provided.

Chapter 6: Long term durability performance of the developed of eco-friendly FRCC

The research delved into a comprehensive analysis of the long-term mechanical properties and durability of the developed composite. This includes examining its compressive and flexural strength at 360-days period, chloride ion penetration resistance, water absorption and dimensional stability. The evolution of ITZ across time was also studied to understand the strength development.

Chapter 7: Performance of the developed FRCC against Environmental Thermal Fatigue

Building upon the concepts introduced in Chapters 4 and 5, this chapter endeavours to mitigate the damage caused by ETF. Repeated ETF cycles between 20 and 60°C was applied and damage to surface, strength and changes to microstructure was studied. SEM, Mercury Intrusion Porosimetry (MIP) and Differential Scanning Calorimetry (DSC) were employed to assess the cause of change in the behaviour of FRCC under ETF conditions.

Chapter 8: Thermal performance enhancers against airfield pavement deterioration conditions

This chapter focused on the suitability of the developed FRCC based on HVFA and SS aggregates by subjecting the mixes 300 combined ETF and aircraft fluid cycles.

Chapter 9: Conclusions and Future Scope

Key findings of all the experimental studies conducted have been provided in this chapter. Also, underlying mechanism for enhanced thermal performance has been put forth. Furthermore, based on the limitations identified in each study, future scope was defined.

1.5 Bibliographical note

Parts of chapter 4 and 6 appear in the following journals and conference proceedings.

- A. Tangirala, S. Rawat, M. Lahoti, High volume fly ash and basalt-polypropylene fibres as performance enhancers of novel fire-resistant fibre reinforced cementitious composites, Journal of Building Engineering 78 (2023). https://doi.org/10.1016/j.jobe.2023.107586
- A. Tangirala, S. Rawat, M. Lahoti, A Year-Long Study of Eco-Friendly Fibre Reinforced Cementitious Composites with High Volume Fly Ash and Industrial Waste Aggregates, Innovative Infrastructure Solutions (2024) **(Accepted).**
- A. Tangirala, S. Rawat, M. Lahoti, Performance of ternary blended Basalt-Polypropylene fibre reinforced cementitious composite at elevated temperatures, in: SiF 2022– The 12th International Conference on Structures in Fire, 2022: pp. 457–465.

1.6 Summary

This chapter introduces a broad overview of the thesis which is focused on achieving high thermal durability while simultaneously considering sustainability. It also covers the designed objectives and the scope of the research. The literature survey presented in the next chapter (Chapter 2: Literature Review) is crucial for solidifying the feasibility and potential success of the objectives set forth in this chapter. It provides a thorough examination of the properties of FA, SS, and BF-PP fibres, along with an exploration of the enhanced thermal performance

achievable through this novel combination of materials. The gap analysis conducted in Chapter 2 also lays the groundwork for the practical and experimental phases of the research, ensuring a well-informed and methodical approach to the study.

Chapter 2
Literature review

2.1 Background

The push towards urbanization, population explosion and spatial limitations, has necessitated the construction of high-rise buildings and underground constructions. These structures which are important for alleviating the demands for housing and transportation are increasingly vulnerable to fire accidents. Enhancing the thermal performance of concrete plays a crucial role in the development of primary infrastructure of a country, such as buildings, tunnels, pavements, and energy systems.

Research highlights that the economic and human impact of tunnel and building fires is profound. The incidents in European tunnels such as the Tauern, Mont Blanc, and Gotthard Road Tunnels resulted in over 60 fatalities combined and caused closures for repair works, affecting the transport infrastructure significantly [34]. The economic losses of these events not only include the costs of repair and reconstruction but also indirect costs such as lost revenue, increased insurance premiums, and the societal impact of lost lives and environmental damage. Fig. 2.1 depicts severe fire accidents in high rise buildings and their consequences.

Also, the thermal performance of concrete should also be considered for repeated exposures to lower temperatures followed by cooling as usually observed in the environment [31]. Significant strength deterioration and consequent loss in durability has the potential to reduce the service life of the structures.

The severity of damage caused by elevated temperatures and sustainability of concrete is primarily influenced by individual components included in the cementitious composite. The main issues pertaining to thermal performance of cementitious composites and concrete are further outlined in the next section.

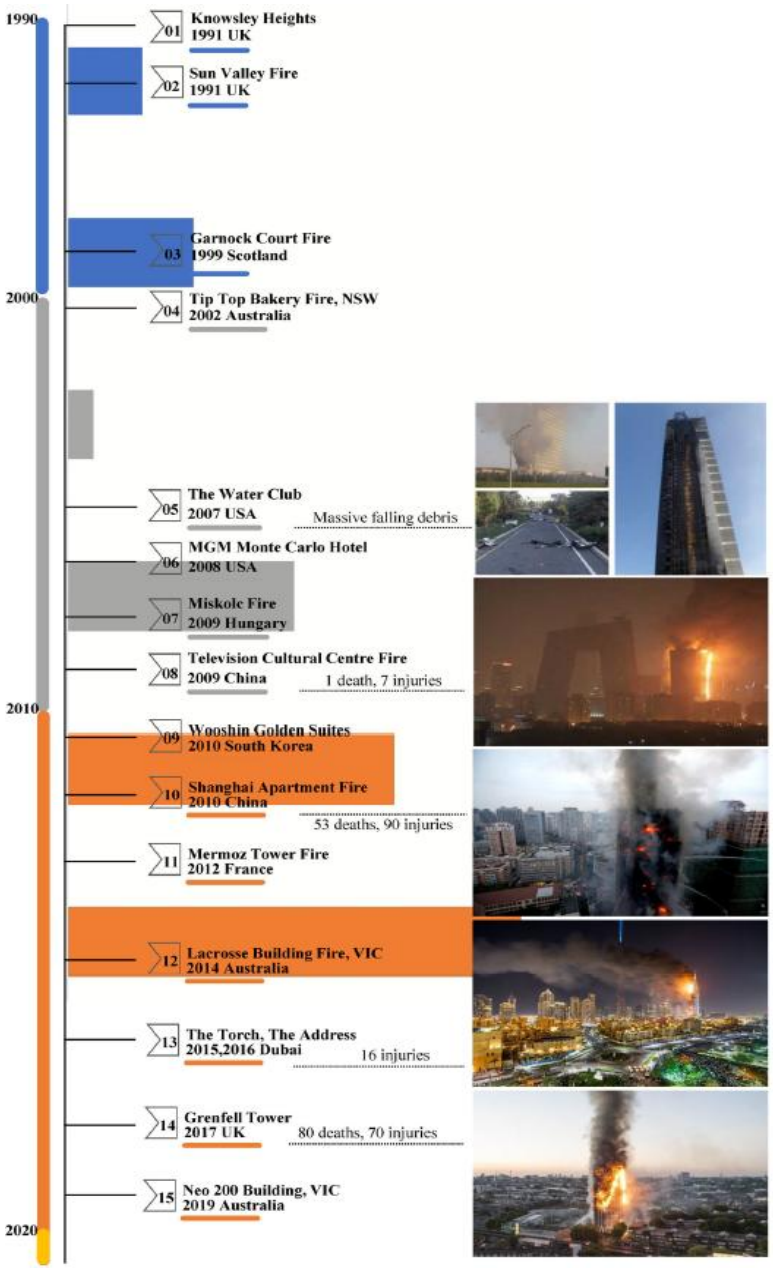

Fig. 2.1. Past multi-storeyed building accidents related to fire [35]

2.2 Problem identification

2.2.1 High temperatures

The structural damage to concrete during fires can be extensive. The impact of elevated temperatures on OPC based cementitious composite involves significant compositional changes, occurrence of spalling and origination of thermal stresses that affect their mechanical properties and durability.

Fig. 2.2 summarises the some of the changes in concrete that occur after subjecting it to elevated temperatures. According to Ma. et al. [36], the compressive strength of concrete does not change, or a marginal increase is observed for temperatures up to 300°C. Significant reduction in compressive strength is observed when it is subjected to temperatures between 300 and 800°C. The concrete loses almost all its compressive strength at temperatures > 800°C.

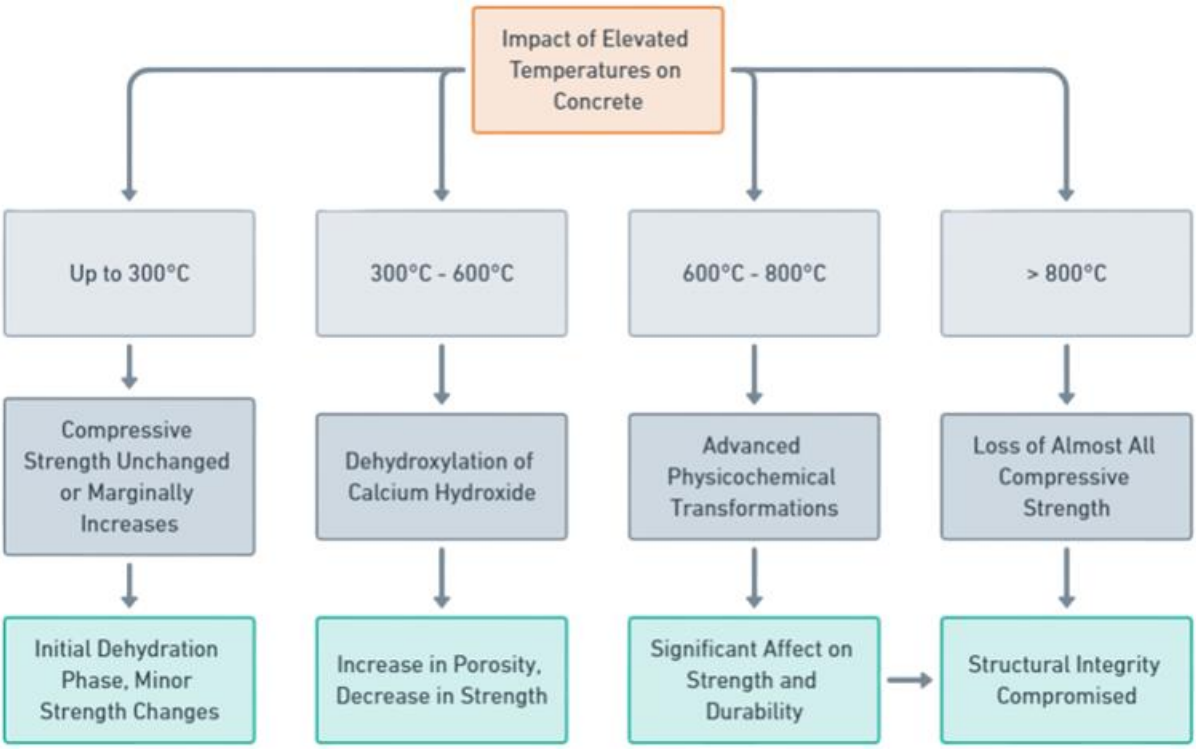

Fig. 2.2. Changes in concrete with increasing temperatures

In the initial dehydration phase, the loss of free and physically bound water from the pores of the concrete is observed. This process leads to a reduction in mass and can also initiate microcracking because of drying of the concrete [37]. Minor changes in strength may occur. The porosity and average pore diameter may begin to increase slightly, affecting the material's permeability and potentially its mechanical properties [38].

Between 300 and 600°C, dehydroxylation of calcium hydroxide (portlandite) forms calcium oxide (lime). These reactions contribute to an increase in porosity and a decrease in strength. The loss of chemically bound water and the decomposition of calcium hydroxide are prominent

in this temperature range [37]. The structural integrity of concrete is further compromised due to the progression of microcracking and the alteration of the calcium-silicate-hydrate (CSH) gel. The thermal expansion of aggregates can also lead to increased internal stresses, exacerbating cracking and leading to a noticeable reduction in mechanical properties [38].

Between 600 and 800°C, advanced physicochemical transformations are observed. The complete dehydration and dehydroxylation, decarboxylation reactions occur. There is also the beginning of the decomposition of CSH gel, which significantly affects the concrete's strength and durability [37]. Overall, dehydration, dehydroxylation of portlandite and decarbonation of calcium carbonate occurs at temperatures between 35-200°C, 450-550°C, 635-750°C respectively [39–41]. Understanding these temperature-dependent changes is important for evaluating fire-damaged concrete structures and to tailor the ingredients of concrete mixes for improved fire resistance properties.

In addition to these transformations, spalling of concrete is an important phenomenon that requires significant attention. The thermo-hygral spalling is attributed to the buildup of pore pressure within the concrete. If the vapor pressure exceeds the tensile strength of the concrete, it can lead to explosive release of chunks of concrete or aggregate that diminishes the load carrying capacity of the structural members. Coarse aggregates are more susceptible to dislodgement from spalling because of their relatively weaker and porous ITZ and therefore could be avoided in the matrix [42]. The addition of polypropylene fibres to concrete has been shown to reduce the possibility of vapour-pressure-induced explosive spalling [43]. Also, differential thermal expansion due to the mismatch in thermal expansion coefficients between the aggregates and cement matrix may causes cracking and degradation of the mechanical properties of concrete [44].

2.2.2 Sub-elevated temperatures

The degradation of concrete can result from the pronounced daily and annual temperature variations prevalent in mid and high latitude areas [31]. These fluctuations in environmental temperatures arise due to changes in incident sunlight and wind patterns. In regions where ambient temperatures exceed 30°C, the temperature of structural elements and pavements can escalate to 60-70°C [32]. After exposure to high daytime temperatures, there is often a substantial drop in temperature either at night or due to changing weather conditions. Repeated exposure to varying environmental temperature causes degradation in concrete properties which is also known as environmental thermal fatigue.

The ETF cycles can initiate cracking at micro and macro levels and cause a degradation to pore structure [45]. This increase in porosity is generally attributed to the evaporation of free water and decrease of crystal water in the concrete. As temperatures rises, there is an increase in the pressure in closed pores of the cementitious composites. This results in the breakdown of the barriers between open and closed pores, which enlarges the pore and the microcracks emerge [46]. Li et al.[31] subjected concrete to temperature differential of 20, 30 and 40°C for 400 cycles. Porosity and total pore volume increased with thermal cycles and the microstructure showed signs of coarsening. The relative impact on porosity was greater in the concrete with strength 49.1 MPa as compared to a concrete of strength 28.5 MPa, indicating a higher susceptibility of concrete to thermal fatigue-induced degradation when the strength is higher.

The consideration of ETF is also essential because concrete is a three-phased material with different thermal expansion coefficients of constituent materials. An et al. [32] utilized FA up to 25% as replacement to cement and subjected the specimens to 135 ETF cycles between 20 and 65°C. Significant strength degradation was observed across all the mixes and the primary cause of deterioration was identified as the substantial disparity in the thermal expansion coefficients between the coarse aggregate and the cement matrix. This mismatch leads to non-

uniform deformation across the concrete components during ETF cycles compromising the mechanical properties of the composite. The magnitude of this degradation was more pronounced for concrete with higher strength grades. Huang et al.[47] also evaluated the impact of ETF on the mechanical properties of concrete by subjecting concrete to temperatures between 20 and 65°C over 330 cycles. The compressive strength initially increased, peaking at around 150 ETF cycles, then decreased significantly with further exposure to ETF. During the strength enhancement stage, unhydrated cementitious materials reacted with moisture, leading to the formation of hydration products like C-S-H gel and ettringite. ITZ microcracks increased in all geometrical parameters (such as total length, area, and width) as ETF cycles increased, indicating more severe degradation in the later stages of ETF. In the strength degradation stage, the porosity near the aggregate edge increased, and the ITZ was more severely affected. Based on the reported results, it is evident that the effect of ETF in concrete material is severe as the structure durability is compromised even after just 300 ETF cycles. This highlights the necessity of a durable material, particularly in the construction zones where temperature fluctuation is very frequent.

2.2.2.1 Special case of airfield pavements under sub-elevated temperatures

This problem is serious in case of the airfield pavements which have large surface areas and cost significantly higher than ordinary pavements. These pavements require 74-370 million USD for their construction and are designed to serve for 20-40 years [48,49]. In case of civilian airports, closing a runway causes an economic loss and higher risks are associated with strategic military airfield pavements. Generally, airfield pavements experience fatigue load, impact load, as well as shrinkage in addition to severe weather conditions. Furthermore, they are exposed to hydraulic oil, lubricating fluid, and air traffic fuel leaked from the aircrafts that cause saponification, scaling, chipping, and strength loss of concrete at higher temperatures as demonstrated in Fig. 2.3 (a) and (b) [33,50,51].

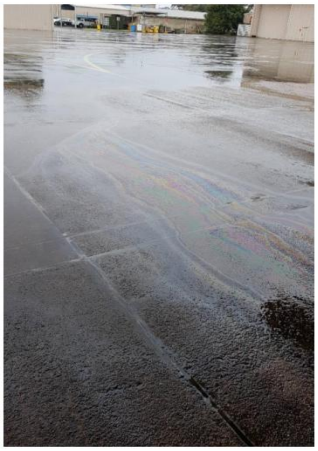

(a) Leaked oil from aircraft with rainfall runoff

(b) Spalling of surface

Fig. 2.3 Airfield pavements exposed to fluids leaked from the aircrafts [52,53]

The aircraft fluids consist of esters of fatty acid, carboxylic acid, phosphate esters etc. Saponification occurs when carboxylic acid from the aircraft fluids reacts with the portlandite in the cementitious system to form calcium carboxylate salts (soap) and water at higher temperatures. Formation of carboxylate salts is also possible with the reaction between calcium carbonate in concrete and esters of fatty acids. The penetration of these deleterious fluids through the cracking caused by ETF can potentially increase the rate of degradation and significantly reduce the service life of pavement.

Also, cracks, spalls, and loose fragments from concrete pavement can create debris on runways, taxiways, and aprons which can be called as foreign object debris (FOD) on airfield pavements. They represent a critical concern for aviation safety, potentially causing extensive damage to aircraft and even leading to accidents. The presence of FOD on airfield pavements can result in tire punctures, damage to aircraft engines, and, in severe cases, catastrophic failures. Moreover, FOD-related incidents increase operational costs due to aircraft repairs and downtime. Also, the considerable rise in air traffic coupled with ongoing enhancements in payload capacity has led to a manifold increase in the maintenance demands for airfield

pavements [54]. Consequently, material selection for the construction of airfield pavements must consider thermal and chemical resistance to enhance the service life of the pavements.

The material to be used in the construction for airfield pavements require specific characteristics, including minimal porosity, resilience to impacts, resistance to abrasion, durability against thermal fluctuations, and protection against chemical attack.

2.2.3 Sustainability and environmental impact

Recently, there is a noticeable shift in the construction industry towards sustainability, particularly in the development of green cementitious composites. This shift is influenced by the urgent need to reduce the environmental impact of construction materials and their production processes. Innovations in clinker substitutes, upcycling of industrial wastes as aggregates, and the incorporation of sustainable fibres have been at the forefront of this transformation [55,56].

The production of cement is notably energy-intensive and a major source of CO_2 emissions, contributing substantially to global warming [57]. Accounting for approximately 8% of worldwide CO_2 emissions, the industry's carbon footprint primarily results from limestone calcination and the burning of fossil fuels [58]. CO_2, being the most detrimental of all greenhouse gases, accelerates the global warming phenomenon at an alarming rate [3]. This environmental impact is further exacerbated by the extraction of aggregates, highlighting the need for exploration of alternative materials as in the form of industrial wastes aggregates [59]. Moreover, the fibres that are incorporated in composites adds to the overall carbon footprint, thereby affecting long-term environmental sustainability [60]. Through proper evaluation and selective substitution of each pollution causing component individually with a sustainable alternative can potentially mitigate the environmental concerns of cement and concrete composites. The cement and aggregates form most of the volume of the concrete and therefore

alternatives must be found. Further enhancements in sustainability are possible through the utilization of ecofriendly fibres. All these aspects are discussed in detail in the following section.

2.2.3.1 Binder

Cement is the primary contributor of greenhouse gases in concrete and consequently, there has been growing demand for cement substitutes that can potentially enhance the properties of the concrete. Fly ash, a by-product of coal combustion in power plants, is the most widely used supplementary cementitious material that has a great potential for ready industry acceptance and therefore can be considered for further research. The practice of replacing a high volume of cement with fly ash not only addresses environmental concerns but also enhances the mechanical, durability and thermal endurance of the composite materials [4,61,62]. Fly ash use in high volumes has also been found effective in improving the workability and long-term strength of concrete [63]. Furthermore, its fine particulate nature contributes to a denser microstructure, enhancing the durability and reducing the permeability of the concrete. The replacement of cement with fly ash in concrete reduces the carbon footprint of the construction material [64]. Therefore, the properties of cement-based composites incorporation of this widely available waste material must be investigated.

2.2.3.2 Aggregate

As highlighted in chapter 1, there is a high likelihood of exhaustion of construction grade RS by the year 2050. Also, sand mining and associated activities are unsustainable as they exploit natural resources and cause irreversible damage to the environment [65,66]. This necessitates use of a sustainable alternative especially in the form of wastes from allied industries which not only allows for resource and environment conservation but also promotes waste upcycling.

Aggregates made of electric arc furnace steel slag is one such alternative which is produced during the steelmaking process in an electric arc furnace. Approximately 40% of global steel production is carried out in electric arc furnace generating 103 million tonnes of SS annually [67,68]. The production process involves melting steel scrap or direct reduced iron with electric arcs, during which impurities are separated and collected as slag.

The consumption of natural aggregates, such as sand and gravel is reduced by utilization of this industrial waste. Also, this conserves natural resources, energy and diminishes the environmental impact related to their extraction and processing [69]. From an environmental perspective, the use of industrial wastes as aggregates helps in the eradication of waste disposal in landfills and reduces the adverse environmental effects associated with the processing and mining of natural aggregates [70]. In terms of mechanical strength benefits, concrete made from industrial waste materials, including SS, has shown good performance in terms of durability and strength [71]. Additionally, the use of SS as fine aggregate in concrete has shown comparable or better results in terms of mechanical properties, compared to natural river sand [72]. Other industrial wastes, such as coal bottom ash, eco sand, and quarry dust, have also shown potential as substitutes for traditional fine aggregates, contributing to the strength and durability of concrete. Furthermore, SS has also been found to enhance the fire resistance of the concrete [73]. In conclusion, the use of SS in concrete not only aids in managing industrial waste effectively but also supports the conservation of natural resources, reduces energy consumption, and enhances the strength of concrete, aligning with the goals of sustainable construction practices.

2.2.3.3 Fibres

Sustainability of the cement-based composites can further be enhanced by adopting BF. Traditional polymer and steel fibres require significant resources and energy, while producing

waste and toxic gases during their production. Basalt fibres are produced by melting crushed basalt rock at 1700°C and then extruding it through small nozzles to produce continuous fibres [74]. BF require approximately 1/3rd the energy required for the steel production in an electric furnace [75]. BF release no toxic fumes at high temperatures, has a high softening point of 960 °C and retains 90% of its strength even at 600°C [76,77]. Also, these fibres require no additives for their manufacturing. These properties could prove to be useful to the improve the performance of the composite especially when exposed to elevated temperatures. Recently, there has been significant interest in utilization of BF because of enhancement in mechanical properties, their thermal stability and sustainability as well.

Therefore, synergistic integration of HVFA-BF-SS aggregates into concrete has the potential to significantly mitigate the environmental concerns associated with the construction industry. HVFA reduces the carbon footprint by substituting a significant amount of cement. This not only curtails greenhouse gas emissions but also enhances the mechanical and durability characteristics of the concrete. Utilization of SS aggregates offers a sustainable alternative to conventional RS and helps in conserving natural resources and minimizing the detrimental environmental impacts of extraction and processing. Moreover, it enhances the compressive strength and fire resistance capabilities. The production of BF necessitates a fraction of the energy required to produce steel and is devoid of toxic emissions, making it a green fibre. Collectively, these materials present an optimal solution for addressing the environmental challenges posed by the construction sector.

2.3. Current state of each of the identified constituents

2.3.1 Effect of HVFA

High-volume inclusions of FA lead to significant variations in the fundamental characteristics of cementitious composites. Following sections provide a comprehensive overview of the effect of FA on various properties including workability, compressive strength, chloride

durability and thermal resistance of cementitious and concrete composites. Also, the reactivity of FA is of utmost importance given that it is being considered as primary SCM. This aspect affects all the properties including fresh state, hardened mechanical properties and thermal performance of the cementitious composites. Therefore, this aspect has also been studied with special focus in the current section.

2.3.1.1 Workability

FRCC usually require high amount of superplasticizer because of usual low water-binder ratio, increased viscosity, friction and surface area and water absorption by fibres [78,79]. Class-F FA reduces the amount of superplasticizer required to achieve desired flowability because of the "ball-bearing" effect of spherical FA particles, thus making the mix economical [80]. Shaikh and Supit [81] investigated the effect of 40 and 60% replacement of OPC with HVFA in their mortar containing nano-$CaCO_3$ and reported an increase in slump flow by ~ 14 and 43%. An increase in FA content resulted in enhancement of the workability. Harera et al. [82] replaced up to 75% of OPC with FA and determined slump and slump loss as a function of time. With increase in FA substitution, a higher slump values were obtained in the range of 10-40 mm and slump loss reduced by 50%. This slump loss is reduced because of slower pozzolanic reaction rate of FA particles.

FA also tends to deflocculate the cement particles because of dilution effect which can increase the workability of the mix [83]. Overall, workability of the mix is enhanced because of ball bearing effect and dilution effect and the mix remains workable for a longer duration because of slower reactivity of FA particles. This is especially useful for designing mixes with higher strengths which generally require low water contents and high concentrations of expensive SP.

2.3.1.2 Compressive strength

The strength of concrete with HVFA was found to be a function of time and replacement level. The compressive strength of HVFA based concrete gradually decreases with increasing fly ash content [84]. At early stages, strength of the cementitious composite is primarily contributed by the hydration of cement particles, whereas at later stages, the participation from FA pozzolanic enhances the compressive strength of plain cement concrete [85]. Herath et al. [86] utilized 65% (HVFA-65) and 80% (HVFA-80) replacement of OPC with FA and observed the variation in compressive strength from 7 to 450 days. The strength of HVFA concrete increased over time, with compressive strength values ranging from 32 to 73 MPa for HVFA-65 and 22 to 71 MPa for HVFA-80. According to Li et al. [83], HVFA slows down the hydration of OPC because of formation of low density and high diffusivity CSH which reduces the Ca/Si ratio and takes longer to stabilize. However, over time, HVFA enhances the degree of hydration of cement particles because of deflocculant action and formation of additional sites for nucleation. Nevertheless, Rashad [11] and Siddique [87] highlight that a compressive strength recovery over time when HVFA is used in concrete. This trend is further evident in Fig. 2.2, which highlights that the strength difference between the control specimen (0% FA dosage) and HVFA concrete diminishes progressively over time. Furthermore, the studies also establish a direct correlation between the reduction in compressive strength and the proportion of cement replaced with FA.

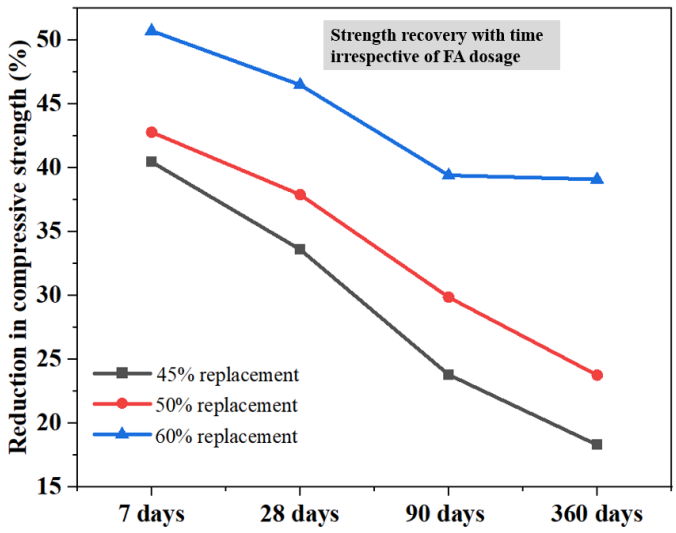

Fig. 2.4. Compressive strength recovery w.r.t time at various FA dosages

A significantly low early age compressive strength may also be because of low portlandite content in the matrix as low calcium FA was used. The use of CaO as an activator in HVFA concrete results in higher compressive strength compared to HVFA concrete without an activator [84]. The addition of SF to HVFA has also been found to accelerate the initial hydration reaction, shortening the setting time, and improving the compressive strength during the initial and middle stage of hydration because of pozzolanic reaction and consequent densification of pore structure [88].

2.3.1.3 Chloride Durability

In case of HVFA, increasing the FA dosage has been demonstrated to enhance the chloride ion penetration resistance [12]. Poon et al. [89] replaced 45% of OPC with FA and measured chloride ion penetration via rapid chloride penetration test (RCPT). They observed a decrease of ~62 and 84% in total charge passed through the specimen at 28 and 90-days curing age respectively. The sample exhibited a RCPT values of 768 and 175 Coulombs (C) at the end of curing ages previously mentioned. FA, because of its pozzolanic reaction, increases the tortuosity and reduces the interconnectivity of the pores, thereby reducing the transport of

chloride ions [90]. Sahmaran et al. [91] also demonstrated a reduction in chloride ion penetration with curing age and with increasing FA dosage as shown in Fig. 2.5.

The penetration of chloride depends on the electrical conductivity of the pore solution, which is directly related to the alkalinity of the cementitious material. As the amount of FA incorporated increases, the alkalinity proportionately decreases, leading to reduction in the RCPT values. The reason for this excellent performance can also be attributed to the physical adsorption on CSH and formation of Friedel's salts from the reaction between C_3A and C_4AF with chloride ions to form calcium chloroaluminates and calcium chloroferrites [91–93].

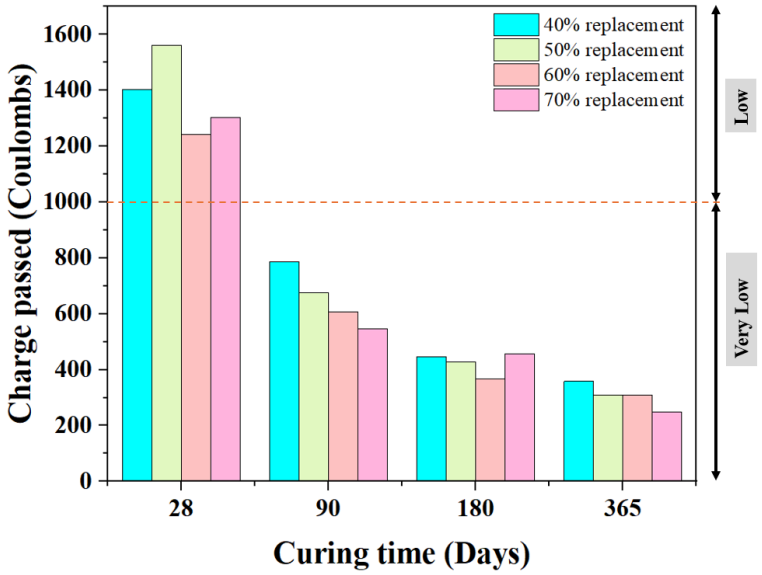

Fig. 2.5. Total charge passed at various time intervals

The chloride ion penetration values of mixes with HVFA can be categorized as 'very low' as per ASTM C1202 [94] for extended curing durations. Therefore, HVFA based mixes can be considered for offshore structures and coastal areas where airborne chloride can cause reinforcement corrosion.

2.3.1.4 Thermal resistance with HVFA

The integration of fly ash in concrete has been proven to enhance its fire resistance. This enhancement is predominantly because of the pozzolanic reactions of FA, which significantly

improve the concrete's mechanical and microstructural properties under high-temperature exposure [95]. FA contributes to denser concrete microstructure, thereby improving thermal stability and reducing permeability when subjected to fire. Additionally, it has been found that higher dosages of FA enhance the residual properties of the concrete. Rashad [4] suggested that formation of a compound known as tobermorite increases the strength of the concrete by up to 2.5-2.9 times the original compressive strength at ambient temperatures at 400 and 600°C. This compound is synthesized under hydrothermal conditions in the presence of reactive silica, portlandite and with Ca/Si ratio ranging from 0.8 to 1.4 [96–99]. These conditions can be achieved using class-F fly ash. Khan and Abbas [100] demonstrated a residual strength greater than 100% after exposure to 400 and 600°C. The formation of tobermorite at 400°C significantly contributed to the strength retention of the concrete [4,101]. Donatello et al. [102] replaced incorporated ~ 80% of FA in their paste with 4% Na_2SO_4 and observed compressive strength retention >100% even after exposure to 1000°C. They observed a reduction in mass loss because of reduction in portlandite, calcite, ettringite and gel-water. Ibrahim et al. [103] created a HVFA-nanosilica based mortar that retained the same strength at 700°C as that of control mix at room temperature. It is evident from this section that a material with high thermal resistance is possible with the incorporation of FA in high volumes.

2.3.1.5 Reactivity of fly ash

The rate of reaction of FA particles in the cement-based composites affect fresh, mechanical and durability properties of the cementitious composite in addition to its thermal performance. Several factors influence its reactivity in the cementitious system as demonstrated in Fig. 2.6.

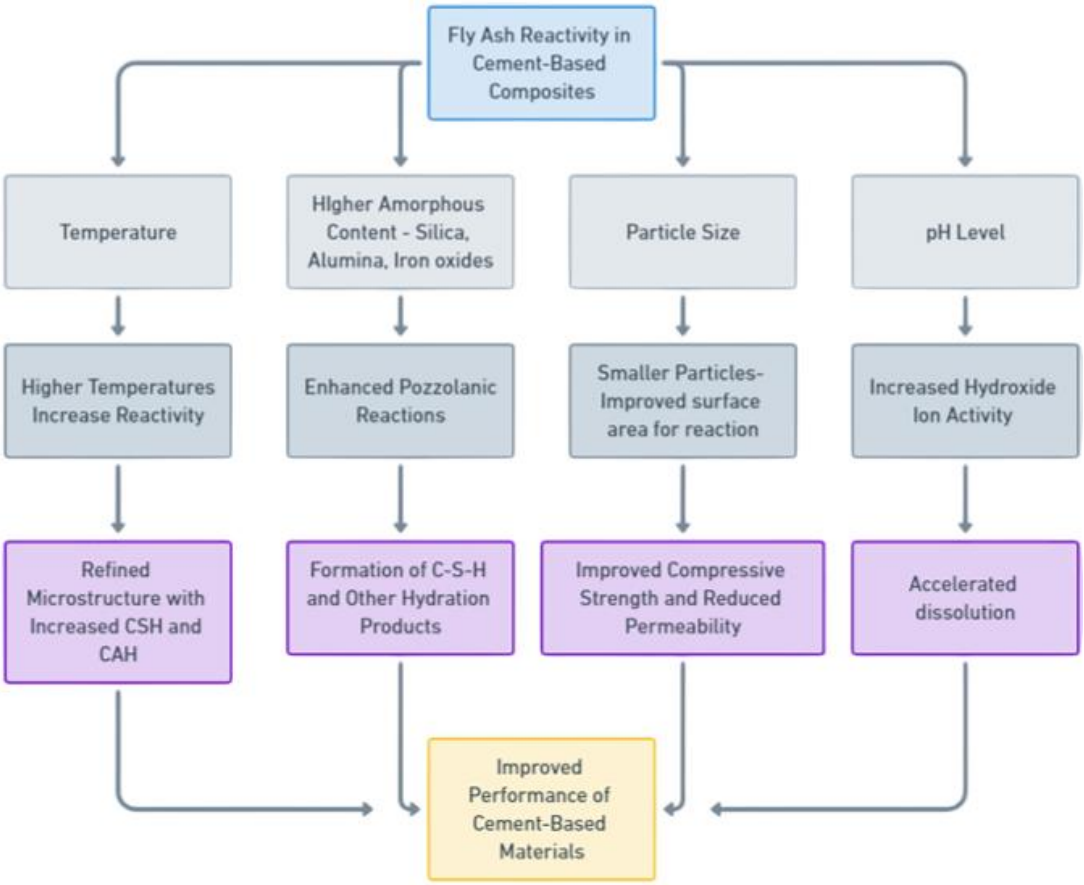

Fig. 2.6. Factors affecting the reactivity of FA in cementitious system

The amorphous content within FA is one of the primary determinants of the hydration kinetics and overall reactivity in cement-based systems. Research by Glosser et al. [104] shows that the composition and properties of FA affect the kinetics of reactions in cementitious pastes. Specifically, the amorphous phases, rich in silica, alumina, and iron oxides, facilitate pozzolanic reactions, leading to the formation of additional CSH and other hydration products.

The dissolution kinetics of these amorphous components are affected by environmental factors and the overall chemical composition of the cementitious system. Higher temperatures and pH increase of the rate of reaction, thus enhancing pozzolanic reactions [105,106]. Higher pH level was found to accelerate dissolution due to increased hydroxide ion activity.

Ji et al. [107] investigated the effect of temperature on reactivity of FA between 20 and 80°C and found that higher temperatures within this range enhance the reactivity of FA. Kang et al.

[108] investigated the effect of steam curing on the pozzolanic reactivity of FA in a cementless binder system composed of FA, hydrated lime, and silica fume. The paper reported that steam curing at 60°C for 3 days significantly accelerated the consumption of FA and portlandite, resulting in the formation of CSH and the development of ultra-high strength (>100 MPa). Similar observations were made by Fernández and Renedo [109] under hydrothermal conditions, particularly at temperatures between 60 and 200°C. This effect continues till 600°C where compressive strength >100% was observed by different researchers as discussed in the previous section.

There has also been extensive research focusing on how the particle size of FA influences its rate of reaction. Haustein and Kuryłowicz-Cudowska [110] investigated the impact of the particle size of fly ash microspheres (up to 200 µm and up to 500 µm) on properties of concrete. It was observed that finer FA microspheres significantly improved the mechanical properties of concrete. Similar observations were made by Lin [111] on reactive ultra-fine FA (particle size 0.1µm - 10µm). It was observed that ultra-fine FA exhibits significantly higher reactivity and is more effective as an additive, contributing to the improved performance in terms of strength and durability.

In summary, the amorphous content and particle size of FA, pH and temperature of the cementitious system determine of the reactivity of FA. Understanding its composition, dissolution kinetics, and the factors affecting its reactivity is essential for optimizing the performance of composites that include fly ash.

2.3.2 Steel slag aggregates

Following sections present a thorough review of the existing studies which utilize SS as aggregate for the development of concrete or cementitious composites. This section first analyses the suitability of SS aggregates as a viable candidate for construction materials,

considering its effects on compressive strength and microstructure. Moreover, it provides information on the impact of adding SS aggregates on thermal performance. The literature related to the use of SS aggregates raises some questions regarding its volume stability within the cementitious system. Therefore, special attention to mitigate the ill effects of volume expansion has been included.

2.3.2.1 Effect on compressive strength

Construction grade river sand is a scarce resource and therefore needs to be replaced with sustainable alternatives. As discussed earlier, the addition of SS as an aggregate in concrete has been shown to increase the compressive strength compared to conventional concrete mixes. This is partly due to the enhanced packing density and the formation of a stronger ITZ between the slag particles and the cement paste. Arribas et al. [112] provided a detailed explanation of this behaviour. The ITZ of ordinary aggregates is generally characterized by higher porosity, water content, calcium hydroxide, ettringite and reduced amount of CSH. The SS aggregates, on the other hand, do not repel the cement grains given that they have similar chemical composition. Also, they retain only a small amount of water on their surface as opposed to ordinary aggregates. Furthermore, the irregular shape of the aggregates and the surface porosity provides a good interlocking with the surrounding matrix. Consequently, a solid ITZ is observed when SS aggregates are used in cementitious composites. These aggregates also release CaO slowly towards the surface of the specimens with time which undergoes carbonation. Adegoloye et al. [113] also suggested that utilization of SS can impart good mechanical properties because of improved adhesion with the paste phase as these aggregates which have a rough texture, higher porosity, and irregular shape. Also, Rashad et al. [114] presented sufficient evidence of increasing compressive strength with incorporation of SS aggregates. The ITZ is critical in defining the overall strength and durability of concrete.

From thermal-endurance perspective, a study by Liang et al. [22] demonstrated a compressive strength retention of 69% at 1000°C with incorporation of SS fines. The enhancement in performance was attributed to the similar chemical composition of OPC and SS, which mitigates differential thermal expansion between the aggregate and paste phase, thereby forming a more continuous ITZ.

2.3.2.2 Volume instability

One of the key problems associated with the utilization of electric arc furnace SS as aggregates is its volumetric instability [112]. The expansion of concrete containing SS aggregate is a complex phenomenon influenced by several factors, including the physical and chemical properties of the slag, the curing conditions, and the particle size of the aggregate. Various researchers have investigated these aspects to understand the mechanisms behind the volume expansion and to assess the performance of SS in concrete applications. The findings have been summarized in Fig. 2.7.

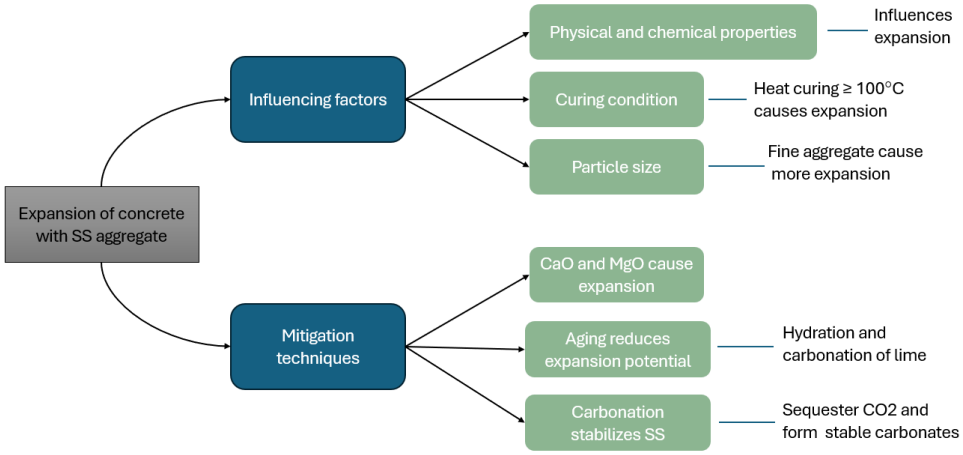

Fig. 2.7. Factors affecting volume stability and mitigation strategies

Kuo and Shu [115] linked this volume instability to the calcium oxide (CaO) and magnesium oxide (MgO) content in SS aggregates and found that the expansion reaction in concrete is influenced by curing temperature. Heat curing at 100°C resulted in significant expansion,

especially for fine aggregates. The expansive reactions within the slag aggregates were less active at lower temperatures, highlighting the temperature dependent expansive behaviour of SS aggregates in concrete applications. Also, the mineralogical transformation of slag components, such as the transformation of wustite into magnetite at temperatures greater than 800°C, can cause expansion in volume, introducing cracks [116].

The aging process of slag aggregate can also mitigate potential expansion issues. The aging process allows for the hydration and carbonation of free lime present in the slag, thereby reducing its expansion potential and improving its suitability as a construction material [117]. Research also showed that SS had low concentrations of expansive compounds, and possible swelling can be reduced by aging the slag for 45 days and consequently improving volume stability [118]. Carbonation is also a prominent method for stabilizing steel slag by sequestering CO_2. This process involves the reaction of CO_2 with calcium and magnesium in the slag to form stable carbonates, such as calcite. Carbonation can significantly reduce the leaching of alkaline earth metals and stabilize hazardous metals converting Calcium-phases into calcite, thereby improving the environmental properties of steel slag [119].

In conclusion, while SS aggregate can cause expansion in concrete, careful selection of particle size, aging or pre-treatment of the slag, and appropriate curing conditions can mitigate these issues, making it a viable aggregate for concrete applications.

2.3.3 Basalt fibre

Fibre inclusions in cementitious composites alters its fresh state, mechanical, durability and thermal properties. The individual fibre parameters such as fibre length and content affect the overall properties of the cementitious composite and therefore must be taken into consideration. These parameters have the potential to alter the workability and mechanical properties and thermal endurance of the cementitious composites. Furthermore, effect of fibre hybridization

on thermal performance has also been incorporated. Some of the key findings from the existing research is described below.

2.3.3.1 Effect of BF on compressive and flexural strength

The inclusion of BF can lead to a decrease in compressive strength in some cases, which may be attributed to the disruption of the cement matrix uniformity and the creation of weak interfaces and voids around the fibres. This effect is particularly noted at high fibre contents which often causes fibre agglomeration and reduction in workability of the concrete mix [120]. Conversely, a moderate addition of BF can enhance compressive strength by improving the microstructure of the concrete and reducing the crack width, which contributes positively to the compressive strength of cement composite. Adesina [74] pointed out that there is still no consensus among researchers about the effect of BF content on the compressive strength of the cement-based composites. The literature suggests that increasing the length of the fibres can have positive impact on the compressive strength of the composite. Jiang et al. [121] demonstrated a higher compressive strength by increasing the length of the BF and they attributed it to the stronger bridging effect of the longer fibres. Therefore, use of longer fibres or hybridization of fibre lengths presents potential to enhance the characteristics of the composite.

From an elevated temperature performance perspective, Afzal et al. [30] incorporated 1% and 2% BF (by % wt. of cement) in high strength concrete and exposed it temperatures up to 800°C. They suggested that BF improves the resistance to surface cracking, reduces the mass loss and improves the relative residual strength of concrete. This improved performance was attributed to thermal stability of BF that maintain the structural integrity of the composite, reduced thermal conductivity with increasing BF content and crack bridging capability of stable BF. Furthermore, they suggested that BF act as additional nucleation sites for hydration products

to justify the improvement in mass retention. Alaskar et al. [76] analysed the effect of 0.25-1% dosage of BF (by %vol.) in concrete after exposure to 300 and 600°C. The benefits of adding BF in the matrix become evident at higher temperatures as products of hydration start to decompose. It was suggested that excellent thermal stability of BF and formation of a fibre network improves the strength retention of the composite.

BF also enhance flexural strength because they act as a bridge across cracks in the composite material. This bridging effect prevents the propagation of cracks and improves the material's toughness and durability. The fibre-matrix bond plays a crucial role in transferring stress from the matrix to the fibres, thereby enhancing the flexural performance [122]. Incorporating BF into concrete mixtures can lead to enhanced flexural strength, fracture energy, and abrasion resistance, albeit at the cost of reduced compressive strength. This improvement is observed even with low BF contents [120]. Basalt fibre reinforcement in cement mortars enhances flexural strength up to 20% but may reduce compressive strength by up to 15%.

The interaction between BF length, content, and the cementitious matrix can further influence the mechanical properties. Shorter fibres are more effective in preventing crack initiation, while longer fibres are beneficial in bridging and controlling the propagation of existing cracks. An optimal balance is required to enhance mechanical properties without adversely affecting the material's density and homogeneity. Moreover, hybridization of fibres is another way to optimize the properties. Usually, a combination of high modulus (or high melting point) and low modulus fibre (or low melting point) fibres is used to achieve a favourable balance between compressive and tensile performance. The optimal combination of fibre types, lengths, and contents can significantly increase both compressive and flexural strengths by providing a balanced reinforcement effect that addresses the weaknesses of each fibre type alone [123]. For

instance, hybridizing basalt fibres with other types of fibres, such as polypropylene, can create a synergistic effect that enhances the mechanical properties of the composite.

Yao et al. [124] incorporated BF up to 0.4% with constant 0.1% of PP and compared it to the performance of individual BF and PP up to 0.4% at an increment of 0.1%. The samples with hybrid fibres exhibited the best performance in terms of mass loss and strength retention up to 800°C which demonstrates the utility of BF-PP hybridization. The spalling was also avoided because of creation of microchannels by melted PP fibres. Su et al. [125] incorporated up to 1.5% (by vol.) of BF-PP in their fibre reinforced rubber concrete. A slower rate of decrease in the relative compressive strength and reduced mass loss was observed in case of concrete reinforced with BF-PP. They identified that a 1% BF (by vol.) and 1.5% PP (by vol.) as most effective in slowing down the loss of compressive strength under elevated temperatures. Koci et al. [126] attempted to study the effect of BF-PP against spalling and overall material behaviour under thermal stress on their reactive powder concrete. They suggested that BF help maintain the structural integrity while PP fibres help mitigate the spalling phenomenon even in concrete with very high strength. Therefore, careful selection of fibre properties can yield a composite not only with good mechanical properties at ambient temperature but also enhance the residual properties at elevated temperature.

2.4 Research gaps

Significant opportunities exist in terms of utilization of slow reactivity of FA particles and associated reaction kinetics with temperature and lime content. These properties may be used to enhance the thermal stability of the composite. The properties of the developed composite may further be enhanced by homogenization of the mix with the help of steel slag fine aggregates.

The performance of steel slag aggregates as a valid construction material is still under question considering the possibility of volumetric expansion. A long-term investigation studying various mechanical and durability properties of the cementitious composite may help alleviate the concerns. In case of any durability related issues, the suggested stabilizing methods such as carbonation and aging may be attempted.

The literature also indicates the ambiguity regarding the role of BF on the compressive strength of the composite. This thesis may help to bridge the gap by utilizing varying contents of BF in the design mixes. These fibres when combined with PP can help create a spalling free cementitious composite.

Therefore, this thesis attempts to develop a green FRCC with enhanced thermal durability at high and sub-elevated temperatures utilizing hybrid BF-PP with a special focus on the waste valorisation of HVFA and steel slag aggregates. The literature pertaining to the behaviour of HVFA based composites at elevated temperatures are very limited [127–129]. Moreover, in those limited works, the intent of addition of HVFA is restricted to sustainability aspect and not from the standpoint of thermal performance enhancement.

At sub-elevated temperatures, the studies related to ETF of concrete and cementitious composites are scarce in current literature despite being a primary exposure condition of most of the concrete based infrastructure. Furthermore, studies related to combined effect of ETF and aircraft fluids does not exist in current literature. This problem is serious from both economic and safety perspective and therefore requires significant attention.

2.5 Summary

This chapter presents a comprehensive literature review on the use of sustainable materials in construction, with a focus on HVFA, SS aggregates, and BF in green cementitious composites.

It highlights the environmental challenges associated with traditional construction materials and the benefits of incorporating industrial by-products. The review outlines the significant advancements in enhancing mechanical properties and durability while emphasizing the need for further research in optimizing thermal durability at high and sub-elevated temperatures. The identified gaps in knowledge form the basis for the proposed research, aiming to develop a green FRCC that leverages the waste valorisation of HVFA and SS aggregates and explores the thermal performance enhancement potential of these materials.

Chapter 3
Experimental program and methodology

3.1 Introduction

The careful consideration of material properties and testing methods is essential for any research project. As the present study considers distinct combination of SCM, aggregates and fibres, it is important to provide a detailed insight of the chemical composition, or the specifications of the ingredients used. This chapter provides a brief description of the material properties used in this project. Moreover, a detailed procedure of specimen preparation and testing methods has also been provided.

3.2 Material properties

Commercially available Ultratech ordinary Portland cement (grade 53) was used for this study. Fly ash was obtained from the disposal sites of National Thermal Power Corporation, Dadri India. The fly ash was classified as low calcium fly ash as per ASTM-C618 [130]. Class-F fly ash was specifically chosen for its slow reacting property, lower calcium oxide content, improved workability, and sustainability. A high-grade SF was incorporated as a secondary pozzolana to improve the rate of strength development. The specific gravity of cement, FA and SF were 3.14, 2.16 and 2.01 respectively. X-ray fluorescence (XRF) spectroscopy was conducted on the binder materials to obtain the chemical composition which has been shown in Table 3.1 along with the maximum particle diameter.

Fine aggregates in the form of normal river sand and electric arc furnace steel slag (specific gravity: 3.10) passing through 300μm sieve were used. In addition to these dry materials, MasterGlenium Sky 8777 polycarboxylate ether-based superplasticizer (SP) was also used to improve the workability of the mix. These ingredients are further shown in Fig. 3.1.

Table 3.1. Oxide composition and particle size of OPC, FA, SF, RS and SS (% mass)

	SiO_2	Al_2O_3	CaO	MgO	Fe_2O_3	SO_3	Na_2O	K_2O	Max particle size
OPC	19.17	06.98	61.42	02.35	02.98	00.5	00.14	00.46	13.8% retained on 45 µm sieve
FA	59.26	30.33	00.96	--	04.41	--	00.94	01.85	21.4% retained on 45 µm sieve
SF	95.11	00.75	00.45	00.39	00.99	--	00.90	01.01	3.9% retained on 45 µm sieve
RS	67.95	13.07	6.45	--	06.77	--	--	--	100% passing through 300 µm sieve
SS	34.58	8.02	47.03	--	3.91	1.14	--	2.26	100% passing through 300 µm sieve

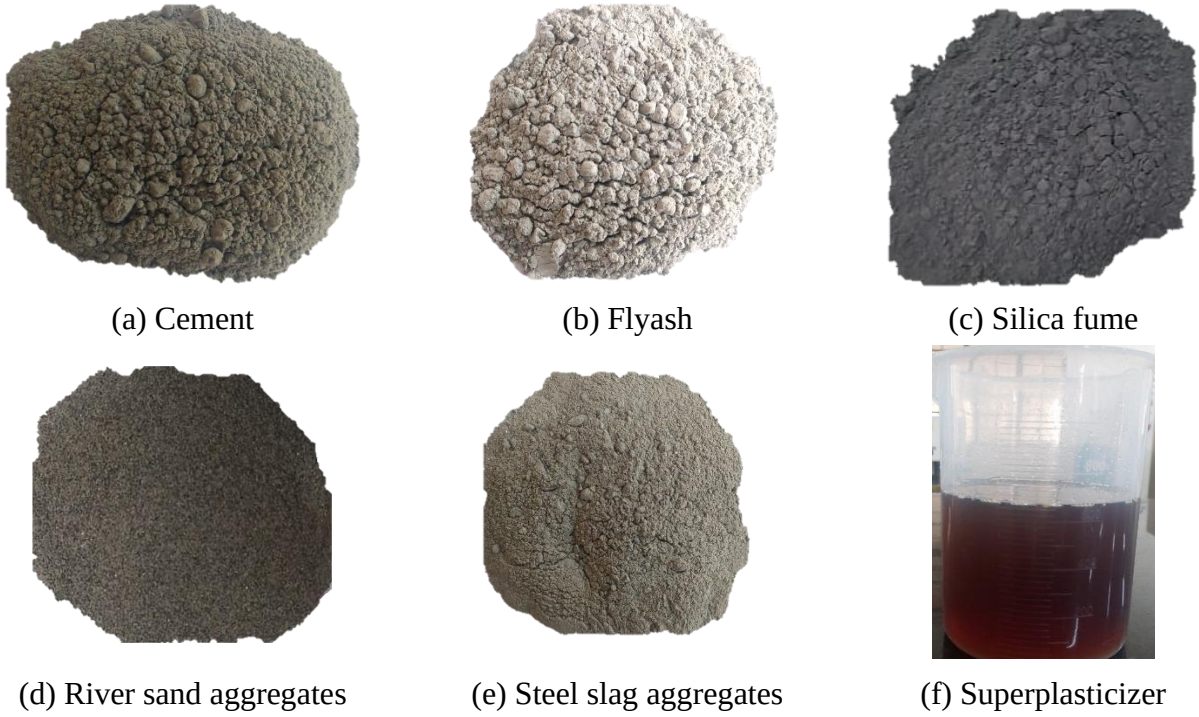

(a) Cement (b) Flyash (c) Silica fume

(d) River sand aggregates (e) Steel slag aggregates (f) Superplasticizer

Fig. 3.1. General mix ingredients used in the present study

This study further utilizes a combination of high melting point BF and low melting PP fibres as shown in Fig. 3.2, and their properties provided by the supplier are specified in Table 3.2. Basalt fibres were used in two different lengths of 12 mm and 18 mm to simultaneously analyse the effect of length of fibre. However, the length of PP fibre was kept constant to 12 mm throughout the study.

Table 3.2. Properties of fibres

Fibre	Specific Gravity	Melting point (°C)	Diameter (μm)	Length (mm)	Coating
Basalt	2.70	1350	17	12 or 18	Silane
Polypropylene	0.91	166	12	12	--

Basalt fibre (12 mm) Basalt fibre (18 mm) PP fibre

Fig. 3.2. Fibres used in the present study

In addition to the above-specified common constituents, several other chemicals were also used for a special study on the effect of aircraft fluid. These include Aeroshell fluid 31, Aeroshell Turbine oil 500 and Air traffic fuel as shown in Fig. 3 which were purchased from Fledge Aero Private. Ltd., Delhi.

(a) Aeroshell fluid 31 (b) Aeroshell turbine engine oil 500 (c) Jet fuel

Fig. 3.3. Aviation fluids used in the present study

3.3 Specimen preparation and curing

The mixing procedure used has been demonstrated pictorially through Fig. 3.4. This procedure was standardized and has been used throughout the project. Firstly, all the dry ingredients were added to the pan and the constituents were mixed for a minute using a variable speed paint mixer. Next, water along with a constant mass of SP was added and mixed for two minutes. Depending upon the flowability and homogeneity of mixture, SP content was further increased, and mixing was continued until requirement of flowable mix was fulfilled. Thereafter, half of the total fibres were added, and the mixing was continued to obtain uniform dispersion of the fibres. This is also done to avoid sudden load on the mixer blades and the motor. Remaining fibres were then added, and the mixing continued for another 3-5 minutes until the same homogenous distribution of fibres achieved.

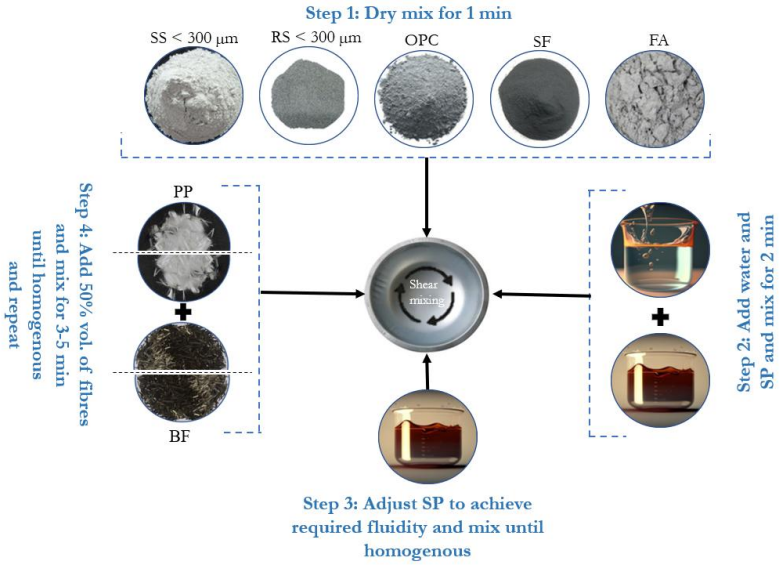

Fig. 3.4. Mixing process for the preparation of FRCC

After ensuring the mix is homogenous, it was poured into different types of moulds depending upon the study. Different types of specimens considered in the project are: cylinder of size 75 mm (diameter) × 150 mm (height), cubes of size 50 ×50 × 50 mm, 160 × 40 × 40 mm and 350 × 40 × 40 prisms and 100 mm (diameter) × 50 mm (height) disks. These moulds were usually demoulded 24-36 hours after casting and were initially water cured for 28 days maintained at

23±1°C. In addition, air curing was also done for another 28 days. The curing duration varied depending on the type of the study. After the completion of curing period, the specimens were either directly tested or were transferred to furnace or environmental chamber for thermal exposure.

3.4 Test methods

The present study included a variety of tests ranging from mechanical properties to durability. A detailed description of the conducted tests and the adopted procedure has been described below.

3.4.1 Flow table test

Flowability test was conducted to ensure all the freshly prepared FRCC mixes have similar flow level and consistency. The test was conducted as per ASTM C1437 [131]. The freshly prepared FRCC mix was poured into the standard cone mould placed on flow table. The mould was filled in two layers of 25 mm each and each layer was tamped 20 times with the help of tamping rod. The mould was then lifted slowly, and the table was given 25 strokes in 15 seconds. In a flow table test, mortar may not spread uniformly across the table. To accurately capture the extent of its spread, measurements were taken in three directions across the spread area and the average values are reported.

Fig. 3.5. Flow table test setup

3.4.2 Mechanical performance tests

Compressive tests were conducted on either cylinder or cubic specimens using a 2000 kN capacity compression testing machine at a loading rate conforming to ASTM C39 [132]. Flexural strength test was conducted on prism specimens of dimensions 160 × 40 × 40 mm (with an effective span of 120 mm) as per ASTM C348-21 [133]. Additionally, larger prisms sized 350 × 40 × 40 mm (effective span 300 mm) were tested for their bending strength at a loading rate of 0.03 kN/s. The setup of both compression and bending tests is shown in Fig. 3.6. These tests were either performed immediately after the end of curing period or were performed at the end of the required thermal exposure as a residual test.

(a) Compression test (b) Flexural test

Fig. 3.6. Mechanical performance tests setup used in the current project

3.4.3 Elevated temperature test

Nabertherm muffle furnace (Fig. 3.7) was used to heat the specimens as required for the study. In general, the specimens were subjected to four target temperatures, 200, 400, 600, 800°C at 1°C/min heating rate and a hold period of 2 hours at respective peak temperature. A heating rate of 1°C/min and a hold duration of 2 hours at respective peak temperature was found sufficient for providing uniform heating inside the muffle furnace after repeated trials. This

was done to ensure the consistency in elevated temperature testing to provide a fair comparison. The samples were allowed to cool without any external interference inside the muffle furnace before further testing.

Fig. 3.7. Furnace used in the project

3.4.4 ETF tests

Part of the project also included exposing specimens to ETF. For this, a programmable environmental chamber (Fig. 3.8) was used to perform continuous temperature cycles.

Fig. 3.8. Environmental chamber used in the project

In general, a normal cycle ranged from 20 to 60°C with a temperature differential of 40°C. The heating rate was set to 1°C/min with a hold period of 2 hours. The selected heating rate and

duration effectively ensured uniform temperature distribution across both the specimen's surface and core. This uniformity was verified through the strategic placement of thermocouples, affixed on the surface of the specimen and inserted to half the depth of the specimen as shown in Fig. 3.9. This was followed by a rapid temperature decrease, inducing thermal shock. Total duration of each cycle was 5 hours and 20 minutes and therefore, each specimen underwent 4 thermal cycles per day. The specimens were tested for compression and flexure after 0, 60, 120, 180, 240 and 300 ETF cycles. All the specimens were tested together to eliminate the effects of maturation.

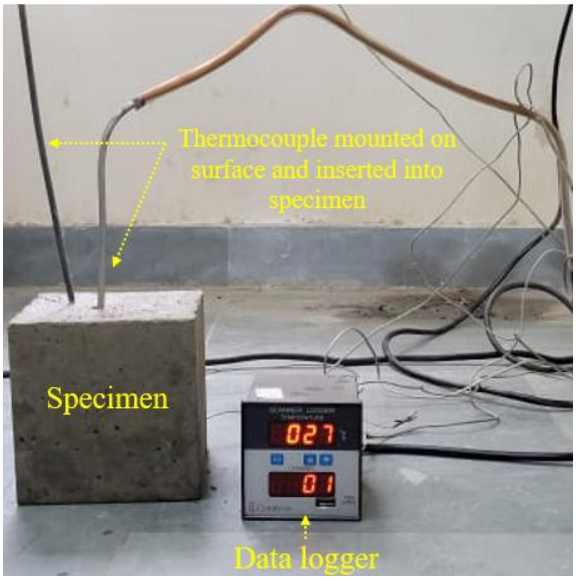

Fig. 3.9. Thermocouple arrangement for determination of temperature across sample cross section

3.4.5 Durability tests

3.4.5.1 Chloride resistance

Rapid chloride penetration test was conducted in accordance with ASTM C1202 [94] to analyse the chloride ion penetration resistance. This approach involves monitoring the electric current flowing through cylindrical concrete disc samples, which have a thickness of 50 mm and a diameter of 100 mm, over a period of 6 hours. A potential difference of 60 V is applied between

the cathode (immersed in a 3% NaCl solution) and the anode (immersed in a 0.3 N NaOH solution).

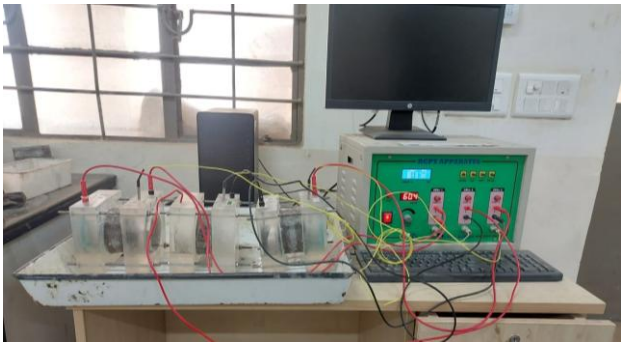

Fig. 3.10. Rapid chloride penetration test apparatus

3.4.5.2 Water absorption test

Water absorption test was conducted to measure the amount of water absorbed by the FRCC specimens as a measure to assess durability. The immersion water absorption test was conducted by first drying the specimen in an oven at 100–110°C for 24 hours to achieve a constant mass. After cooling, the oven-dried mass was recorded to the nearest 0.1g. Then specimen was then submerged in water for 24 hours at room temperature. Once the immersion period was completed, the specimen was removed and surface-dried with a cloth to remove excess water and weighed to obtain the saturated surface-dry mass. The water absorption was calculated as a percentage of the oven-dry mass, based on the difference between the saturated and dry weights.

3.4.6 Microstructural characterization tests

After the mechanical testing, a small sample was also extracted from the core of specimens of each set and stored in acetone for 72 hours to inhibit further hydration reaction. The collected sample was then dried in a desiccator to prevent any contact with moisture. A small part of the dried sample was gold coated and used for the SEM imaging to analyze the microstructure of the composite. Field emission scanning electron microscope (FE-SEM) of FEI make (Apreo

LoVac model) was used for this purpose. The gold coating was done for 120 seconds using a Quorum Tech. sputter coater. MIP analysis was also conducted to determine the pore size distribution of the extracted FRCC samples. A 3-5 mm sized sample was used in MIP under the pressure between 0.10 and 60000 psi and contact angle of 130°, and the volume of intruded mercury was recorded at each applied pressure.

The rest of the collected sample was powdered using a mini ball mill and passed through 70 µm sieve to be used for X-ray diffraction (XRD). The analysis was conducted in a tabletop XRD 600W Rigaku MiniFlex in the range of 10-50° and scan-rate of 0.48°/min. Thermogravimetric analysis (TGA) and differential scanning calorimetry (DSC) analysis was performed either using the Perkin Elmer TGA-4000 machine or with the Netzsch STA 449F5 Jupiter. Approximately 10-50 mg of the sample was weighed and placed in a crucible. The crucible was then heated at a rate of 5-10°C per minute in a nitrogen atmosphere, with the temperature gradually increasing from 35°C up to 800°C.

3.5 Summary

This chapter provides an overview of the material properties and specimen preparation procedures utilized in the current study. Additionally, it presents detailed information on the test setup and the methodology adopted. The subsequent chapters will concentrate on the experimental investigation concerning the development of FRCC with improved fire performance and its durability assessment.

Chapter 4

Utilization of HVFA and hybrid basalt-polypropylene fibres for development of thermally enhanced FRCC

4.1 Introduction

Reducing dependence on OPC is crucial for mitigating greenhouse gas emissions, conserving resources, and minimizing energy requirements in the construction industry. An effective strategy involves incorporating industry by-products as SCMs. While FA is widely accepted due to its availability, its use has been restricted to only lower amount due to slower setting and the inferior early age strength properties. These issues associated with rate of strength development and setting times can be mitigated by ternary blending with SF which acts as nucleation sites for FA reaction and improves the setting and strength properties of the HVFA system as explained previously. Moreover, recent literature suggests that HVFA may offer superior strength retention at elevated temperatures, making it a promising alternative. Another environmental concern is the high carbon emissions from the steel industry, which can potentially be addressed by incorporating sustainable fibres such as basalt.

Therefore, the use of BF and HVFA cementitious composites emerges as a viable solution not only from a sustainability standpoint but also from fire resistance requirements. However, literature pertaining to the behaviour of HVFA based composites at elevated temperatures are very limited [127–129]. Moreover, in those limited works, the intent of addition of HVFA is restricted to sustainability aspect and not from the standpoint of fire performance enhancement. Therefore, the focus of this chapter is novel from the perspective of its approach towards enhancement in properties by utilization of a new combination of matrix and fibres. Additionally, a novel incentive is proposed that prioritizes the fire performance enhancement of HVFA over traditional sustainability measures. The study involves designing mixes with varying HVFA dosages and SF content, examining their compressive strength and mass loss

properties. Furthermore, a systematic analysis of underlying mechanisms at different temperature ranges is conducted through microstructural investigation to understand the improvement or decline in performance.

4.2 Materials and methods

4.2.1 Materials

The materials used for the current study included Ultratech ordinary Portland cement, class F Fly ash, SF, and locally available river sand passing through 300μm sieve. In addition, MasterGlenium Sky 8777 polycarboxylate ether-based SP was used to achieve uniform flowability. Moreover, this study utilizes a combination of high melting point BF and low melting PP fibres.

4.2.2 Mix proportion and sample preparation

In this chapter, a total of 4 mixtures were selected with varying contents of SCMs as shown in Table 4.1. The control mix was cast with approximately 10% replacement of OPC with SF. The next two mixes 50FA and 60FA were ternary blended with incremental FA contents replacing OPC by 50% and 60% by weight respectively at a constant SF content of 10%. The final mix R60FA was cast with 60% FA reducing the SF content to 5% to study the influence of variation of silica fume at a constant FA content. A lower SF content and higher cement content may allow the final mix to have slightly higher CH content that may participate in the pozzolanic reaction at elevated temperature and have a significant impact on the residual compressive performance of the composite. Water-binder ratio (w/b) was kept constant (0.24) in all mixes and SP was varied to ensure that the mixes had similar flow table spreads of approximately 210-220 mm as demonstrated in Fig. 4.1. As can be observed from Table 4.1, the amount of SP required to maintain same workability reduced with an increase in FA content and decrease in SF content. Hybrid combination of basalt and PP fibres were utilized, maintaining a constant total fibre content (2% BF + 0.11% PP) in all the mixes. This was done

to prevent spalling and maintain integrity of specimens at very high temperatures as explained previously.

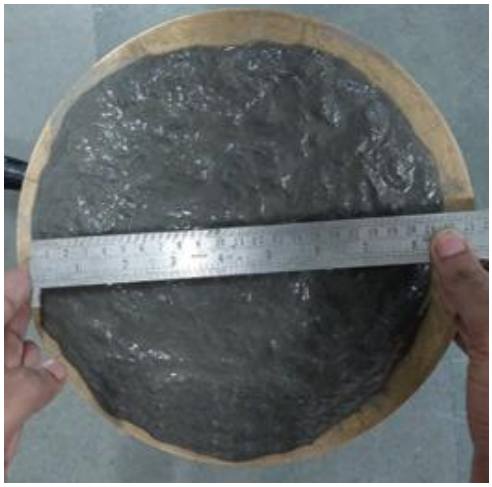

Fig. 4.1. Flow table spread of the control mixture

Table 4.1. Mixture proportions of cementitious composites

Mix ID	*Cement	FA	SF	Sand	w/b	SP (kg/m^3)	BF (%Vol.)	PP (%Vol.)
Control	1289	0	143	573	0.24	8.75	2	0.11
50FA	644.5	644.5	143	573	0.24	6.29	2	0.11
60FA	451	838	143	0.40	0.24	5.47	2	0.11
R60FA	522.5	838	71.5	0.40	0.24	4.87	2	0.11

*Values presented for binders, sand and SP are in kg/m^3

The standard mixing procedure as described previously in Section 3.3 was used. Six cylinders of dimensions 75 mm (diameter) x 150 mm (height) were cast for each mix amounting to a total of 96 specimens. Three of the six cylinders from each batch were used to ascertain the compressive strength of the composite at ambient temperature and the remaining were used for obtaining the residual compressive strength after exposure to elevated temperatures. This was done to establish a control benchmark for each batch of casting and the same data of each batch was used to normalise the results for providing a relative comparison. The cylinders were demolded 36 hours after casting and were initially water cured for 28 days and then air cured for another 28 days to account for the slower reaction time of FA particles.

4.2.3 Test Methods

Cylindrical specimens reserved for ambient temperature testing were tested at the end of 56-days curing period. The specimens reserved for high temperature testing were first weighed before transferring into the furnace. Next, the specimens were subjected to four target temperatures, 200, 400, 600, 800°C at 1°C/min heating rate and a hold period of 2 hours inside a muffle furnace as explained in Section 3.4.3. The samples were allowed to cool inside the furnace and were again weighed before further testing. Compressive tests were then conducted on all the specimens of a single batch using the procedure described in Section 3.4.2. A minimum of three samples were tested per mix, and the average compressive strength has been reported.

After testing for compressive strength, a small sample was also extracted from the core of specimens of each set and stored in acetone for 72 hours to inhibit further hydration reaction. The collected sample was then dried in a desiccator to prevent any contact with moisture. A small part of the dried sample was gold coated and used for the SEM imaging to analyze the microstructure of the composite. The rest of the collected sample was powdered using a mini ball mill and passed through 70 μm sieve to be used for XRD and TG analysis conducted as per the procedure mentioned in Section 3.4.6.

4.3 Results and discussion

4.3.1 Visual appearance and surface characteristics

The surface characteristics of all the mixes has been presented in Fig. 4.2. Cementitious composites normally undergo cracking, surface degradation and colour change when subjected to elevated temperatures. Cracking may occur as a result of the establishment of thermal gradient, rise in pore pressure, drying shrinkage or due to the difference in thermal expansion coefficient of different constituents [134–136].

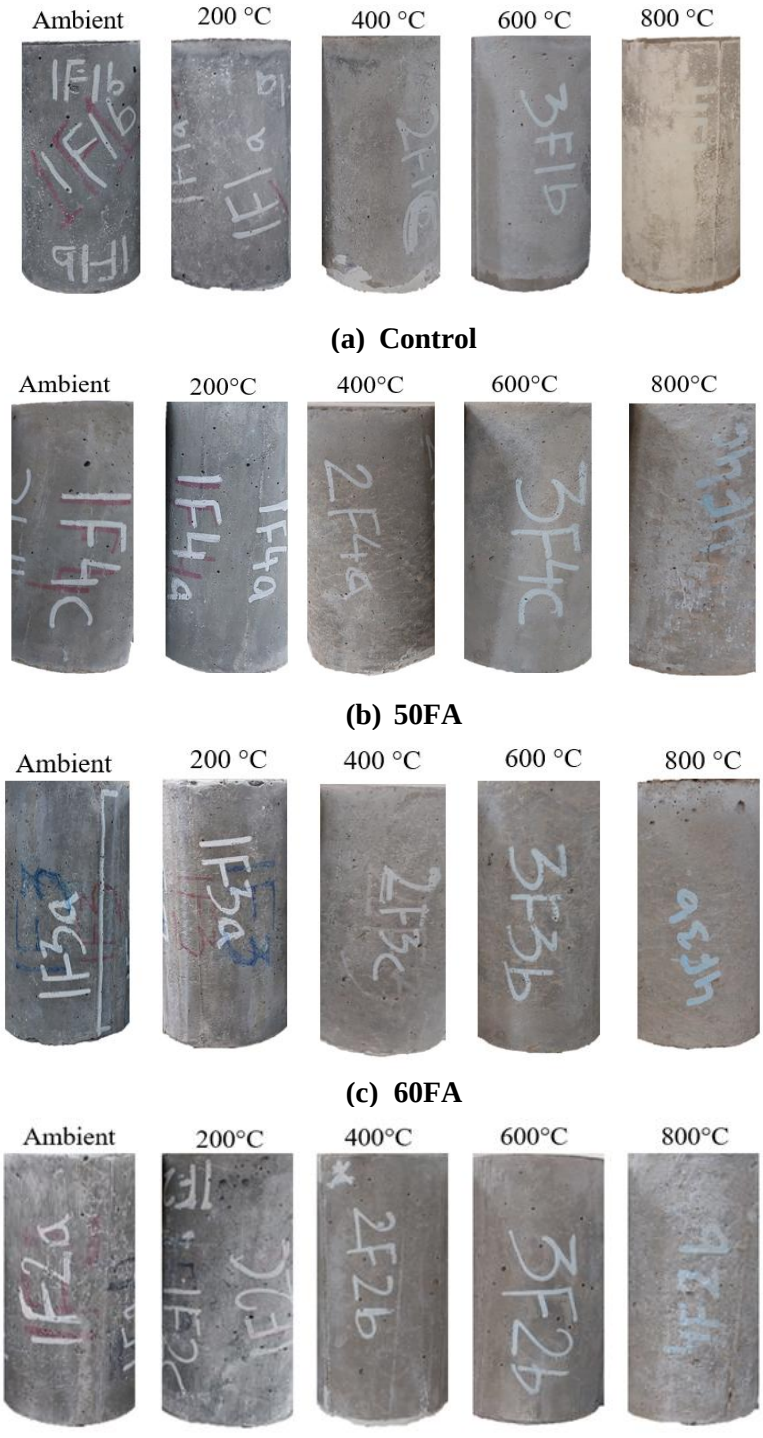

Fig. 4.2. Surface characteristics of the samples at various temperatures

The developed FRCC showed remarkable resistance to surface cracking at all exposure conditions. The absence of larger coarse aggregates and use of natural river fines may have mitigated the cracks originating from differential thermal expansion. Moreover, vacant channels generated due to the melting of PP fibres may have further helped in the dissipation

of pore pressure. Overall, the combination of BF-PP was found to be very effective in crack inhibition and no surface cracks were observed in any of the control mix specimens even at 800°C. Same trend was observed for the mix containing blends of silica fume and HVFA. In general, silica fume increases the chance of spalling and degradation due to thermal exposure [24]. However, this can be mitigated using HVFA as observed in this study. The addition of fly ash leads to the generation of additional hydration compounds on increase in temperature leading to pore refinement and hence, the crack density may have reduced.

In addition to the surface cracking, change in colour can also be an easy indicator of the damage sustained by the composite. In case of control mix, the specimens progressively turned to light grey on increasing the temperature to 200-400°C. At 600°C, the brick red colour started to appear on the specimens. At 800°C, the colour changed to orange-brick red as shown in Fig. 4.2. For HVFA mixes, the specimens were dark grey at ambient temperature and no visible surface cracking was observed. On exposure to 200°C, the colour changed from dark grey to dull grey which further transformed to a much lighter shade of grey at 400°C. Upon further increase in temperature to 600-800°C, the colour of the whole specimen changed to dull brick red. All the HVFA samples demonstrated almost similar surface and colour characteristics irrespective of the content of SF or fly ash.

4.3.2 Mass loss

At various stages of heating, mass loss is caused by release of free, adsorbed, chemically bound water, and decomposition of hydration products. Escape of free water completes at around 120°C [137] and capillary and gel water is released between 150-300°C [138]. Consequently, cement composites exhibit maximum amount of mass loss up to 400°C. This can also be observed from Fig. 4.3 which depicts the mass loss exhibited by all the mixes at different temperature range. As shown in Fig. 4.3, on initial increase in temperature, mass loss increased

to 5.83-6.76% at 200ºC and 10.24-10.78% at 400ºC. Thereafter, the rate of rise in mass loss decreases and only 11.49-12.23% loss in mass was observed at 600ºC.

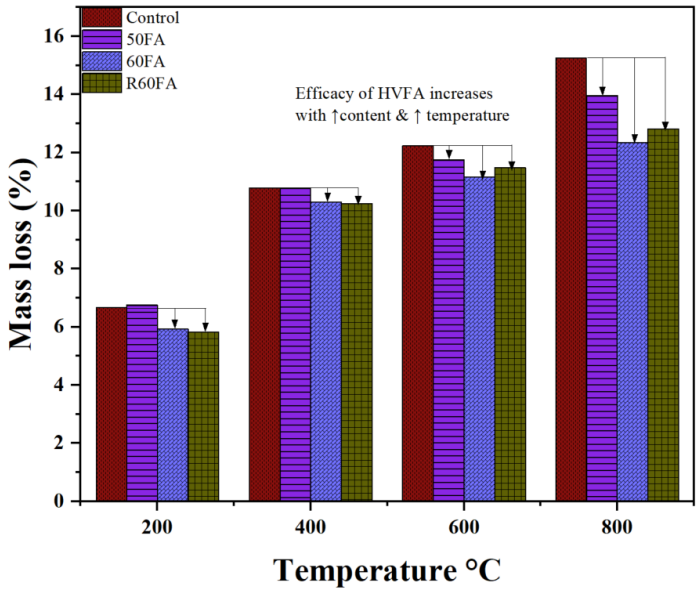

Fig. 4.3. Mass loss reduction owing to HVFA usage in FRCC mixes.

For temperatures greater than 400°C, mass loss is a result of decomposition of products of hydration [139]. Portlandite starts to dehydrate at 400°C and decomposes at 600°C [140]. This is the reason that the specimens of OPC rich control mix containing higher concentrations of portlandite showed higher mass loss at 600°C. On the other hand, pozzolanic reaction from HVFA and lower OPC content ensures relatively lower amounts of CH in the HVFA based mixes resulting in a lower mass loss as shown in Fig. 4.3. Additionally, FA also impedes the dehydration by reacting with CaO to produce more stable tobermorite [141,142] . Mix 60FA contained least cement content and consequently least portlandite of all the mixes and its performance in terms of mass retention at 600°C and 800°C was found to be best of all the mixes in this study followed by R60FA and 50FA. Furthermore, the performance of control mix may have worsened because of higher concentrations of calcite originating from the clinker rich OPC. Loss in mass between 600-800°C is also due to the removal of chemically bound water in the remaining hydration products of cement paste and crystal transformation of quartz [139,141].

Overall, mass loss is directly proportional to the portlandite and calcite available in the system and inversely proportional to the FA replacement percentage. The advantages of utilization of HVFA become increasingly apparent with rising temperatures.

4.3.3 Compressive and residual compressive properties

The average compressive strengths (with standard deviation) of the mixes and their corresponding relative residual strengths have been highlighted in Fig. 4.4. The control mix achieved a high strength 74.5 MPa at ambient temperature, whereas the strengths of HVFA mixes, 50FA, 60FA, and R60FA were found to be 48.7, 47.8, and 52.3 MPa, respectively. A decline in compressive strength was observed in mixes containing high volumes of FA because of the slow reaction of FA particles and limited availability of CH in the mix for continued pozzolanic reaction [143,144]. The presence of SF in the mix may have counteracted this strength loss to some extent due to the filler effect and presence of additional nucleation sites [4,12]. Consequently, the HVFA mixes achieve appreciable compressive strength suitable for structural applications. Also, any further increment in fly ash from 50 to 60% did not have a detrimental effect on the 56-days compressive strength. This further confirms the suitability of HVFA in the design of a greener cementitious composite. It should also be noted the unhydrated FA particles which are found in abundance in HVFA mixes at ambient temperature act as a filler in the composite. These unhydrated FA particles play a much larger role in strength retention at elevated temperature.

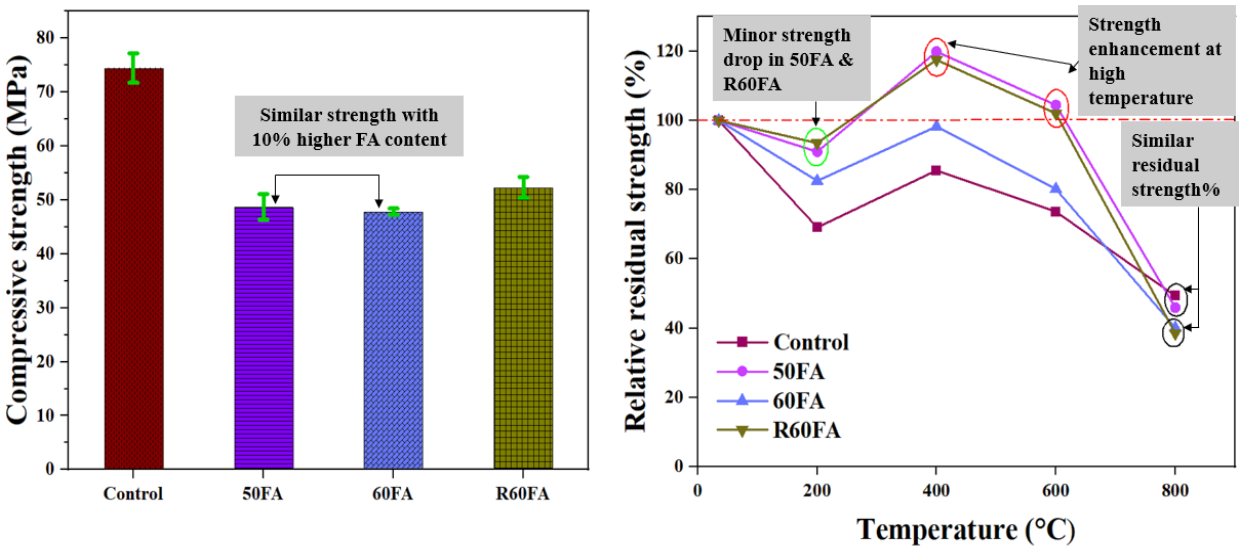

Fig. 4.4. Average compressive strength and relative residual compressive strength of FRCC mixes

As observed from Fig. 4.4, there was an initial decrease in compressive strength with increase in temperature to 200°C. Control mix lost nearly 31% of its compressive strength. However, mix 50FA and R60FA retained 90.97% and 93.46% of their compressive strengths and the least performance among HVFA mixes was observed in 60FA with only 17.47% strength loss. The loss in strength was primarily because of formation of channels inside the composite owing to the melting of PP fibres. The so-called 'disjoining pressures' generated by the swelling of water layers within the cement paste may also be responsible for a decrease in compressive strength [145]. Despite formation of channels and increase in porosity of the cementitious composite, the HVFA mixes retained higher strength because of improved rate of pozzolanic reaction and increased friction among failure planes which is initiated by water evaporation [146].

On exposure to 400°C, all the mixes gained strength as a result of the improved rate of pozzolanic reaction which caused the conversion of portlandite to denser CSH [103,147]. The mixes 50FA and R60FA respectively retained an additional 40% and 37% strength over the control mix. In addition to the improved rate of pozzolanic reaction, the formation of a compound known as tobermorite that is stronger as compared to CSH, may have caused a

sudden rise in the compressive strength at this temperature. The strength of tobermorite is reported to be 200-300% of that of CSH [148,149].

At 600°C the control mix retained the least strength of 73.63% and the mix 60FA retained 80.14%, whereas the residual strengths of both 50FA and R60FA were greater than their respective ambient temperature compressive strengths even at 600°C. The CSH gradually deteriorates with the rising temperature causing some strength loss. This results in reduction in residual strengths of approximately ~104% and ~102% in 50FA and R60FA, respectively. Therefore, both 50FA and R60FA demonstrated a 15% loss in compressive strength at 600°C with respect to the samples exposed to 400°C, yet maintaining a residual strength greater than 100%. On the other hand, significant strength degradation of 26.36% was observed for the control specimens. After exposure to 800°C, a large reduction in relative residual strengths was observed for all mix types as a result of the severe degradation of hydration products and a comparable performance was observed for all mix types. The control exhibited the highest relative residual strength of 49.28% at 800°C. This was followed by 50FA which retained 45.92% of the compressive strength. The mixes 60FA and R60FA performed almost similarly with a strength retention of 40.06% and 38.48%.

In general, the performance of 50FA and R60FA was found to be almost identical at ambient and elevated temperatures, and these mixes demonstrated better elevated temperature than the control mix especially up to 600°C. Therefore, higher replacements of FA may be allowed in case of FRCC for better relative strength retention at high temperatures. The basis of improved performance with HVFA is the slower pozzolanic reaction of FA along with availability of portlandite which converts to CSH at elevated temperatures. In the current scenario, the primary contributor of CH is cement, as low calcium FA was used. In the case of 50FA, a higher amount of CH can be expected because of higher cement content in the mix. A low cement fraction combined with same SF content in 60FA reduces the CH in the matrix.

Contrarily, as SF is reduced in the R60FA, the higher concentrations of available portlandite reacts with unhydrated FA and thereby causes an enhancement in the performance of the mix at elevated temperatures. Based on the analysis of residual strength results, the presence of portlandite was identified as a crucial factor influencing the outcomes. The distinguishing factor among the HVFA mixes was the availability of portlandite within each mix. The mixes 50FA, 60FA and R60FA differ in their respective cement and SF contents which causes a variation in available CH in the mix. Due to this difference in the quantity of CH, there was a consequent variation in the pozzolanic reaction with unreacted FA, leading to differences in the enhancement of strength. Appropriate quantity of portlandite along with unhydrated FA particles play a key role in strength enhancement and retention of the cementitious composites during fire scenarios.

4.3.4 Microstructural observations

The variations in the microstructure with varying content of SCMs at ambient temperature has been shown in Fig. 4.5. A denser microstructure was observed in the control mix as compared to other mixes corroborating the higher strength development in this mix.

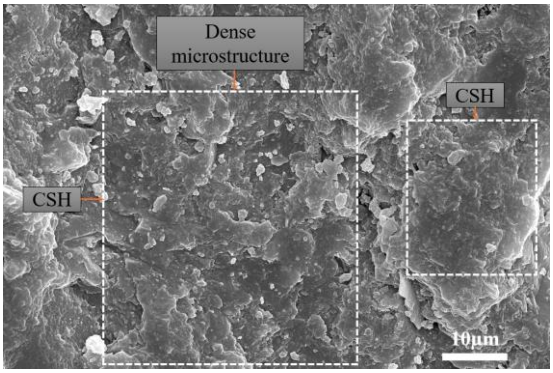

(a)Control

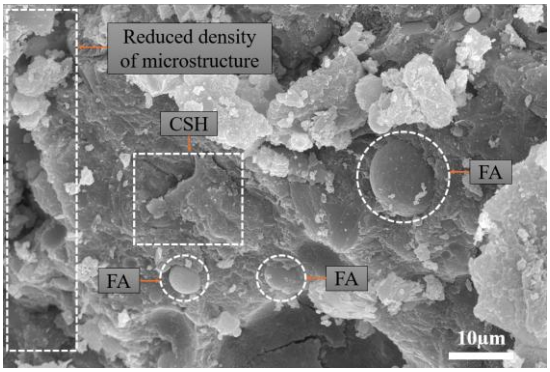

(b)50FA

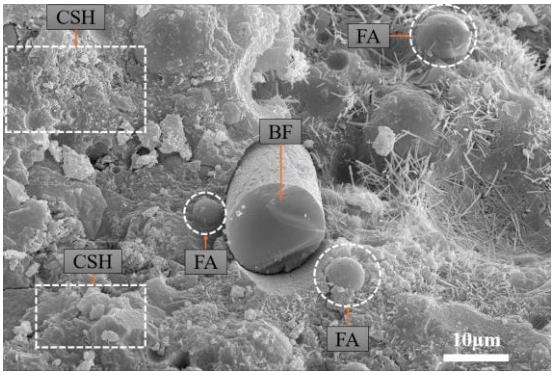

(d)R60FA

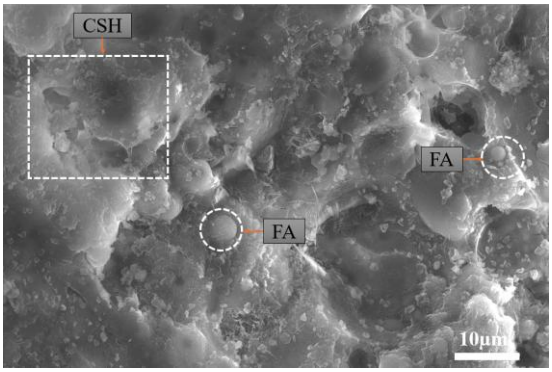

(c)60FA

Fig. 4.5. Morphology of all the mixes at ambient temperature

As can be seen from Fig. 4.5, unhydrated or partially hydrated FA particles were widely spotted in HVFA mixes, suggesting their slow pozzolanic reactivity which makes them available for participation as elevated temperature performance enhancers.

A comparison between the control mix and R60FA has been made in Fig. 4.6 to study the influence of morphology on the elevated temperature performance. At 200°C, both the matrices exhibited slightly higher porosity caused by the melting of PP fibres as can be seen from Fig. 4.6 (a-b) and Fig. 4.7.

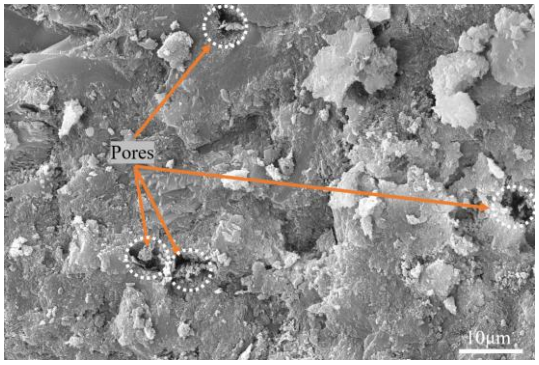

(a) Control - 200°C

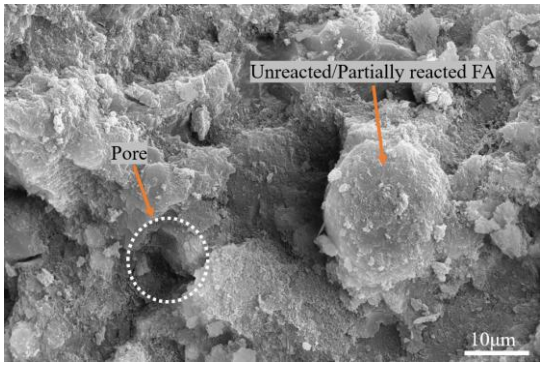

(b) R60FA – 200°C

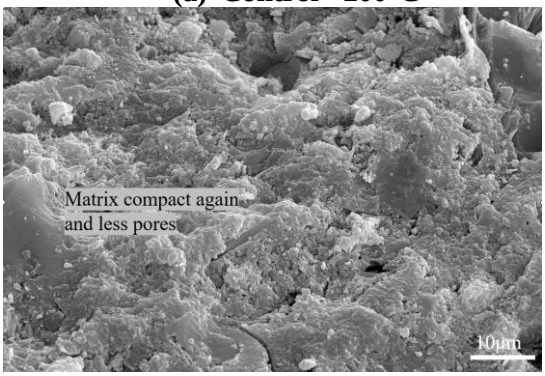

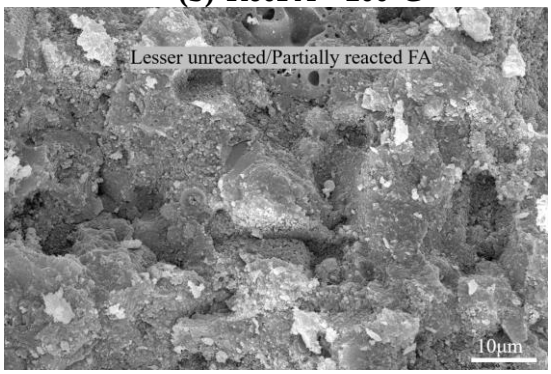

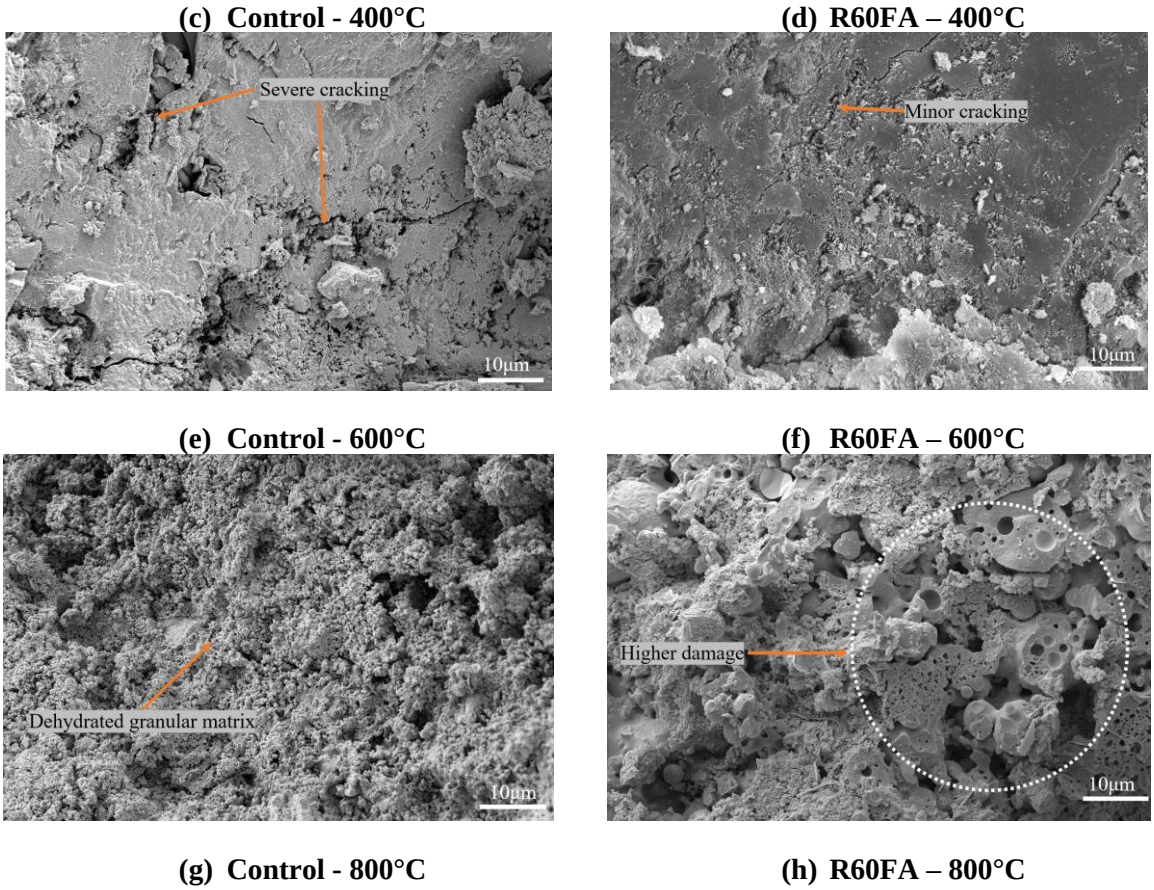

Fig. 4.6. Morphology of control mix and R60FA at various temperatures

The R60FA mix exhibited a strength loss of 6.53% of its strength in contrast to 30.93% in the case of the control mix. This is attributed to the increased hydration and pozzolanic reaction of unhydrated FA particles at high temperature [141]. The SEM imaging of the mix 60FA at various temperatures has been demonstrated in Fig. 4.6a.

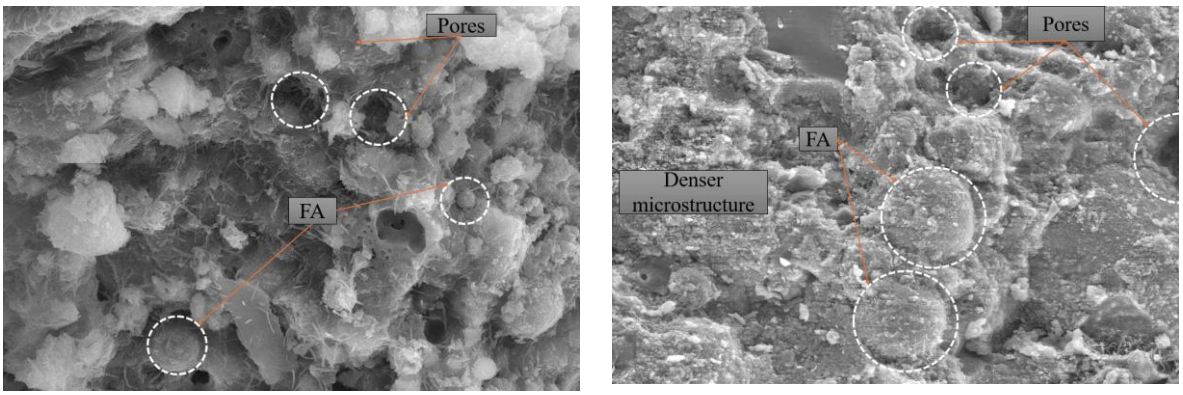

200°C 400°C

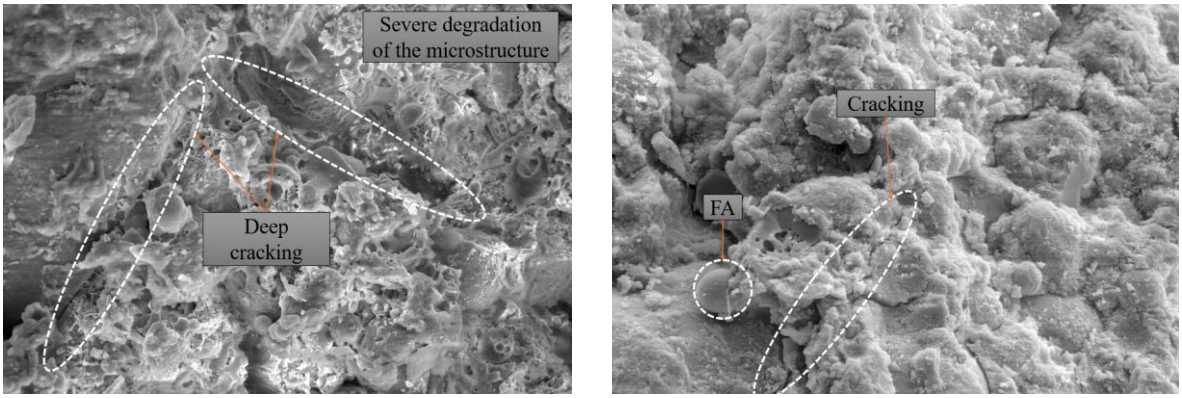

800°C 600°C

Fig. 4.6a. Microstructure of 60FA at various temperatures

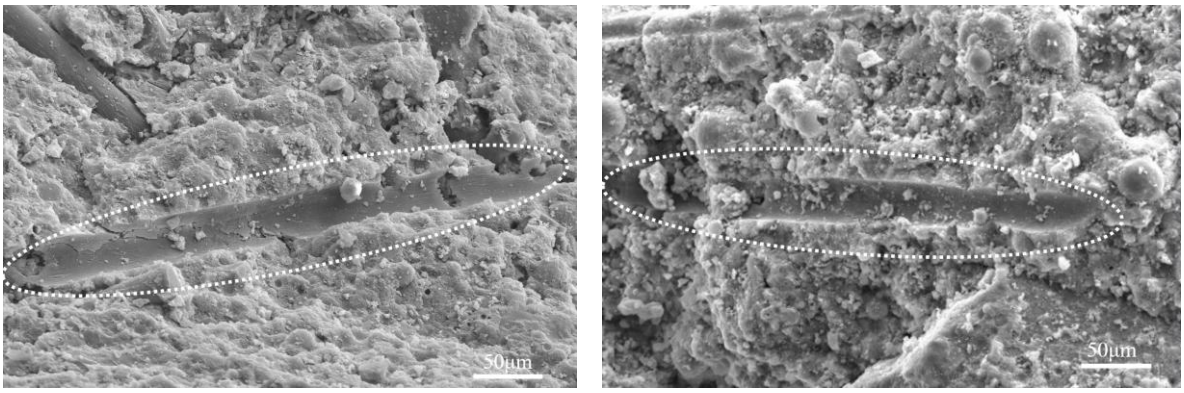

(a) Control **(b) R60FA**

Fig. 4.7. Formation of vapor-escape microchannels in (a) control and (b) R60FA at 200°C

At 400 °C, both the matrices appear to have regained the compactness as evidenced by their improvements in the relative residual compressive strengths. R60FA demonstrated lesser prevalence of unhydrated FA particles suggesting their pozzolanic reaction and their subsequent contribution to strength enhancement. For the same reasons, Sahmaran et al. [141] suggested that the cumulative pore volume > 0.1 µm decreases at 400 °C. In addition, formation of strong and thermally stable tobermorite at 400°C as shown in Fig. 4.8 plays an important role in strength enhancement [150] in comparison to their ambient temperature counterparts. At 600 °C sharp contrast in the crack formation between the control and R60FA mix can be observed. The decrease in thermal conductivity with increasing FA content may have protected the interior of the matrix. At 800°C, severe matrix degradation and cracking caused a steep loss

in strength in both the mixes. CSH phases were found to be disintegrated at this temperature. The loss in strength is attributed to loss of chemically bound water, and disruption of phase boundaries of the hydration products.

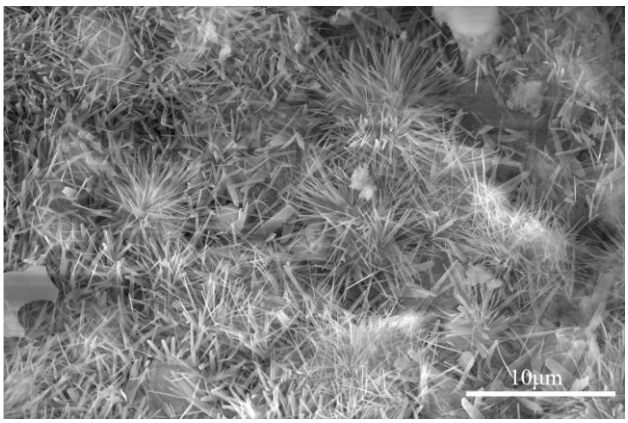

Fig. 4.8. Formation of high strength tobermorite crystals in R60FA at 400°C

In addition to the selection of thermally compatible binder material, a combination of low melting point PP fibres and high melting point BF fibres was also strategically used to enhance the elevated temperature performance. PP fibres played important role in mitigation of the pore pressure and spalling prevention through melting (Fig. 4.7), whereas basalt fibres were helpful in maintaining the integrity of the specimens after the melting of PP fibres. As can be seen from Fig. 4.9, BF remained intact and stable in all the mixes due to their high melting point (1350°C). These fibres maintained the tensile capacity of the matrix at elevated temperatures and ensured remarkable stability against the cracking and surface degradation. Furthermore, the stability of the fibres at elevated temperature is important from compressive strength perspective because of their crack bridging mechanism under load. The study conducted by Yao et al. [124] on mortar with BF-PP fibres demonstrated that minor cracking and spalling from 200°C and deep cracking from 600°C. They also observed the complete disintegration of BF by 800°C. Also, the study conducted by Rashad [4] with unreinforced HVFA demonstrated larger microcracks in the interior of the matrix. Contrarily, the current study has demonstrated

exceptional resistance to surface cracking confirming that the addition of hybrid PP-BF may have positive impact at elevated temperatures if used with suitable matrix constituents.

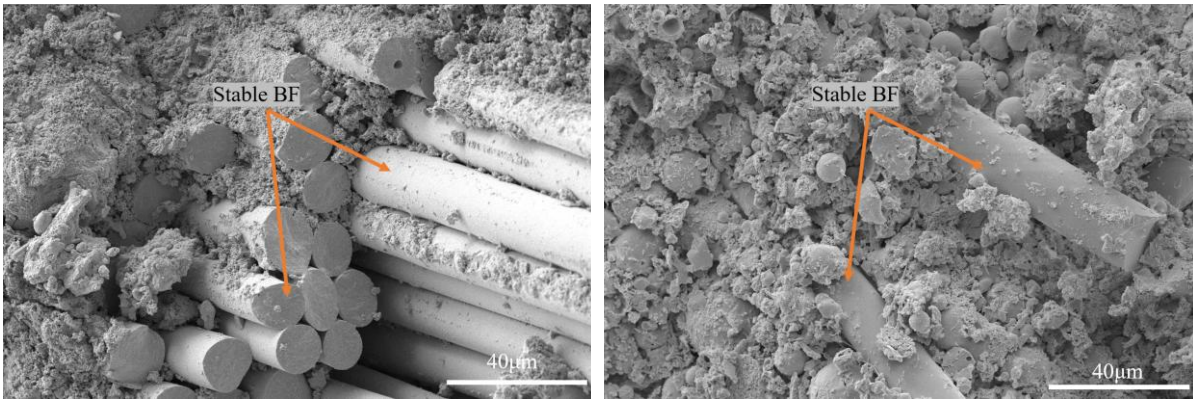

(a) Control **(b) R60FA**

Fig. 4.9. Stable BF in (a) control mix and (b) R60FA after exposure to 800°C

4.3.5 Phase change using X-Ray diffraction analysis

XRD analysis was conducted on samples of control and R60FA to ascertain the transformation of various compounds in the matrix and correlate it to the performance of the composite at elevated temperature. X-Ray diffractograms of control mix and R60FA are presented in Fig. 4.10. The crystalline phases that were detected in control mix were portlandite (P), alite (C_3S), β-C_2S, quartz (Q), calcium carbonate (C), ettringite (E) and semi crystalline CSH. The decomposition of CSH gives rise to alite and β-C_2S and their common peak is represented as CnS [151]. Therefore, variations in their peaks can be used to determine the extent of degradation. The peaks of ettringite were observed only in the samples analysed under normal temperature conditions. However, these peaks disappeared after exposure to higher temperatures, suggesting that ettringite might have undergone decomposition. A minor reduction in peaks of portlandite at 200°C suggests the initiation of elevated temperature hydration. However, the compressive strength of the composite reduced because of the formation of channels from melted PP fibres and the bond weakening caused by the disjoining pressure as discussed before.

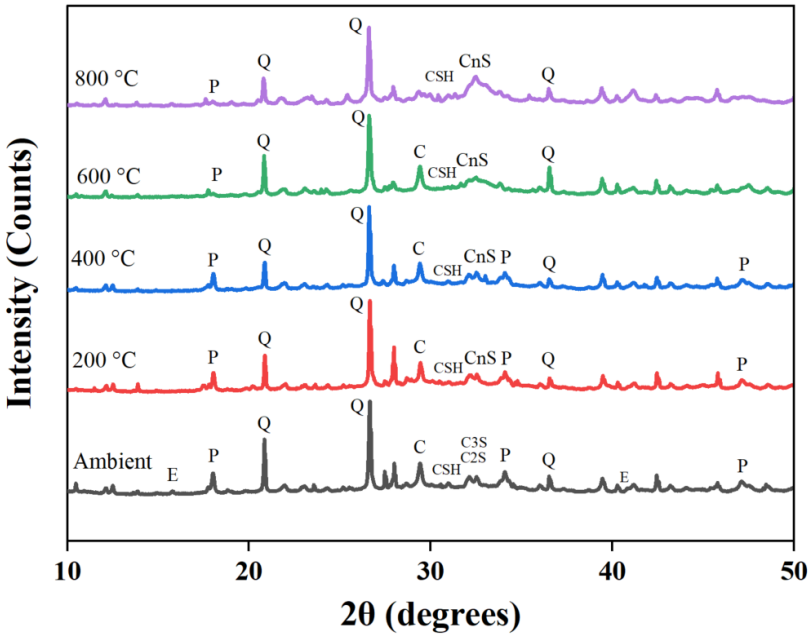

(a) Control

Q-Quartz, C-Calcite, P-Portlandite, CnS-C_3S+ β-C2S, E-Ettringite

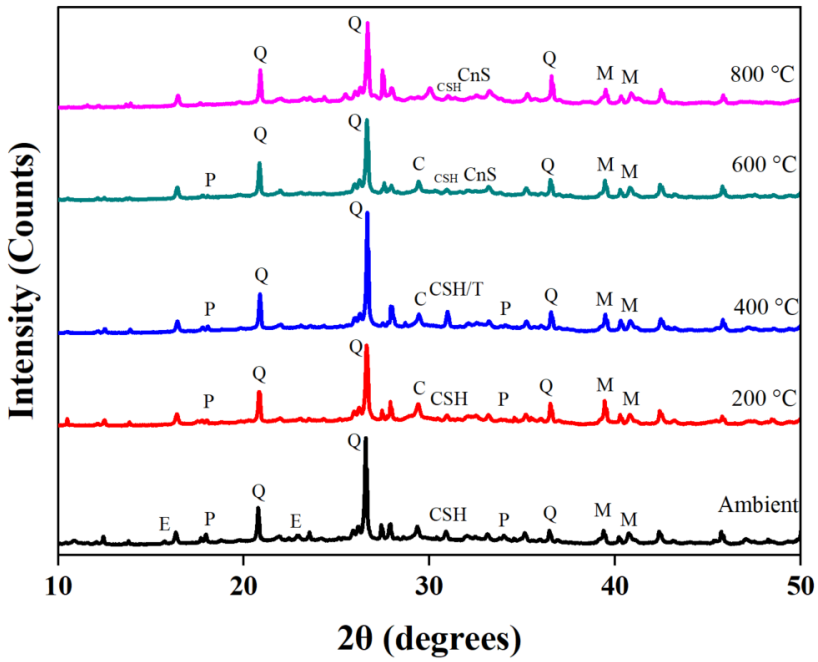

(b) R60FA

Q-Quartz, C-Calcite, T-Tobermorite, P-Portlandite, M-Mullite, CnS-C_3S+ β-C2S, E-Ettringite

Fig. 4.10. X-Ray Diffraction patterns of (a) control mix and (b) R60FA at various temperatures

At 400°C, the highest relative residual strength of ~86% despite the reduction in CSH peak. This is attributed to the increased Van der Waals forces between gel layers caused by evaporation of water [146]. The peaks of portlandite reduced significantly for samples

subjected to 600°C suggesting its decomposition. At 800°C, significant drop in the CSH peak and highest peak of C_nS representing the degradation of CSH was observed which is validated by a drop in compressive strength. Also, peaks of calcite disappeared at 800°C which may also have contributed to both strength and mass loss.

In R60FA, alite (C_3S), β-C_2S, quartz (Q), tobermorite (T), mullite (M), Ettringite (E) and semi crystalline CSH were observed. Similar to the case of the control specimens, the peaks of the ettringite disappeared as a result of exposure to elevated temperature in the R60FA as well. The pozzolanic reaction from HVFA and lower cement content reduced the amount of available portlandite and therefore some peaks disappeared, and others were observed to be relatively shorter. Peak of semi-crystalline CSH diminished at 200°C which may also have resulted in a minor drop in strength. At 400°C, the pozzolanic reaction and hydration is accelerated, as evidenced by the increase in CSH peak. The peak associated with strong and thermally stable tobermorite appeared and contributed to highest relative residual compressive strength of 117.47% at this exposure condition. The peak for tobermorite disappeared at 600°C and the composite maintained a relative residual compressive strength of over 100%. At 800°C, the height of the CSH peak reduced significantly that resulted in a strength retention of approximately 40%. The performance of the mix 50FA was found to be almost identical to the R60FA and therefore similar findings can be expected.

Delayed cement hydration, large reductions in CH at appropriate temperature and formation of tobermorite form the basis of improved performance of HVFA composites. These reactions must be properly utilized to tailor the matrix for enhancement in performance of the composite.

4.3.6 Thermogravimetric analysis

TGA has been utilized to estimate the thermal stability and the extent of degradation of mixes at elevated temperatures and the results from TGA analysis have been shown in Fig. 4.11. The

samples (without fibres) undergo mass loss during TGA because of exit of compounds or their decomposition at high temperatures. Major stages of mass loss are associated to the primary hydration products of cement pastes such as CSH, CH, calcium aluminates and a tertiary product in the form of calcium carbonates.

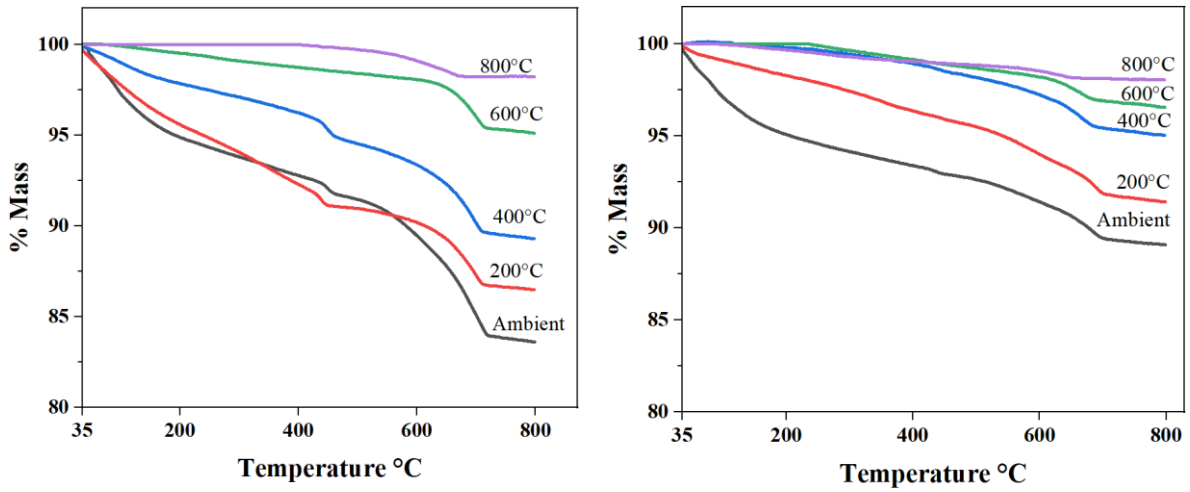

(a) Control **(b) R60FA**

Fig. 4.11. Thermograms of (a) control mix and (b) R60FA after exposure to various temperatures

Dehydration, dehydroxylation of portlandite and decarbonation of calcium carbonate occurs at temperatures between 35-200°C, 450-550°C, 635-750°C respectively [39–41]. Peaks corresponding to decomposition of CSH which happens between 105-120°C [152] and dehydroxylation can be observed from the curves corresponding to ambient, 200°C and 400°C in both control and R60FA whereas decarbonation mechanism can be observed throughout. The cumulative weight loss of control and R60FA respectively at key stages has also been compiled in Table 4.2 demonstrating the superiority of the HVFA mixes. As observed previously, control specimens demonstrated higher mass loss at 400°C and 600°C which further accelerated at 800°C. On the other hand, a smaller mass loss was observed in R60FA samples at elevated temperatures.

This can further be understood through the CH and calcium carbonate content in the matrices of R60FA and control mix as shown in Table 4.3. The availability of portlandite in the matrix

initially may have increased because of increased hydration reaction of unhydrated/partially hydrated cement particles at elevated temperature and then reduces because of its reaction with the available pozzolana or eventual dehydroxylation mechanism.

Table 4.2. Percentage mass loss for temperature-exposed control and R60FA during key stages of TGA

Sample exposed to	Stage						Cumulative mass loss %	
	Dehydration 35-200 °C		Dehydroxylation 450-550 °C		Decarbonation 635-750 °C			
	Control	R60 FA	Control	R60 FA	Control	R60 FA	Control	R60FA
Ambient	5.09	4.63	1.27	0.83	4.51	1.69	10.87	7.15
200°C	4.13	1.58	0.477	1.02	3.01	1.88	7.62	4.48
400°C	2.03	0.21	1.25	0.73	3.18	1.51	6.46	2.45
600°C	0.47	0	0.33	0.44	2.54	1.11	3.34	1.55
800°C	~0	0.33	0.35	0.21	0.46	0.21	0.81	0.75

As discussed before, the concentration of portlandite and calcite in the matrix between the temperatures of 400 and 800°C may play a crucial role in terms of mass retention at elevated temperatures. For samples exposed to 400°C, control mix has 77.30 % higher CH and 120% higher calcite as compared to R60FA. These two compounds decompose between 400 and 800°C and form the major contributors to mass loss. On the whole, the mass loss associated with dehydroxylation and decarbonation mechanism is higher in case of control mix because of its higher availability as evidenced by Table 4.3. The contents of calcium hydroxide and calcium carbonate was calculated based on the method suggested by Dash et al.[39]. Therefore, utilization of calcium rich clinker negatively impacts the elevated temperature performance of the composite.

Table 4.3. Portlandite and calcium carbonate content in control and R60FA mix at various temperatures.

Sample exposed to	Calcium hydroxide (%)		Calcium carbonate (%)	
	Control	R60FA	Control	R60FA
Ambient	5.68	3.66	11.60	4.21
200°C	2.15	4.34	7.62	4.56
400°C	5.39	3.04	7.81	3.55
600°C	1.37	1.83	5.91	2.58
800°C	1.46	0.85	1.06	0.49

4.4 Discussion

The objective of this chapter was to simultaneously improve the sustainability and fire endurance of the cementitious composite. Overall, this has been successful considering the avoidance of spalling and cracking, reduction in mass loss, and higher relative residual strengths. The theories governing the improvement in these properties exist in the current literature and can be utilized for enhanced performance of cementitious composite.

Plain concrete may experience a strength gain when exposed to elevated temperatures [148]. Between the temperatures of 150-350°C, evaporation of water increases strength because of improvement in friction among the failure planes [146,153]. Also, a mechanism called dry hardening is invoked where water evaporation causes increased Van der Waals force that brings the gel layers closer to each other making the microstructure denser and more compact [148]. Furthermore, autoclaving conditions prevail during a fire scenario which promote hydration and consequently an improvement in strength is observed [36,153]. This enhancement is more pronounced in case of matrices containing HVFA because of formation of tobermorite. This compound has higher thermal stability and is stronger than traditional CSH [127]. Furthermore, the reaction coefficients of FA obey Arrhenius law [154] which suggests that rate of reaction of FA particles increases with increasing temperature. The utilization of slow reacting FA in high volumes ensures the presence of unhydrated FA particles in the matrix. These particles whose reactivity is enhanced at elevated temperatures have the potential to further improve the strength of the cementitious composite. Nevertheless, longer setting time and slower rate of strength development is often associated with the use of HVFA in cementitious composites. However, existing literature recommend the doping of SF in HVFA system to address these concerns. SF particles act as additional nucleation sites in the system and promote the rate of reaction and formation of the products of hydration [4]. In addition, they also fill the micro-voids and ITZ properties thus improving the overall properties of the composite. Wei et al.

[155] suggested that SF accelerates the reaction of FA because of its high specific surface area and also readily reacts with Portlandite to form CSH. Therefore, addition of SF is useful from strength and sustainability perspectives.

Utilization of SF doped HVFA system has indirect benefits in the form of reduction in mass loss as well. The SF increases the rate of pozzolanic reaction and thereby accelerates the consumption of CH. After initial dehydration, primary contributors to the mass loss are CH and calcite. As the amount of CH is reduced, a consequent reduction in the mass loss is observed. Also, utilization of low calcium FA reduces the calcite formation as well which further improves the performance of the composite from a mass loss perspective. HVFA-SF may also contribute to post-fire form and strength retention of the composite because large reduction in portlandite by pozzolanic reaction at ambient and elevated temperature. This may avoid the cracking in the microstructure caused by expansion of rehydrated portlandite if it is exposed to post-fire curing at later stages.

Furthermore, the void structure of the HVFA-SF system varies significantly with OPC-SF based system. From Fig. 4.5, it can be observed that the HVFA-SF system is more porous and less dense initially. A porous and less dense microstructure allows effective removal of water and thereby causes less internal cracking [156]. Additionally, as the temperature increases, there is a gradual formation of CSH and hydration compounds, in contrast to the OPC-SF system, which experiences deterioration at higher temperatures. This unique characteristic of the HVFA-SF system allows for delayed CSH and tobermorite formation with increase in temperature while reducing the presence of portlandite and calcite.

In addition, incorporation of HVFA helps retain additional strength because of formation of ceramic bond which can resist higher temperature in comparison to hydraulic bond [157]. Proper utilization of these properties can give rise to a sustainable fire-resistant fibre reinforced

cementitious composite (FR-FRCC). The sustainability was improved by using BF which has demonstrated good utility in holding the matrix together at elevated temperatures and prevented the occurrence of spalling and excessive cracking. All things considered, these elements when used appropriately, have the potential to remedy the problems associated with the sustainability aspect of cementitious composites and significantly improve its fire endurance.

Overall, a composite that is thermal resistant and sustainable can be designed using HVFA-SF and BF. The mechanism of strength improvement has been clearly summarized in Fig. 4.12.

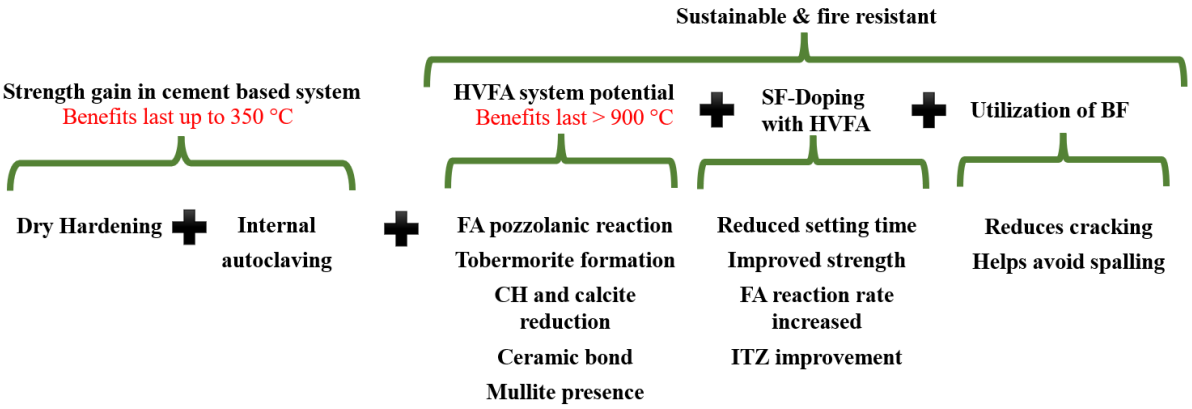

Fig. 4.12. Mechanism of improved fire-performance and sustainability with BF-HVFA system

It must be noted that the change in fibre content will also affect the thermal performance of the composite. In the current study, only one kind of fibre content was used and the thermal performance of HVFA-SF FR-FRCC system under compressive loads was thoroughly investigated. Future works must take into account the variation in fibre content and the tensile, flexure, and toughness behaviour of FRCC must also be evaluated.

4.5 Summary

This chapter focused on the FRCC made with a novel combination of BF-PP HVFA-SF. This combination has been successfully demonstrated to be suitable for manufacturing a sustainable FR-FRCC with potential for ambient and high temperature applications. Based on the detailed experimental investigations, the following conclusions can be summarized.

- Surface cracking was completely avoided in the system suggesting the suitability of the matrix and the hybrid fibre combination at ambient and high temperatures.
- The combination of BF-PP effectively mitigated spalling phenomenon and helped to maintain the structural integrity of the specimen. BF were found to be intact and stable even at 800°C with no surface deterioration and therefore can be considered for high temperature applications.
- Increase in the HVFA dosage reduced the mass loss of the composite. The HVFA system is especially advantageous at higher temperatures because of reduced CH and calcite.
- Increasing the FA from 50 to 60% did not have any detrimental effect on the ambient temperature compressive strength. Both 50FA and 60FA exhibited a similar strength of approximately 48 MPa indicating the positive influence of SF on counteracting the detrimental effect of HVFA inclusions in cementitious composites. Also, reducing the amount of SF by 5% and increasing the cement content in the mix R60FA increased the compressive strength of the composite by 9.4%.
- PP fibres played important role in mitigation of the pore pressure and spalling prevention through melting, whereas basalt fibres were helpful in maintaining the integrity of the specimens. Consequently, the 50FA and R60FA based composites maintained a residual strength greater than 100% up to 600°C.
- The pozzolanic reaction and the consequent formation of tobermorite at 400°C in HVFA mixes proved instrumental in strength enhancement of the composite. Even at 600°C, the mixes 50FA and R60FA demonstrated exceptional strength retention of approximately 104 and 102% respectively. The strength retention at 800°C was also relatively better with approximately 46, 40 and 38% retention for 50FA,60FA and R60FA respectively.

- HVFA and BF can now be viewed as novel sustainable solutions for fire performance enhancement of FRCC.

Chapter 5

Enhancement of the fire performance of developed FRCC with additional utilization of steel slag fine aggregates

5.1 Introduction

Chapter 4 focused on the development of FRCC with enhanced elevated temperature performance. The primary objective was to replace OPC with suitable industry-by products. The study revealed that the mixture containing HVFA, with over 50% replacement of OPC, exhibited outstanding residual performance, retaining more than 100% up to 600°C. Additionally, the combination of BF-PP was effective in maintaining the integrity of the specimens and providing necessary spalling resistance. This confirmed that the synergistic utilization of HVFA, and hybrid BF-PP fibre could serve as a sustainable solution for the fire performance enhancement of FRCC.

In addition to the selection of right SCM, the choice of the aggregate can also play important role in improving the fire performance as well as the sustainability. Traditional construction grade river sand, the main aggregate used in FRCC, is now considered as 'new gold' considering its scarcity and projected exhaustion by 2050 [19]. Sand mining and associated activities are unsustainable as they exploit natural resources and cause irreversible damage to the environment [65,66]. As an alternative, slag generated from the production of steel using electric arc furnace could serve as potentially substitute for river sand aggregates. Researchers have shown the positive impact of utilization of SS in cement and concrete composites in terms of improved sustainability, and fire durability performance [21,22]. The improvement in performance is mainly because of the similar chemical composition of OPC and SS which can mitigate the differential thermal expansion between the aggregate and the paste phase, forming a continuous ITZ. However, the studies on the utilization of SS to improve the fire performance

of FRCC are scarce and further research is required to corroborate the actual effect of SS under thermal exposure. Therefore, considering the opportunities in fire performance enhancements, utilization of HVFA and steel slag fine aggregates in cementitious composite appears to be highly advantageous.

Therefore, this chapter attempts to further enhance the sustainability and fire performance of the previously developed FRCC with a special focus on integration of steel slag fine aggregates as fire performance enhancers. A novel holistic approach of preservation of the composite at elevated temperatures from enhancements in matrix, aggregate, ITZ and spalling protection has been demonstrated. Investigations pertaining to compressive properties, microstructural and phase change analysis have been conducted to assess and demonstrate the effectiveness of this novel approach.

5.2 Materials and methods

5.2.1 Materials

The materials used in this study included OPC, fly ash, silica fume, river sand, steel slag fine aggregates, polycarboxylate-ether based SP, and basalt and polypropylene fibres. The chemical composition of the main ingredients as well as the fibres has been described in Table 3.1 (section 3.2). Fine aggregates in the form of normal river sand and electric arc furnace steel slag passing through 300μm sieve were used.

5.2.2 Mix proportions

Five mixes were selected in the present study to analyse the effect of steel slag fine aggregates and fibre hybridisation as highlighted in Table 5.1. Four variations to the control mix were made in terms of fibre length, fibre content and steel slag (as partial or complete replacement to river sand) with an intent to enhance the fire performance characteristics of composite. The literature suggests that increasing the length of the fibres can have positive impact on the

compressive strength of the composite. Jiang et al. [121] has demonstrated a higher compressive strength by increasing the length of the BF and they attributed it to the stronger bridging effect of the longer fibres. Therefore, hybridization with longer fibres presents potential to enhance the characteristics of the composite and consequently, both 12 and 18mm fibres have been incorporated in the 12BF18 mix. In the third mix, volume of PP has been increased to 0.22% of volume of the composite for more effective pore pressure removal. Construction grade river sand is a scarce resource and therefore needs to be replaced with sustainable alternatives. Initially, 30% of river sand is replaced by SS in the fourth mix to study the ambient and elevated temperature performance. This is in accordance to the findings of Qasrawi et al. [158], that indicated a low sand replacement level of 30% with unprocessed electric arc furnace steel slag can cause an improvement in compressive strength. Thereafter, complete replacement of RS has been carried out for the fifth mix to analyse the effect on fire performance by simultaneously achieving higher sustainability.

Table 5.1. Mix proportions of the composites

Mix	*Cement	FA	SF	RS	SS	w/b	SP	BF (%Vol.)	PP (%Vol.)
Control	522.5	838	71.5	573	0	0.24	4.87	2	0.11
12BF18	522.5	838	71.5	573	0	0.24	6.56	1%12+1%18	0.11
2PP	522.5	838	71.5	573	0	0.24	4.87	2	0.22
30SS	522.5	838	71.5	401	172	0.24	8.75	2	0.11
100SS	522.5	838	71.5	0	573	0.24	14.22	2	0.11

*Values presented for binders, sand and SP are in kg/m^3

5.2.3 Sample preparation

The method of mixing was kept the same as previously explained in Section 3.3. After obtaining the homogenous mix with well dispersed fibres, the mix was poured in cylindrical moulds of size 75mm (diameter) x 150mm (height). A total of 120 cylinders were cast with 6 cylinders for each batch as demonstrated in Table 5.2. Three cylinders to ascertain ambient

temperature strength were cast separately for each batch to ensure that the normalised residual strength at each temperature is accurately assessed.

Table 5.2. Calculation of number of samples per mix (A = Ambient testing, E= Elevated temperature testing)

200°C		400°C		600°C		800°C		Total
A	E	A	E	A	E	A	E	24
3	3	3	3	3	3	3	3	

The hardened cylindrical specimens were demoulded 36 hours post casting and immediately transferred to a water bath maintained at room temperature for 28 days. After 28 days, the specimens were removed from the water bath and cured in air for 28 more days to allow further pozzolanic reaction of FA. The specimens were then considered ready for ambient and high temperature testing.

5.2.4 Test methods

At the end of curing period, uniaxial compression test was conducted on three specimens from each batch as demonstrated in Table 5.2 to determine the ambient temperature compressive strength. The remaining specimens were heated to 200, 400, 600 and 800°C as per the procedure described in Section 3.4.3. After the predetermined period of exposure to elevated temperature, specimens were allowed to naturally cool inside the furnace. Thereafter compressive strength tests were conducted as per the procedure described in section 3.4.2. After testing of cylinders for their compressive strengths, broken fragments of the specimens were collected from its core and stored in acetone for 3 days to stop any further hydration. They were then dried inside a desiccator. A small flat fragment was chosen to study the morphology of the specimen under SEM and the remaining broken fragments was powdered to size finer than 70μm for XRD analysis as described in Section 3.4.6.

5.3 Results and discussion

5.3.1 Surface characteristics

Exposure to elevated temperature generally causes a change in colour and surface cracking in cementitious composites because of multiple factors such as drying shrinkage, temperature differential between layers of concrete, decomposition of the hydration compounds etc. Therefore, change in colour and surface properties can provide a quick assessment on the suitability of constituent materials and the damage to the composite in a fire scenario. In the current study, all the mixes demonstrated a high degree of surface stability, and no cracking was observed even after exposure to 800°C. The surface characteristics of 12BF18 and 100SS are shown in Fig. 5.1 for similarities and comparison. It can be observed that incorporation of SS in HVFA composite did not significantly alter the surface characteristics and colour change. At ambient temperature, the 12BF18 specimens were grey in colour while a lighter shade was observed in case of 100SS. Between 200 and 400°C, both the mixes demonstrated progressively lighter shades of grey. At 600°C, patches of red brown appeared on both mixes, with a higher concentration on 12BF18. The reddish-brown appearance was evenly spread throughout the surface of samples of both the mixes at 800°C. This is attributed to the presence of the iron oxide compound in the binder materials which upon exposure to high temperature, produces pigmentation in the samples.

The variation in colour of these HVFA based mixes varies significantly from the ordinary concrete containing silicious aggregates. The concrete initially turns pink to red in the temperature range of 300-600°C and whitish-grey between 600-900°C [159,160].

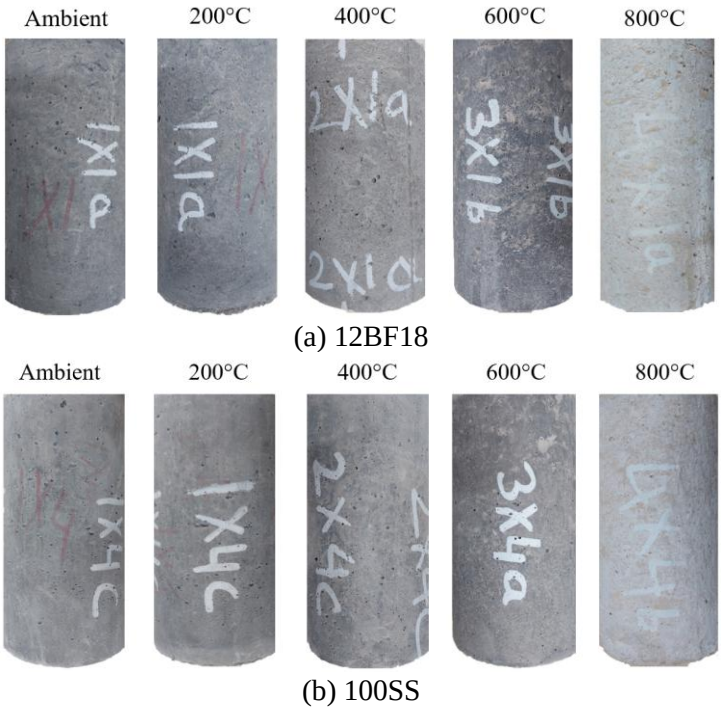

Fig. 5.1. Surface characteristics of (a)12BF18 (b)100SS

All the specimens showed remarkable surface stability despite prolonged duration of exposure. Furthermore, no spalling was observed in any of the mixes suggesting the effectiveness of hybridization of BF-PP under elevated temperature conditions. It should be noted that this improvement also depends on the selection of the right matrix constituents and their compatibility with the fibres. For instance, Yao et al. [124] used 0.4%BF- 0.1% PP hybrid fibre combination in their cement-based mortar which demonstrated surface cracking when the composite is exposed to temperatures beyond 200°C. This suggests that improvement in surface characteristics is only achieved when a matrix and fibre volume (2% and 1% of BF by vol. in current study) are chosen appropriately.

5.3.2 Compressive strength

Average compressive strengths and residual compressive strengths (%) have been plotted in Fig. 5.2. It can be observed that the average compressive strengths of the five mixes lie in the range of ~ 45 to 52 MPa. The variation in length or dosage of BF and PP fibres did not have any significant effect on the compressive strength at ambient temperature. With the

replacement of RS with 30% and 100% of SS, a small decline in compressive strength was observed which can be attributed to the utilization of higher SP content leading to increase the air content in the matrix [161].

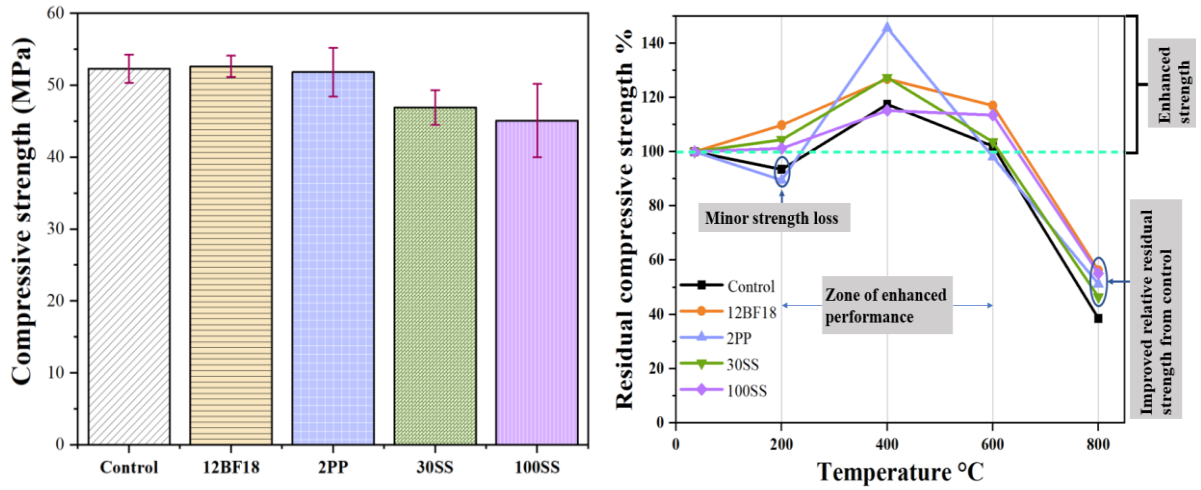

(a) Average compressive strength at ambient temperature

(b) Residual compressive strength after elevated temperature exposure

Fig. 5.2. Variation in compressive strength with temperature

At 200°C, the residual compressive strength of all the mixes (except 2PP and control) underwent a slight increase. This strength increase may have been due to the accelerated pozzolanic reaction of FA particles with available CH to form strength providing CSH [141]. The minor strength loss of ~ 6.5% in control mix is attributed to the creation of vacant conduits from the melting of PP. This is further exacerbated in 2PP mix in which twice the volume of PP has been incorporated which caused a strength loss of 10.5%.

On the other hand, 12BF18 demonstrated an improvement in retained strength, owing to the usage of BF of different lengths along with increased rate of pozzolanic reaction. The longer BF allows better fibre-bridging and stress transfer [162,163]. In case of 30SS and 100SS, the improvement in strength is attributed to the improvement in bonding caused by the partial hydration reaction on SS fine aggregate surface and surrounding paste phase at elevated

temperature which has been demonstrated in section 5.3.3.2. Similar observations on the ITZ of SS aggregates were made by Jing et al. [164].

When exposed to 400°C, all the mixes demonstrated their peak performance in terms of strength enhancement. This enhanced performance may have been possibly due to the autoclaving condition and the dry hardening leading to increased Van Der Waals force [36,148,153]. Furthermore, formation of tobermorite at this temperature may also contribute to increase in the strength of the composite as demonstrated in section 5.3.3.1. Also, the residual compressive strength % of the mix 2PP was found to be the highest at this exposure level. This may be attributed to the better removal of water vapour due to their melting and avoidance of associated microcracking at the early stages of heating. For 30SS, the elevated temperature may accelerate the reaction of unreacted FA and SS aggregates that strengthens the matrix and the bonding between aggregate and paste phase [164]. Consequently, a stronger and consistent ITZ that provides better mechanical properties were achieved. Further investigations on ITZ properties and analysis have been discussed in section 5.3.3.2. The mix 30SS exhibited slightly better performance as compared to 100SS at this temperature. A higher SP content in 100SS may have increased the air content causing a strength reduction in the mix. At 600°C, similar relative residual compressive strength was demonstrated by 12BF18 and 100SS followed by 30SS and 2PP. A higher strength retention of 100SS as compared to 30SS can be explained by improved bond performance between SS aggregate and paste phase of cementitious composite. When exposed to 800°C, rapid deterioration to hydration compounds caused a decline in strength in all the mixes. Both 12BF18 and 100SS showed similar relative residual strength at 800°C. The mixes 12BF18, 30SS and 100SS outperformed the control mix at all elevated temperature exposure levels suggesting the suitability of hybrid length BF and sustainable SS.

5.3.3 Microstructural observations

5.3.3.1 Paste phase microstructural observations

The Fig. 5.3 demonstrates a comparison between the microstructural observations of the best performing mixes 12BF18 and 100SS that differ in fibre composition and aggregates. At ambient temperature, the un-reacted/partially reacted FA particles which are spherical in shape [165] can be seen throughout the microstructure. These FA particles act as filler material at ambient temperature and has the potential to enhance the properties of the composite at elevated temperatures.

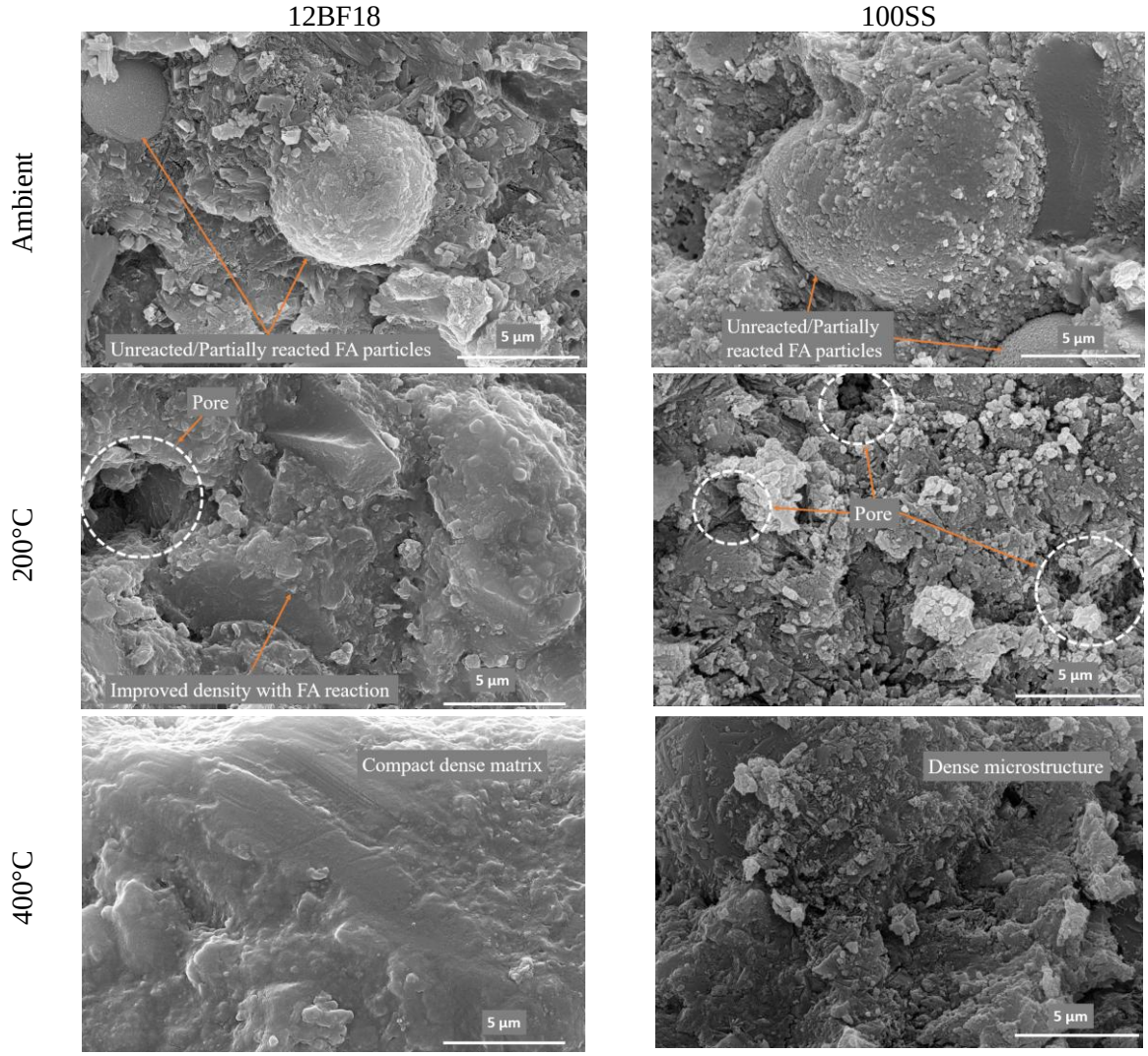

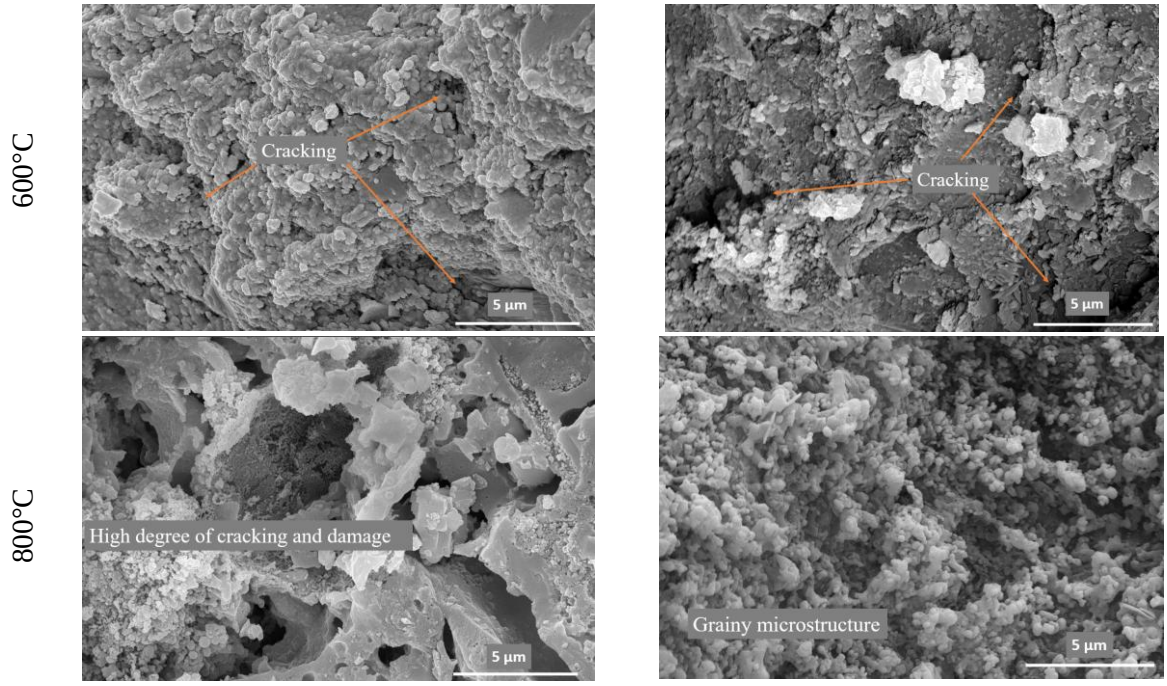

Fig. 5.3. Morphology of 12BF18 and 100SS at various temperatures

At 200°C, the matrix densification is initiated by the accelerated pozzolanic reaction of FA. Consequently, a marginal improvement in strength was observed in all the mixes except control and 2PP. For both 12BF18 and 100SS, the fibre bridging action, the improvement in ITZ and densification caused by improved FA reaction compensated for the loss of strength from increased porosity caused by PP fibre melting as their relative residual compressive strength was found to be 110% and 101% respectively. The matrix densification continued at 400°C and all the mixes demonstrated highly compact microstructure with less porosity as compared to the samples at 200°C. This caused an increase in relative residual compressive strength across all the mixes as shown before.

At 600°C, though a minor reduction in strength (in comparison to the strength at 400°C) was observed for 12BF18, 30SS and 100SS owing to early-stage minor crack formation as highlighted in Fig. 5.3. Nevertheless, these mixes-maintained strength greater than their ambient strength counterparts. This is attributed to the formation of tobermorite as can be seen from Fig. 5.4.

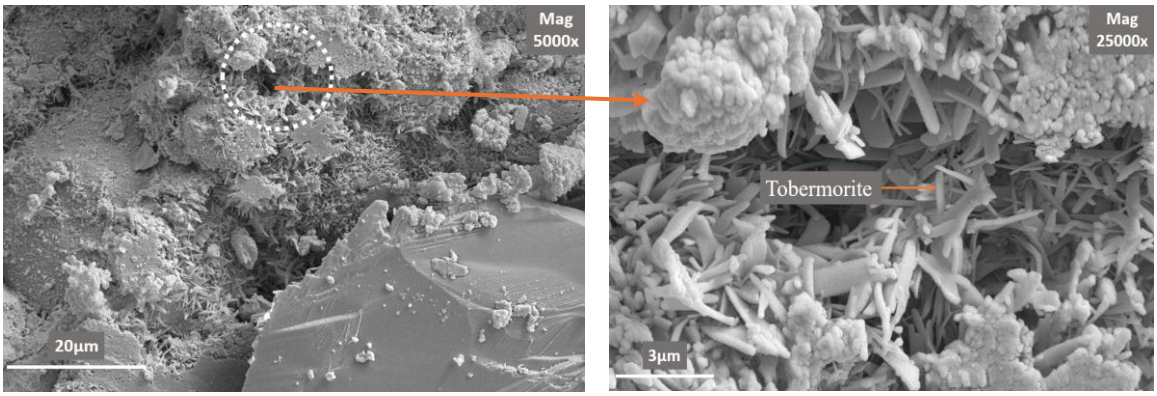

Fig. 5.4. Tobermorite formation in 12BF18 mix

At 800°C, the products of hydration start to decompose causing a drop in strength. Despite exposure to 800°C, the 100SS did not completely dissociate and grainy non-coherent microstructure was seen. In the 12BF18 mix, large cracks and pores were widely spotted. Both the mixes outperformed the control mix with ~17% higher relative residual compressive strength.

5.3.3.2 ITZ microstructural observations

Interfacial transition zone plays a key role in mechanical performance of cementitious composites. During casting, the anhydrous cement grains and sand particles are loosely packed around the aggregate which results in higher porosity and water-cement ratio [36]. As SS aggregates have similar chemical composition to that of cement, significant improvements to this region may be expected. A comparison of ITZ between the RS and SS has been made using SEM imaging as shown in Fig. 5.5.

As can be seen from the Fig. 5.5, the ITZ in 12BF18 mix is clearly porous and discontinuous. On the other hand, the paste phase in the vicinity of SS is continuous and does not demonstrate any major discontinuity.

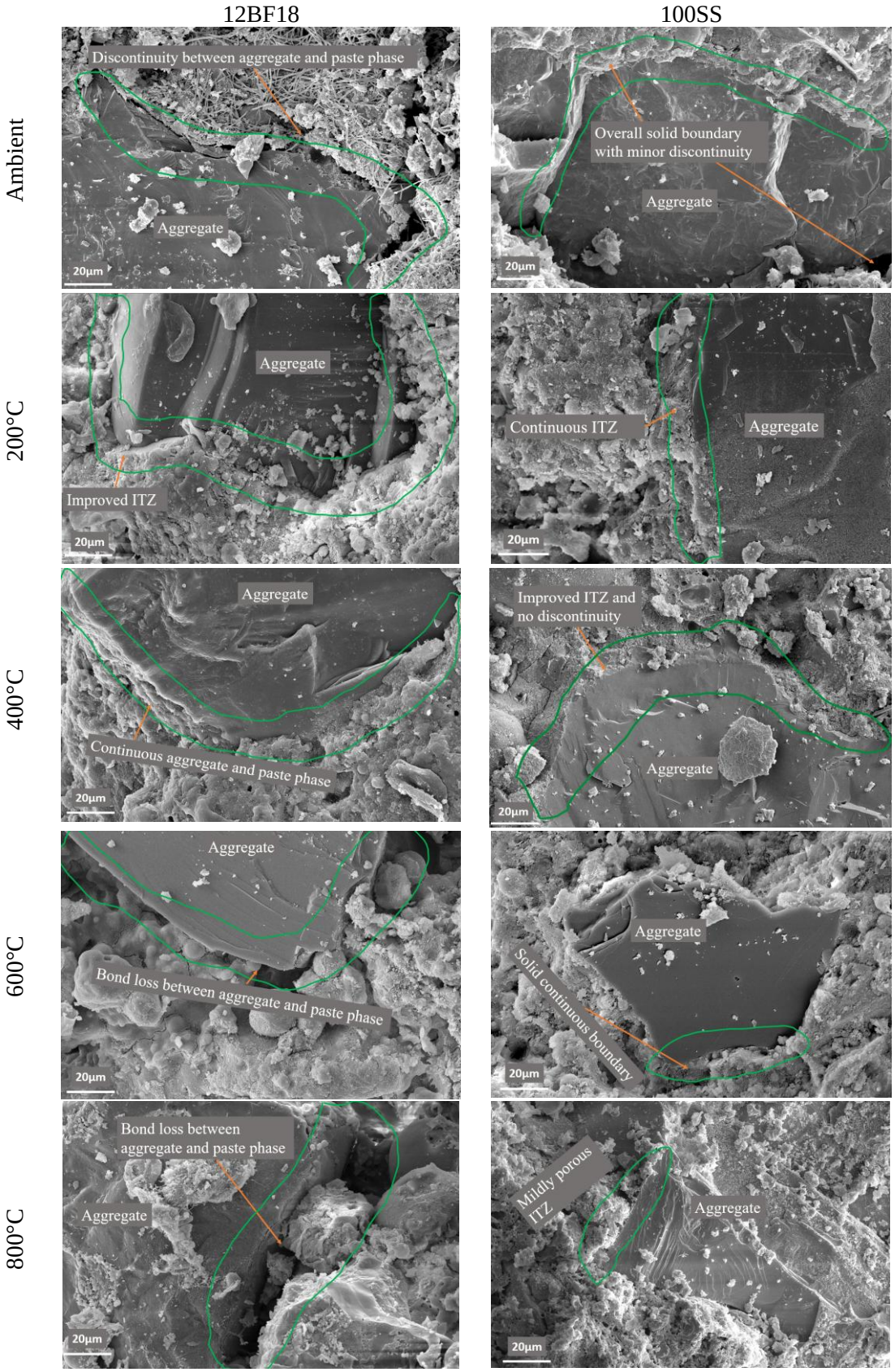

Fig. 5.5. ITZ comparison between 12BF18 and 100SS

The SS aggregates have similar chemical composition to that of cement which avoids the repelling of the cement grains around the aggregates. Furthermore, the sharp corners and honeycombed surface texture of SS aggregates allows it to have strong interlocking capabilities [166]. Furthermore, Arribbas et al. [112] suggested that in case of SS aggregates, the wall effect is reduced because of accessible porosity, surface texture and its chemical composition.

When exposed to 200°C, an improvement is observed in the ITZ surrounding RS as the discontinuity between the aggregate and the paste is reduced. Similar observations were made for the mix 100SS. The temperature of 400°C was found to be crucial for 12BF18 with river sand as it marked the formation of best bond with the paste phase. This is even more pronounced in case of 100SS where aggregate and paste phase appear to have bonded very strongly. At 600°C, a minor drop in strength of ~10% is observed in 12BF18 owing to the weakened ITZ and cracking as shown in Fig. 5.5. On the other hand, the bonding of the SS aggregate with surrounding paste remains unaffected causing only a small reduction in compressive strength. At 800°C, the SS still maintained the bonding, whereas a large gap is visible for traditional RS. This characteristic allows the mixes with SS to improve the strength when exposed to elevated temperature as it maintains a strong bond with the surrounding paste even after exposure to such high temperatures.

This section clearly demonstrates that incorporation of SS aggregates causes an improvement in ITZ properties with increasing temperatures. The improvement is attributed to the enhancement in bonding caused by the partial hydration reaction on SS aggregate surface and surrounding paste phase [164]. This may have been accelerated with the temperature rise forming a stronger bond that stays intact even at 800°C. Consequently, the SS aggregates have demonstrated the properties to be eligible to be a part of TPEs that enhance the performance of the composite with rising temperatures.

5.3.4 X-Ray Diffraction Analysis

XRD analyses was conducted on all the samples to identify the phase changes of the compounds when subjected to various high temperatures. Results of XRD analysis of 12BF18 and 100SS are plotted in Fig. 5.6 for comparison. The compounds that were identified are calcium hydroxide (P), quartz (Q), tobermorite (T), calcium carbonate (C), mullite (M), C_3S, C_2S and β-C_2S. The breakdown of CSH generates C_3S and β-C_2S, and their overlapping peak is denoted as C_nS [151].

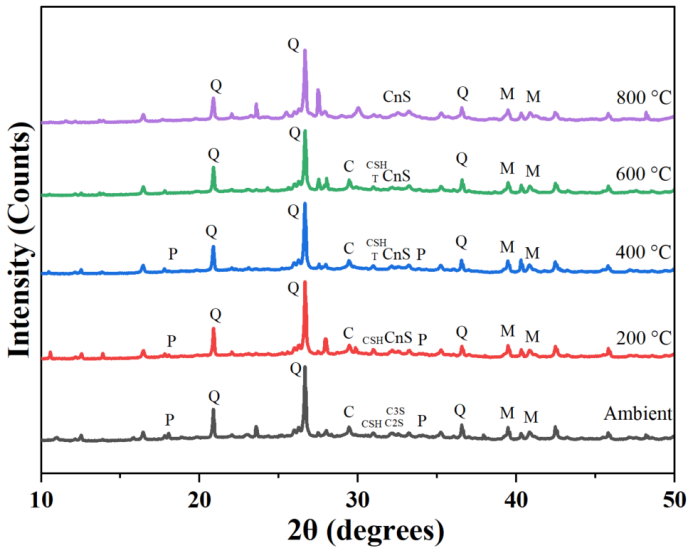

(a) 12BF18

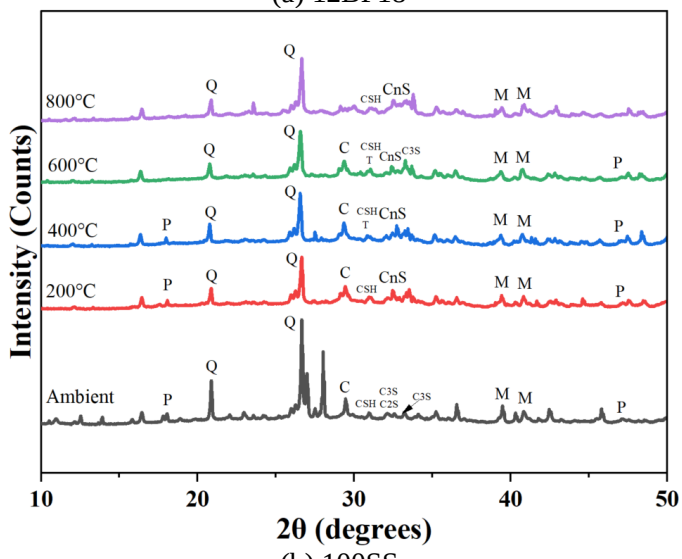

(b) 100SS

Fig. 5.6. XRD analysis of mixes (a) 12BF18 and (b) 100SS at various temperatures

Samples of 12BF18 and 100SS exposed to ambient temperature demonstrate the presence of unhydrated/partially hydrated cement particles as the peak of C_3S and C_2S can be seen from the Fig. 5.6. At 200°C, height of some peaks of portlandite reduced in 12BF18 and 100SS, suggesting the elevated temperature pozzolanic reaction which enhanced their relative residual compressive capacities to 127% and 115%, respectively. Several researchers have demonstrated the formation of tobermorite at 400°C that increases the residual strength of the composite significantly, and dissociates at 600°C. Similar observations can be made for both the mixes under consideration at 400°C. However, the tobermorite was found to be stable even at 600°C (as demonstrated in section 5.3.3.1) that may have contributed to the high relative residual strength of 117% and 113% in 12BF18 and 100SS, respectively.

At 800°C, a rise in C_nS peak was observed which represents degradation of the cementitious composite. Also, the peak of calcite was found to be absent in samples exposed to 800°C. Yet the mixes 12BF18 and 100SS maintained a high relative residual compressive strength of 56% and 55%, respectively.

5.4 Mechanism of SS and HVFA system

Traditionally, concrete has been mixed with fibres of high and low melting points to prevent spalling and help maintain the structural integrity. With advancements in concrete technology, enhancements beyond spalling-prevention must be attempted. The cement-based composites are considered a three phased material containing paste, aggregates and the ITZ. Careful selection and tailoring of materials to enhance these phases can result in desired performance as demonstrated in Fig. 5.7.

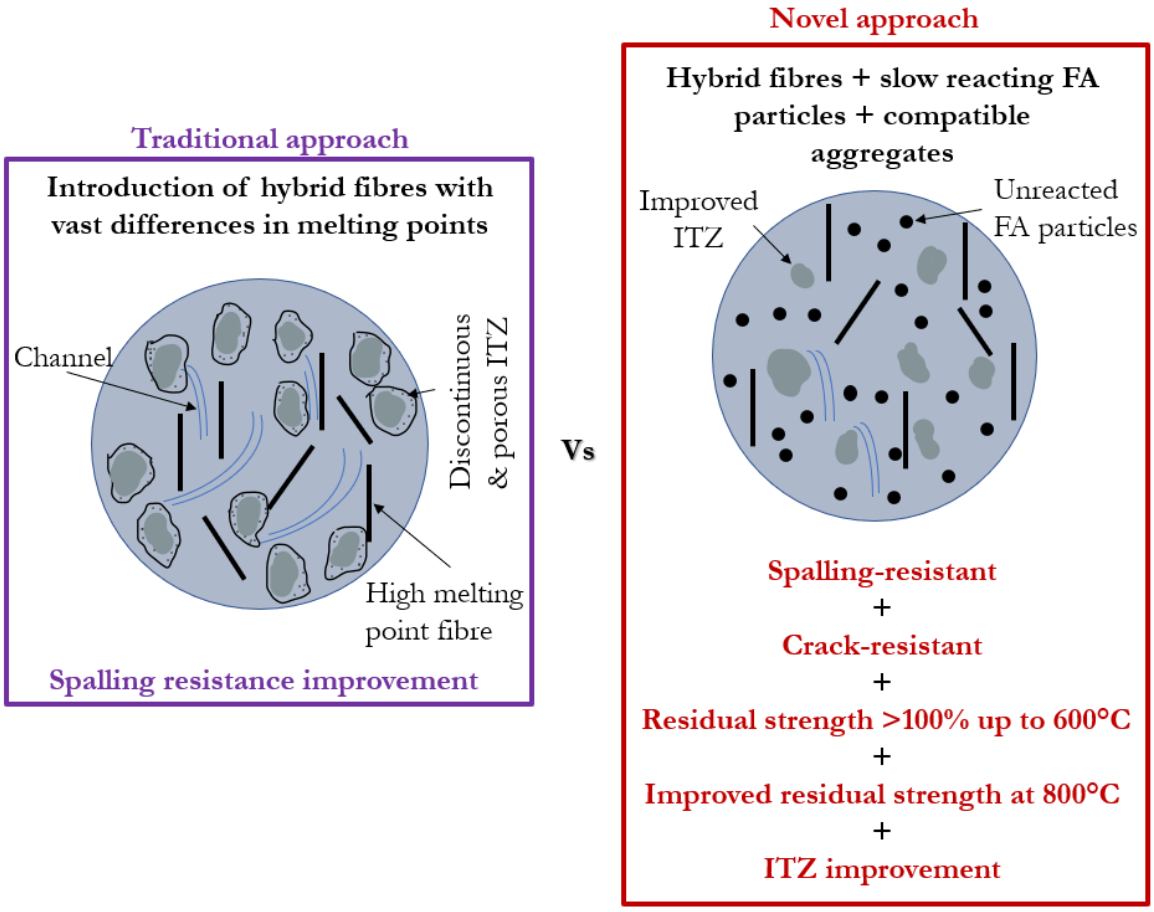

Fig. 5.7. Influence of fire performance enhancers in cementitious composites

In the current study, the compressive strength of the composite continually improved up to 400°C and maintained the compressive strength without loss at 600°C. As per the existing literature, there is an enhancement in properties of the composite between 150-350°C because of the evaporation of water that causes increased friction among failure planes, increased Van der Waals force, and autoclaving conditions [36,148,153]. The unhydrated/unreacted particles in the paste phase can therefore prove to be beneficial for improved thermal performance. The HVFA system incorporates unreacted/partially reacted FA in the hardened state [167]. As the reaction coefficients of FA follow Arrhenius law, their reaction is accelerated at elevated temperature [154]. In addition, researchers have observed the formation of strength providing tobermorite at 400°C, which is 200-300% stronger as compared to CSH [148,149]. The essential precondition for the formation of tobermorite is autoclaving environments where the

amorphous CSH transforms to tobermorite [168]. At high temperatures, the environment is conducive for the formation of strength providing compounds. Consequently, an improvement in the strength of the composite can be expected.

Further enhancements to the composite can be achieved through ITZ refinement. Although it has been demonstrated that incorporation of HVFA improves the ITZ properties at elevated temperatures, a poor bonding between aggregate and cement paste at ambient temperature and at temperatures ≥ 600°C may have a detrimental effect on the residual properties. In addition, incompatible aggregates may cause differential thermal expansion under fire scenario. Utilization of aggregates with similar chemical composition to that of the paste phase containing cement can prove to be beneficial for fire endurance as they can form a strong bond with the surrounding paste. The SS aggregates perfectly fit this requirement as they have similar chemical composition to that of cement, accessible porosity and the presence of hydrophilic silicates and hydrophobic iron oxides reduce the water-binder ratio in the ITZ. Furthermore, the bonding is improved because of the rough surface texture of these aggregates. These aggregates may also participate in the hydration reaction further improving the strength of the composite.

Overall, sustainability of the composite and its thermal performance must be targeted as a multiphase approach with incorporation of suitable constituents. Alterations in paste phase, aggregate, ITZ and usage of greener fibres can result in a green cementitious composite that is also fire resistant.

5.5 Summary

This chapter focused on experimentally investigating the elevated temperature performance of basalt-PP reinforced HVFA based cementitious composite with steel slag aggregates. A series of tests including compressive strength, SEM and XRD analysis were carried out to understand

the behaviour of the composite with increase in temperature. The following conclusion can be drawn based on the test results:

- Utilization of HVFA consistently enhances thermal performance of the composite up to 600°C as a result of the elevated temperature pozzolanic reaction and tobermorite formation.
- Improvements in the properties of the cementitious composite at higher temperatures requires modifications in paste phase, aggregate phase, ITZ and fibres.
- The mix with hybrid length BF demonstrated high relative residual compressive strength of 110, 127, 117, 56% at 200, 400, 600, and 800°C respectively, indicating that the length of the BF is crucial in the residual strength performance.
- Incorporation of steel slag aggregates in addition to being a sustainable solution, was found to be highly beneficial with their unique property of improving the ITZ properties via surface reaction and interlocking behaviour. The residual compressive strength in the mix with 100% SS aggregates was found to be 101%, 115%, 113%, 55% at 200, 400, 600, and 800°C, respectively.

The slow reaction of FA in cement composites have been turned beneficial in this study as they bear potential to react when exposed to high temperature and consequently improve the matrix properties with rising temperatures. Besides, SS aggregates improve the ITZ properties with rising temperatures as they have potential to form hydration compounds to improve the homogeneity of the overall composite. Therefore, it is shown that with the selection of right combination of material, advantages in terms of thermal performance enhancement can be achieved in addition to improved sustainability in the modern construction industry.

Chapter 6

Long term durability performance of the developed eco-friendly FRCC

6.1 Introduction

Chapters 4 and 5 were dedicated to advancing the development of sustainable FRCC with enhanced fire performance. Utilization of HVFA and SF blends as SCM, SS as fine aggregate and hybrid basalt-PP fibre were recommended for achieving superior fire performance. However, use of significant proportions of SCMs with distinct properties raises concerns about the long-term durability of the developed composite. This is mainly important in the mix containing SS as fine aggregates. Existing literature presents contradictory opinion regarding their use. Some researchers have reported significant enhancements in the properties of the ITZ with the use of SS aggregates[169]. A study conducted by Adegoloye et al. [113] suggested that SS can significantly enhance mechanical properties due to its rough texture, higher porosity, and crushed shape, promoting enhanced adhesion with the paste phase. Nevertheless, the literature also cites disadvantages, such as volume instability and reduced durability, which is attributed to the high content of CaO and MgO in these aggregates[23]. Due to these contradictory findings and limited research, further efforts are necessary to ascertain the volume stability of cementitious composites, particularly over an extended period, as incorporation of SS fine aggregates demonstrates great potential to enhance the mechanical properties via enhancements in ITZ.

Furthermore, studies on FRCC with basalt fibres have indicated deterioration in the fibre-matrix interface, as reported by several investigations. For instance, Jiang et al. [121] examined the mechanical and bonding behaviour between BF and the matrix and noted a positive effect of longer BF on mechanical properties owing to the stronger bridging effect and pull-out

resistance. However, deterioration of the bond between fibre and matrix was observed at 28 days. Nevertheless, the available studies are insufficient to draw conclusive statements about this behaviour.

Considering the distinct properties of various components in the developed FRCC, a long-term study on HVFA-SF FRCC is essential since significant changes in microstructure are expected with time which could influence the mechanical and durability performance of FRCC. Moreover, it is also clear that detailed investigation into the bond evolution between BF and the matrix over an extended period is needed for the acceptance and practical implementation of the new FRCC. Therefore, this chapter focuses on the analysis of long-term mechanical (compressive and flexure) and durability performance (chloride ion penetration resistance, water absorption, and volume stability) of the developed FRCC. Age-related ITZ modification of RS and SS fine aggregates has also been investigated.

6.2 Materials and Methods

6.2.1 Materials

OPC, FA, and SF were the chosen binders for this study. Moreover, both RS and SS passing through 300 µm sieve were selected as fine aggregate to compare the durability performance. Hybrid combination of fibres in the form of BF-PP was also incorporated similar to the previous chapters. Additionally, polycarboxylate ether-based SP was used to adjust the fluidity of the mixture.

6.2.2 Mix proportions

A total of five FRCC mixes were designed, as shown in Table 6.1, to ascertain the influence of SS aggregates and fibre composition. The binder content was kept constant in all the mixes and variations in aggregates, fibre length and content were carried out. The control mix contained 2% BF and 0.11% PP fibres and 100% RS. The mix HL-BF with hybrid length BF was used

to ascertain the influence of BF length on flexural properties of the composite. As research suggests contradictory views on the influence of BF content on compressive strength, the effect of variation in its dosage was analysed through mix 1V-BF. Moreover, to assess the suitability of steel slag aggregates, 30% and 100% of RS (by wt.%) was replaced by SS fine aggregates in the mix P-SS and F-SS respectively.

Table 6.1. Mix proportions of the fibre reinforced cementitious composites

Mix ID	***Cement**	**FA**	**SF**	**RS**	**SS**	**w/b**	**SP**	**BF (#%Vol.)**	**PP (%Vol.)**
Control	522.5	838	71.5	573	0	0.24	4.87	2	0.11
HL-BF	522.5	838	71.5	573	0	0.24	6.56	**1%12+1%18**	0.11
1V-BF	522.5	838	71.5	573	0	0.24	03.50	**1**	0.11
P-SS	522.5	838	71.5	401	172	0.24	8.75	2	0.11
F-SS	522.5	838	71.5	0	573	0.24	14.22	2	0.11
*Values presented for binders, fine aggregate and SP are in kg/m^3									
HL-BF- Hybrid length BF, 1V-BF-1% Vol. of BF, P-SS- Partial replacement (30%) with steel slag, F-SS- Full replacement (100%) with steel slag									

6.2.3 Sample preparation

Mixing procedure specified in section 3.3 was followed to achieve a flowable mix with uniform distribution of fibres. The homogenous mix was then cast into cubical moulds of size 50 mm for compressive strength and water absorption tests, 160 × 40 × 40 mm prism for 3-point bending tests and cylinders of 100 mm (diameter) × 50 mm (height) for the determination of resistance to chloride penetration. The samples were demoulded after 36 hours and immediately transferred into a water-bath maintained at room temperature. After 28 days of water curing, samples for 360 day testing were separated and maintained at 25 ± 2 °C and 35 ± 2 % relative humidity. These conditions represent the average temperature and humidity of the study region (Pilani, India). Four cubes each for compressive strength and water absorption, 3 numbers of prisms and cylinders for flexural strength and chloride-ion penetration resistance tests, respectively, were cast for each mix.

6.2.4 Testing methods

Compressive strength tests on cubes and flexural strength test on prisms were conducted as per the procedure mentioned in section 3.4.2, respectively. Additionally, the chloride ion penetration resistance test and water absorption test were carried out in accordance with the procedure detailed in the section 3.4.5. After conducting these tests, SEM analysis was undertaken on fractured fragments collected from the core of specimens. This analysis aimed to discern morphological variations that may underlie the observed outcomes in the compressive strength, water absorption, and chloride ion penetration resistance tests.

6.3 Results

6.3.1 Compressive strength

The variation in compressive strengths for all the mixes has been demonstrated in Fig. 6.1. The incorporation of SF in the mix to ameliorate slow strength gain was found to be successful as strength > 35MPa was achieved in all the mixes within 28 days. All the mixes showed an improvement in strength with age in the range of ~17.63-42.21% at 360 days as compared to 28 days. Improvement in compressive strength over time suggests that the individual ingredients do not adversely affect the compressive performance over time. Individual effect of fibres and aggregates was studied, and observations has been discussed below.

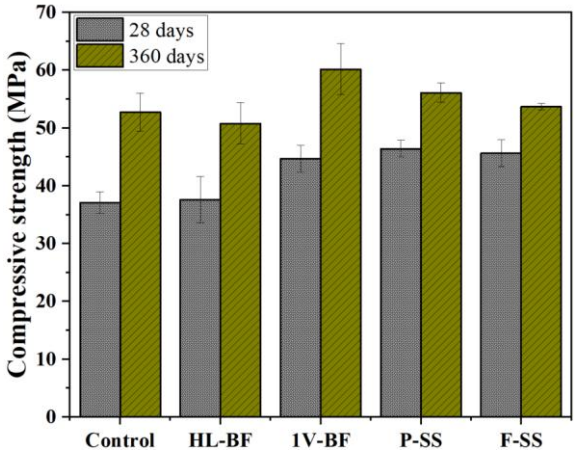

Fig. 6.1. Compressive strength of the FRCC mixes

6.3.1.1 Effect of fibres on compressive strength at 360 days

Incorporation of hybrid length BF in the matrix yielded compressive strength similar to that of the control mix at 28 and 360 days. On the other hand, BF content was found to have a significant impact on the compressive strength of the composite. With 1% of BF in the mix, enhancements of ~20.48% and 14.10% in compressive strength with respect to the control mix (containing higher BF content) at 28 and 360 days respectively. A higher BF content increases voids in the system which results in compressive strength reduction. This has been demonstrated in the microstructure section 6.4.1.

6.3.1.2 Effect of steel slag aggregates on compressive strength at 360 days

Replacement of 30% natural RS by SS aggregates was found to have a positive impact on compressive strength with an increase of 25.15% and 6.38% respectively at 28 and 360 days with respect to control mix. This is attributed to the improved ITZ properties and better interlocking of steel slag fine aggregates with the surrounding paste as demonstrated in section 6.4.1. The mix F-SS demonstrated an increase in strength of ~23.04% and ~1.78% over control mix at 28 and 360 days respectively. Therefore, it can be inferred that SS aggregates have great potential to be a suitable candidate for the replacement of construction grade RS, while improving the sustainability aspect of the composite.

6.3.2 Flexural strength

The observations of flexural strength with variations in fibre and aggregates is pictorially demonstrated in Fig. 6.2. The BF content and the type of the fine aggregates were found to have significant influence over the flexural strength properties of the composite. The effect of individual parameters on flexural strength is discussed below.

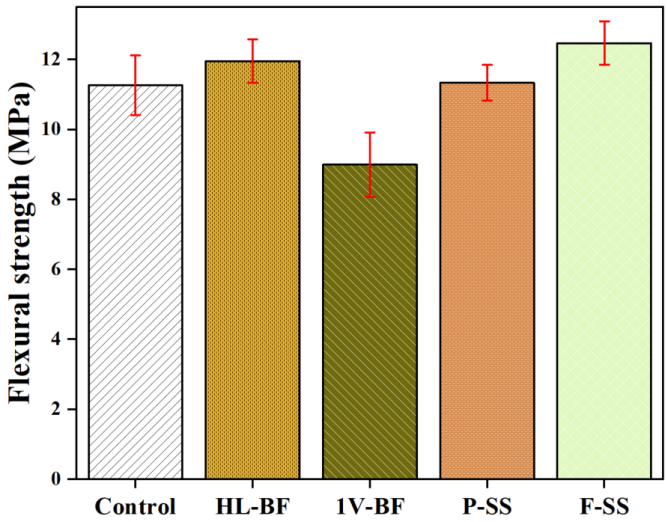

Fig. 6.2. Flexural strength of the FRCC mixes at 360 days

6.3.2.1 Effect of fibres on flexural strength at 360 days

An improvement in flexural strength of ~6% was observed with incorporation of hybrid length BF (HL-BF mix). Jiang et al. [121] suggested that the presence of longer fibres results in a stronger anchorage and bridging effect, contributing to improved flexural strength. A reduction in flexural strength of ~20% was observed when BF content was reduced to 1% in 1V-BF mix. The BF bridges the components of the composite and improves its flexural strength. Therefore, reducing volume fraction of BF reduces the bending strength of the composite.

6.3.2.2 Effect of steel slag aggregates on flexural strength 360 days

Utilization of 30% of SS as partial replacement of RS did not have a significant effect on the flexural strength and achieved a similar flexural strength as that of the control mixture. Contrarily in the case of 100% SS fine aggregates, a strength increase of ~10.72% with respect to the control mix was observed. This may be because of enhanced ITZ properties of the SS fine aggregates. Therefore, it can be clearly observed that the utilization of hazardous SS as partial or complete replacement to conventional river sand does not have any detrimental effect on the strength properties of the composite and therefore poses as a viable replacement of river sand.

6.4 Morphological investigation

6.4.1 General microstructure

The microstructure of the mixes has been analysed using SEM imaging at 28 and 360 days as shown in Fig. 6.3 and 6.4. Unreacted FA particles were visible at 28 days and 360 days as can be seen from Fig. 6.3. These fly ash particles act as filler material inside the composite and therefore can be effective way to utilize the hazardous material. These unreacted/ partially reacted particles continually participate in the pozzolanic reaction in the composite and gradually increase its strength. This caused an improvement in strength of ~42% in the case of control mix. For the same reason, improvements in strengths were observed for all mixes at 360 days owing to the similar mix composition.

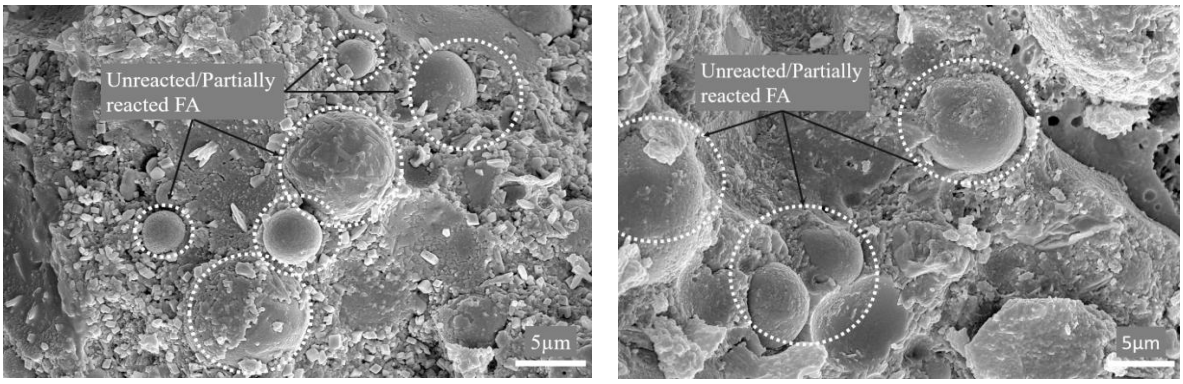

(a) Control - 28 days (b) Control - 360 days

Fig. 6.3. Microstructure of the control mix for different curing periods

The reduction in the volume of fibres in the matrix of 1V-BF mix resulted in a microstructure that appeared comparatively denser and more compact as can be seen in Fig. 6.4. At lower volumes of BF in cementitious composites, lower volume of porous microstructure can be expected. This led to a composite with comparatively higher compressive strength in the case of 1V-BF which has a lower fibre volume content. Formation of porous microstructure with incorporation of BF has been demonstrated in Fig. 6.5.

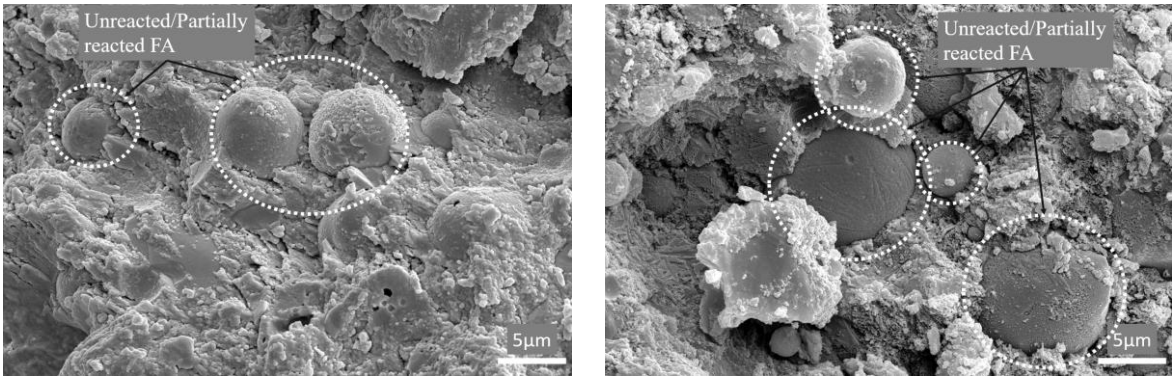

1V-BF F-SS

Fig. 6.4. Morphology of HVFA based mixes after 360 days of curing

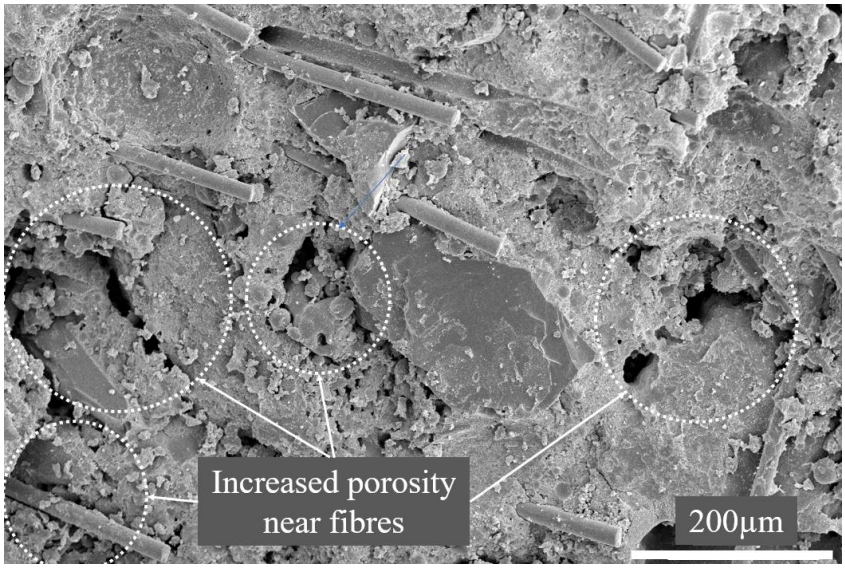

Fig. 6.5. Porosity increases near fibres

6.4.2 Interfacial transition zone

At 28 days, the ITZ with ordinary river sand in the control mix clearly demonstrates a discontinuity and a porous interphase as shown in Fig. 6.6. This adversely affects the strength and durability properties of the composite. The improvement in the strength of the composite in the mix P-SS (30% replacement of RS) and F-SS (100% replacement of RS) is because of the compact and continuous ITZ properties of the mix. The solid ITZ in the vicinity of an SS aggregate is the primary reason for the strength enhancement of the F-SS in comparison to the control mix. Similar observations were made by Jing et al. [164].

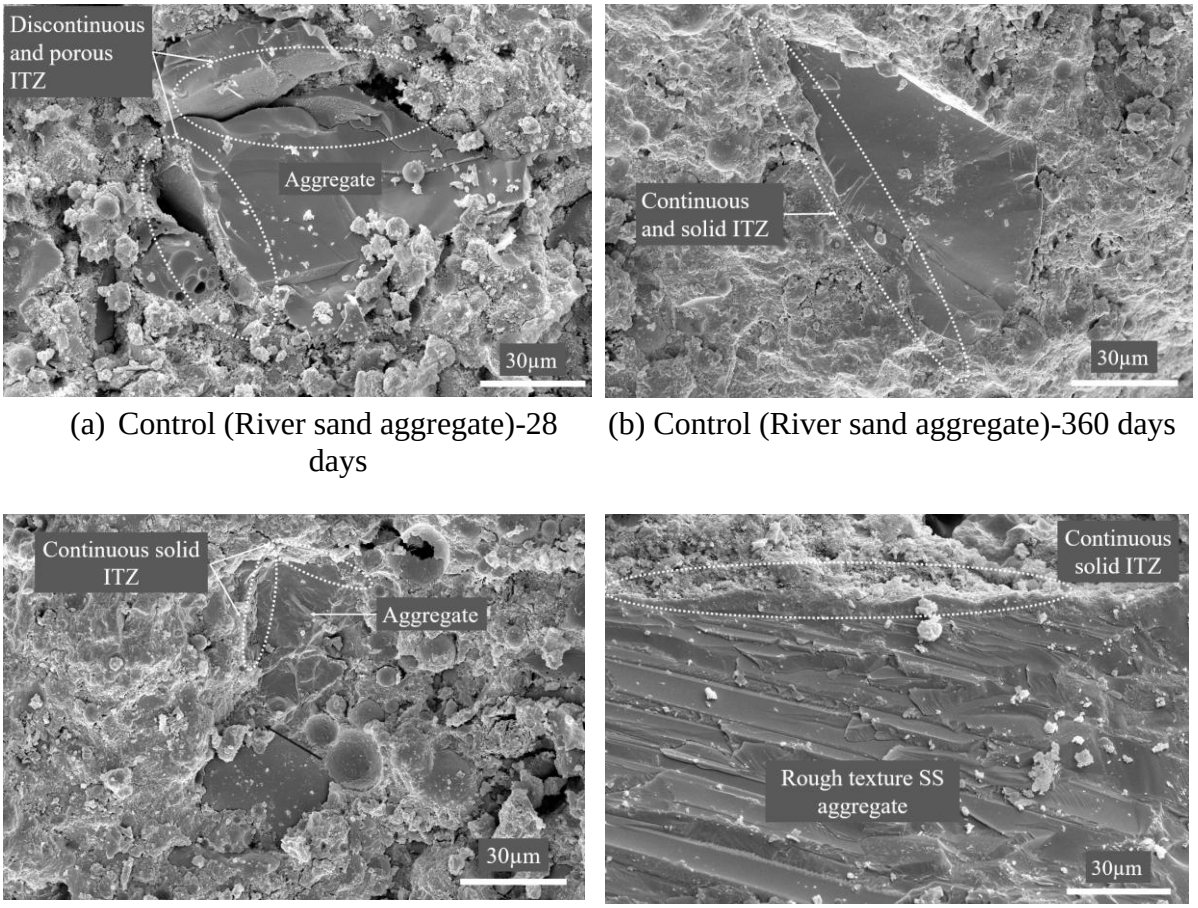

(a) Control (River sand aggregate)-28 days

(b) Control (River sand aggregate)-360 days

(c) F-SS-(Steel slag aggregate)-28 days

(d) F-SS-(Steel slag aggregate)-360 days

Fig. 6.6. Comparison of ITZ between RS and SS aggregates at 28 and 360 days

At 360 days, the ITZ around RS demonstrated an improvement in ITZ over time as shown in Fig. 6.6 (a-b). In addition to the general improvement in strength with the pozzolanic reaction, the ITZ enhancement with time also caused an improvement in strength in mixes containing RS. As can be seen from Table 6.2, on average about 37.33% of strength increment was observed in mixes containing only RS, signalling to the contribution of enhancements in general microstructure and ITZ across time. On the other hand, the mix with 100% SS aggregates (with continuous ITZ), demonstrated an increase of ~17.63% at 360 days.

Table 6.2. Strength improvement with age

Mixes	28-day strength	360-day strength	Improvement %
Control	37.10	52.76	42.21
HL-BF	37.60	50.80	35.13
1V-BF	44.70	60.20	34.67
P-SS	46.43	56.13	20.88
F-SS	45.65	53.70	17.63

The ITZ between the fibre and the matrix also plays a crucial role in the mechanical and durability properties of the cementitious composite. BF are known to have poor bonding with the surrounding matrix because of their smooth surface, dissimilar chemical composition to that of matrix and water absorbing property. Unlike the aggregates, the bond between BF and the matrix did not improve over time as can be seen Fig. 6.7.

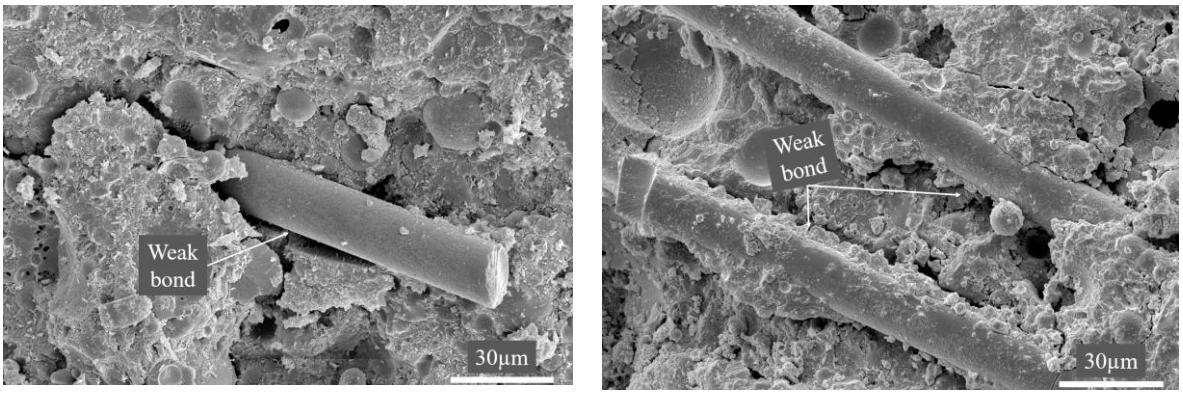

(a) Control- 28 days (b) Control- 360 days

Fig. 6.7. ITZ of fibre-matrix interface- Control at different curing age

6.5 Durability properties

6.5.1 Water absorption

The water absorption of the developed mixes has been pictorially demonstrated in Fig. 6.8. The water absorption test holds significance in evaluating concrete durability, serving as an indirect measure of its open porosity [170].

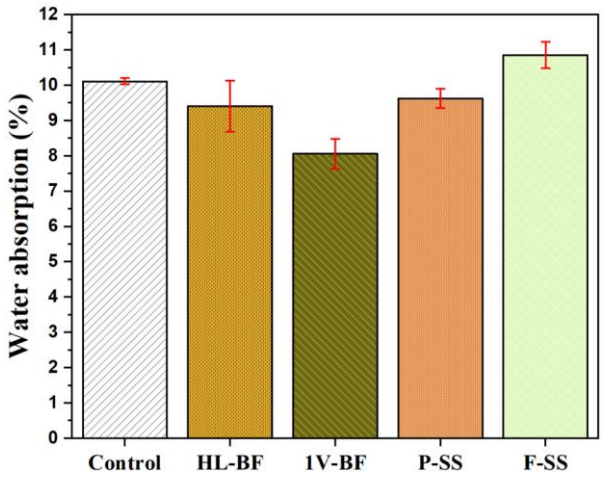

Fig. 6.8. Water absorption of the FRCC mixes

6.5.1.1 Effect of fibres on water absorption

As can be observed, length and content of BF have an effect on the water absorption properties of the composite. The mix with hybrid length BF (HL-BF) exhibited higher resistance to water absorption as compared to the control mix. The content of BF was found to be even more significant in water absorption as in mix 1V-BF with 1% less volume of BF demonstrated highest resistance to water ingress with respect to the control mix. This is attributed to the decrease in porosity with decrease in fibre content as discussed in section 6.4.1.

6.5.1.2 Effect of steel slag aggregates on water absorption

The mix P-SS demonstrated a water absorption very similar to that of the control mix owing to low fine aggregate replacement rate. On the other hand, F-SS had marginally higher water absorption as compared to the control mix owing to the porous nature of the SS aggregates that increases the water absorption capacity of the composite [114]. The performance of the mix F-SS decline only slightly as compared to the control mix. Therefore, SS fine aggregates can be considered as a viable replacement of natural fine aggregates. However, necessary modifications to the paste phase may be necessary to control the water absorption.

6.5.2 Rapid chloride penetration test

RCPT results for all the mixes have been plotted and demonstrated in Fig. 6.9. The cumulative charge passed during the RCPT offers an indirect evaluation of the concrete's ability to resist chloride penetration. A lower charge passed suggests a greater capacity to prevent chloride intrusion.

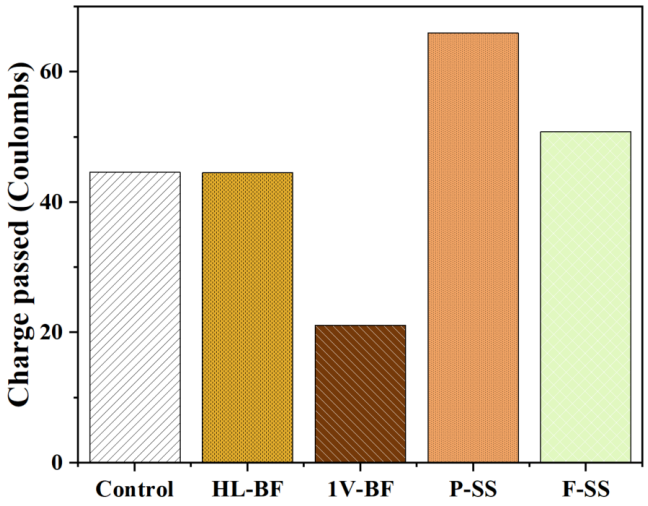

Fig. 6.9. RCPT results for the FRCC mixes

The charge passed through the control mix was found to be 44.6 Coulombs. The charge passed through the mix with hybrid length BF (HL-BF) was 44.5 Coulombs which is same as that of control mix. Again, the mix 1V-BF demonstrated excellent performance even in chloride ion penetration resistance because of its lower porosity. The mixes with SS fine aggregates also demonstrated excellent resistance to chloride ion penetration and only a marginal increase in charge-passed was observed over the control mix. As per ASTM C1202 [94], the charge passed less than 100 Coulombs can be considered as negligible.

The enhanced performance of the mixes in the current study can be explained through chloride binding and physical adsorption. The utilization of HVFA increases the chloride ion penetration resistance of the concrete [12]. Alumina reacts with the chloride ions to form stable

chlorocomplexes [85]. As can be seen from section 3.2, FA contains approximately 8 times more alumina content than OPC. Also, the tri-calcium aluminate (C_3A) reacts with the chloride to form calcium chloroaluminate hydrate, also known as Friedel's salt [92]. Furthermore, Hirao et al. [93] demonstrated the capacity of CSH to physically adsorb the chloride ions. In the case of HVFA, the formation of secondary CSH through pozzolanic reaction is prevalent. Therefore, for prolonged curing durations, higher surface area for adsorption will be available for HVFA based composites. Furthermore, the chloride resistance is inversely proportional to the water-binder ratio and age of the concrete. The current study has a fly ash replacement level of 60%, with a low water-binder ratio of 0.24 and cured for 360 days. Therefore, very low values of charge passed were observed for all the mixes.

6.5.3 Dimensional stability

The presence of oxides in the form of CaO and MgO in the aggregates pose significant threat to the durability aspect contributing to volume expansion. However, no expansion or cracking was observed even after 360 days. Table 6.3 provides the information on the dimensions of the specimens measured at 28 days and 360 days. The mixes P-SS and F-SS both demonstrated excellent dimensional stability without any indication of expansion or cracking potential. Pellegrino et al. [171] associated the expansion potential of the aggregates to the availability of the free oxides. The avoidance of expansion indicates that the SS aggregates have limited free oxides that cause the expansion phenomena.

Table 6.3. Dimensional stability of the mix with 100% SS aggregates (all values are in mm)

Mix	L-28 days	L-360 days	B-28 days	B-360 days	H-28 days	H-360 days
P-SS	50.17	50.10	50.21	50.19	51.01	51.05
F-SS	50.16	50.16	50.73	50.70	49.54	49.51

As a result, the incorporation of SS aggregates has great potential to enhance the mechanical properties while improving the sustainability aspect of the composite.

6.6 Discussion

The sustainability aspect of the whole composite was enhanced with the incorporation of HVFA and SS aggregates. Also, as discussed earlier, the fibres incorporated in the mix in the form BF, consume 1/3rd the electricity required to produce steel [75] and require no other additives for their production. Therefore, a green cementitious composite is possible with the usage of these materials without significant compromise on the properties of the composite.

Incorporation of HVFA, SS aggregates and BF provide unique benefits in terms of strength, cost, environmental sustainability and long-term durability. All the mixes achieved a strength greater than 50 MPa by 360 days and in particular 1V-BF achieved a strength >60 MPa. The rate of strength development of HVFA based cementitious composites is slower because of the slower reaction rate of FA particles. This can be compensated to a certain extent by enhancement in ITZ properties of the aggregates. The SS aggregates are especially beneficial at early ages as their incorporation resulted in compressive strength improvement of ~25 and ~23% in P-SS and F-SS respectively. All these benefits are in addition to the obvious enhancement in the sustainability of the mixture.

Furthermore, as can be seen from the Table 6.4, significant cost savings are possible through the utilization of HVFA and SS aggregates. The mix with no HVFA and SS and containing RS and BF-PP content (c/b=0.90, SF=0.10, RS=1, SS=0, SP= 8.75) adopted from chapter 4 has been compared to the control mix, P-SS (30% SS aggregates) and F-SS (100% SS aggregates). Replacement of cement with FA and reduction of SP content reduces the cost of the composite by ~53%. With the incorporation of SS aggregates, there is an increase in cost of the composite (w.r.t control) because of the requirement of higher quantity of SP. Nevertheless, a reduction of ~47% and ~38% was observed in P-SS and F-SS respectively in comparison to the mix with 100% cement and RS.

Table 6.4. Cost reduction with utilization of HVFA and SS aggregates

Component	Cement	SF	RS	SS	SP
Price/kg (Rs.)	8.2	28	1.2	1	287.4
	Mix	No HVFA	Control	P-SS	F-SS
	Price reduced (%)	--	52.89	46.81	38.42

In addition, chloride durability properties of the composite are enhanced because of HVFA. Under chloride attack conditions, HVFA may protect the underlying reinforcement. To further enhance the durability, BF content must be optimised to achieve lower total volume of penetrable pores.

6.7 Summary

This study demonstrated the long-term mechanical and durability performance of high-volume fly ash and steel slag aggregates with hybrid BF-PP fibres. Tests were performed to evaluate compressive strength, flexural strength, water absorption and chloride ion penetration resistance. Morphology was studied using SEM with a special emphasis on ITZ properties.

- The complex ingredient composition was found enhance the compressive strength of the cementitious composite over time.
- Utilization of HVFA was found to be extremely suitable in applications that require high resistance to chloride ion penetration. This is because of the high alumina content in FA that forms chlorocomplexes when exposed to chloride.
- BF content was found to be influential from both strength and durability perspective. Reducing the content of BF by 1% improved the compressive strength while it reduced the flexural strength and water absorption.
- Utilization of hybrid length BF has an impact on the flexural strength and an enhancement of 6.12% was observed w.r.t the control mix.

- Incorporation of SS fine aggregates in cementitious composites was found to be an excellent way to valorise a hazardous material without any compromise on the mechanical properties. A small increase in water absorption and negligible increase in charge passed through the samples during RCPT test can be expected. Utilization of SS aggregates posed no threat to the volumetric stability of the composite. The SS aggregates with limited free oxide composition, are a feasible alternative for substituting natural river sand in construction materials.
- Significant improvements in ITZ around RS can be expected over time.
- The ITZ properties around BF did not improve over time as opposed to that of the aggregates. An improvement in the fibre matrix interface has the potential to positively influence the mechanical and durability performance of the composite. Consequently, future research must concentrate on this important feature of the FRCC.

Chapter 7

Performance of the developed FRCC against Environmental Thermal Fatigue

7.1 Introduction

While the durability of cementitious composites is traditionally emphasized in the context of general shrinkage, chloride penetration, carbonation, etc happening over the lifespan of the structure, a relatively fast degradation can also occur from the pronounced daily and annual temperature variations prevalent in mid and high latitude areas [31]. In regions where ambient temperatures exceed 30°C, the temperature of structural elements and pavements can escalate to 60-70°C [32]. These repeated ETF cycles can initiate cracking at micro and macro levels and cause a degradation to pore structure [45]. This increase in porosity is generally attributed to the evaporation of free water and decrease of crystal water in the concrete. As temperature rises, there is an increase in the pressure in closed pores of the cementitious composites which results in the breakdown of the barriers between open and closed pores, leading to enlarged pore structures and the emergence of microcracks [46]. Based on the reported results as described in Chapter 2, it is evident that the effect of ETF in concrete material is severe as the structure durability is compromised even after just 300 ETF cycles. This highlights the necessity for any new material to undergo rigorous testing against ETF, particularly if it is intended for implementation in construction zones where temperature fluctuations are frequent.

The newly developed FRCC with HVFA and SF as SCM, SS and RS as aggregates and hybrid BF-PP fibre demonstrated outstanding fire resistance and durability properties under normal environmental conditions. To further advance its application, it is crucial to assess the durability of this material against the degradation induced by ETF. There is very limited research on the ETF of cementitious composites and the majorly available findings highlight a

clear necessity of a durable material against ETF. Considering the anticipated rise in temperature and the frequent fluctuations in weather patterns expected in near future, it is crucial to direct research efforts towards the development of a material that exhibits excellent resistance to ETF.

Therefore, this chapter aims to bridge this gap by analysing the potential of the newly developed FRCC against ETF. The performance of developed cementitious composites have been studied under compressive and flexural loads after exposure to 60, 120, 180, 240 and 300 cycles between 20 and 60°C. To assess the microstructure and understand the underlying mechanisms, SEM, DSC and MIP analyses have been employed.

7.2 Materials and methods

7.2.1 Materials and mix proportions

This study utilized OPC, FA and SF as the binder material and RS and SS passing through 300µm sieve as fine aggregate. In addition, hybrid BF and PP fibres were also used as suggested in the previous chapters. Table 7.1 presents the different fibre-reinforced cementitious composite mixes considered in the present study. Five mixes were formulated to examine the influence of fibre composition and SS aggregate. These mixes were same as that adopted in Chapter 6 for long term durability study.

Table 7.1. Mix proportions of the fibre reinforced cementitious composites

Mix ID	*Cement	FA	SF	RS	SS	w/b	SP	BF (#%Vol.)	PP (%Vol.)
Control	522.5	838	71.5	573	0	0.24	4.87	2	0.11
HL-BF	522.5	838	71.5	573	0	0.24	6.56	**1%12+1%18**	0.11
1V-BF	522.5	838	71.5	573	0	0.24	03.50	**1**	0.11
30SS	522.5	838	71.5	401	172	0.24	8.75	2	0.11
100SS	522.5	838	71.5	0	573	0.24	14.22	2	0.11
*Values presented for binders, fine aggregate and SP are in kg/m³									
HL-BF- Hybrid length BF, 1V-BF-1% Vol. of BF, 30SS- Partial replacement (30%) with steel slag, 100SS- Full replacement (100%) with steel slag									

7.2.2 Sample preparation and test methods

The mixing procedure was kept same as described in Section 3.3. To evaluate the compressive strength of the composite, four 50 mm cubes of each mix were cast at each ETF testing level. For flexural strength, three prism specimens with dimension 350 mm × 40 mm × 40 mm of each mix were cast at each exposure level. A total of 120 cubes and 90 prism specimens were cast for this study. The specimens were demoulded 36 hours after casting and cured first in water and then in air for 28 days each.

After the curing period, the specimens were marked and transferred into environmental chamber which was programmed to perform regular temperature cycles between 20°C and 60°C as depicted in Fig. 7.1 and further explained in Section 3.4.4. The heating rate was set to 1°C/min with a hold period of 2 hours. The primary aim with this heating and cooling rate was to ensure thorough heating of the specimens to the core, followed by a rapid temperature decrease, inducing thermal shock. The specimens were tested for compression and flexure after 0, 60, 120, 180, 240 and 300 ETF cycles. The compressive and flexural strength tests were conducted as per the procedure outlined in Section 3.4.2. For microstructural analysis and a detailed examination of variations in morphology, SEM, MIP and DSC tests were carried out after the testing.

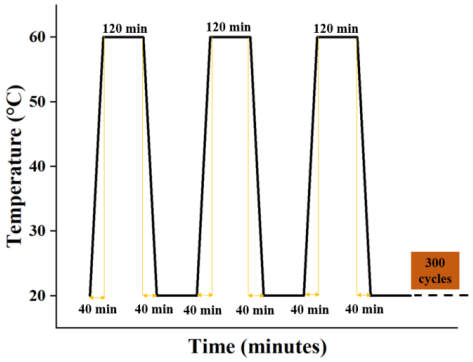

Fig. 7.1. ETF simulation by variation in temperature with respect to time

7.3 Results and analysis

7.3.1 Surface characteristics

Fig. 7.2 demonstrates the surface characteristics of the samples of all mixes before and after exposure to ETF cycles. All the specimens exhibited excellent surface characteristics and did not demonstrate any form of surface degradation even after 300 cycles of temperature fluctuations.

Control HL-BF 1V-BF 30SS 100SS

(a) Without exposure

Control HL-BF 1V-BF 30SS 100SS

(b) Exposure to 300 thermal cycles for all mixes

Fig. 7.2. Surface characteristics of all the mixes before and after exposure to ETF

In general, the structures exposed to ETF exhibit surface cracking and deterioration because of general drying and thermal expansion and contraction. The incorporation of BF-PP improved the tensile strength and the resilience of the composite against cracking. Additionally, HVFA in the cementitious composite can also lead to continued formation of CSH with increasing ETF cycles that may also have deterred the formation of thermal cracks.

7.3.2 Compressive strength

The compressive strength of all the mixes prior to thermal cycles is shown in Fig. 7.3. It should be noted that the cube specimens for 0-ETF cycle case were also tested at the same age as the

rest of the specimens under ETF exposure. This was done to take into account the influence of maturity.

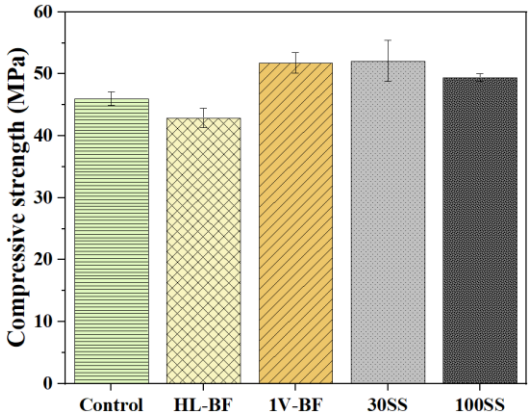

Fig. 7.3. Compressive strength of all FRCC mixes without exposure to ETF cycles

The control mix exhibited a compressive strength of 46 MPa. The compressive strength of the mix with hybrid length BF (HL-BF) exhibited a slightly lower compressive strength of ~43 MPa. Contrarily, reducing the BF volume increased the compressive strength of the composite by ~12%. This rise in compressive strength with reduction in BF volume was due to the reduced porosity of the composite as demonstrated using SEM analysis in the later part of the chapter.

The positive effect of SS aggregates on the compressive properties of the composite is also evident from Fig. 7.3 as both mixes with 30% SS (30SS) and 100% SS (100SS) exhibited a slightly higher compressive strength as compared to the mix with 100% RS (control). The increase in strength for these mixes is attributed to the enhanced ITZ properties caused by similar chemical composition and the rough texture that provides better interlocking through hydration reaction on the surface of the SS aggregate.

7.3.3 Compressive strength after exposure to ETF

It is evident that incorporating TPE to mitigate the effects of thermal fatigue was successful given that there is a progressive increase in compressive strength initially with exposure to ETF

cycles and all the mixes retained strength greater than that at ambient temperature at all ETF levels. The variation in the compressive strength can further be understood through Fig. 7.4

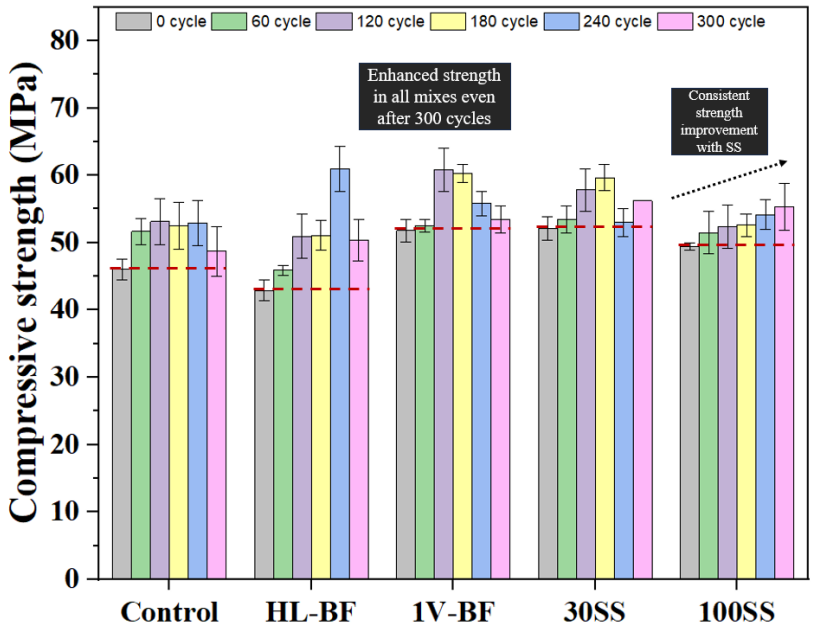

Fig. 7.4. Residual compressive strength variation of all mixes with ETF cycles

Among all the mixes, control, 1V-BF and 100SS showed superior performance. The control mix and the HL-BF (mix with hybrid length BF) demonstrated an increase of ~12% and ~7%, respectively in the initial 60 thermal fatigue cycles. On the other hand, the mixes 1V-BF, 30SS, and 100SS had a marginal improvement in compressive strength of ~1.5%, 2.5%, and 4%, respectively. This trend of rise in strength continued to 120 cycles of thermal exposure (with respect to strength at 60 cycles). The residual strength of all the mixes remained almost similar between 120 and 180 cycles of thermal fatigue exposure. At 240 cycles, some contrasting behaviour was observed among different mixes with river sand. Control mix and mix HL-BF showed the continual rise, however, the strength of mix 1V-BF and 30SS declined. A decline of ~8.6% and 12.7% in compressive strength was observed in the mix 1V-BF and 30SS, respectively. This may have been due to their initial higher strength with denser microstructure. The porosity and pore volume increase with exposure to ETF and this is more pronounced in

concrete with higher compressive strength [31]. The higher compressive strength creates a denser ITZ, which is less capable of accommodating the thermal stresses. Consequently, the bond between aggregate and matrix is weakened upon exposure to ETF. However, the strength of both 1V-BF and 30SS mix remained at a higher level with respect to the strength at ambient temperature.

A decline in compressive strength (w.r.t the strength at 240 cycles) was observed after exposure to 300 cycles in all the mixes containing RS. This may be because of unavailability of unhydrated cement particles or absence of portlandite for continued pozzolanic reaction of FA particles. Consequently, the minor differential thermal expansions and consequent microcracking especially near ITZ may have weakened the bond between aggregate and the cement phase. On the other hand, the strength improvement was found to be steady in case of mix 100SS with 100% SS aggregates and more importantly, the residual compressive strength never declined suggesting the importance of homogenizing the mix with an aggregate with similar chemical composition to cement.

Nevertheless, even after 300 cycles of thermal exposure, none of the mixes demonstrate strength lower than their original strength at ambient temperature. This was mainly due to the use of TPE in the form of HVFA. At high volume replacements, the microstructure is characterised by abundance of unreacted or partially reacted FA particles. The reaction between slow reacting FA particles with portlandite accelerate between the temperatures of 50-70°C following Arrhenius law leading to the development of more CSH [172]. Thereby, the utilization of HVFA allows for strength enhancements at repeated thermal loads when most mixes without this TPE demonstrate a decline in compressive strength. Further discussions on the enhancements in the ITZ can be found in section 7.3.5.

7.3.4 Flexural strength observations

Table 7.3 presents the flexural strength variations for different mixes. Incorporation of hybrid length BF was found to have a beneficial effect on the flexural performance of the composite as HL-BF achieved approximately 7% higher strength in comparison to the control mix. This was due to the stronger anchorage and bridging effect of longer fibres, contributing to improved flexural strength. Reduction in the volume of BF in the mix 1V-BF caused a reduction in flexural strength by ~19%. Incorporation of 30% of SS in the cementitious composite did not have any significant effect on the bending strength. On the other hand, complete replacement of RS with SS aggregates enhanced the strength of the composite by ~4%. Therefore, it can be clearly observed that the utilization of SS as partial or complete replacement to conventional river sand does not have any detrimental effect on the strength properties of the composite and therefore poses as a viable replacement of river sand.

Table 7.2. Variation in flexural strength at different ETF levels (in MPa)

	Control	**HL-BF**	**1V-BF**	**30SS**	**100SS**
Ambient	16.41	17.59	13.59	15.94	17.11
60 cycles	19.22	21.09	16.88	17.81	20.16
120 cycles	20.86	23.20	18.98	18.52	22.27
180 cycles	21.33	21.80	19.45	19.45	22.73
240 cycles	14.41	15.82	12.89	14.77	15.94
300 cycles	12.42	15.00	12.42	12.89	14.53

Fig. 7.5 demonstrates the flexural performance of the FRCC with increasing ETF cycles. Enhanced pozzolanic reaction and hydration reaction at elevated temperature initially improved the flexural strength of all the mixes up to 180 cycles. An improvement of approximately 17, 20, 24, 12 and 18% over their ambient temperature flexural strengths was observed in control, HL-BF, 1V-BF, 30SS and 100SS respectively at 60 TCs. All the mixes (except HL-BF) demonstrated their best performance after exposure to 180 TCs where an improvement in flexural strength of approximately 30, 23, 43, 22 and 32% were observed in

control, HL-BF, 1V-BF, 30SS, and 100SS, respectively. The pattern of variation of all the mixes resembled to that observed under compression, except that a steep decline in bending strength was observed post 180 cycles. At 240 cycles, initiation of thermal cracking and pore coarsening can be expected which may have caused a steep decline in the bending capacity of the composite.

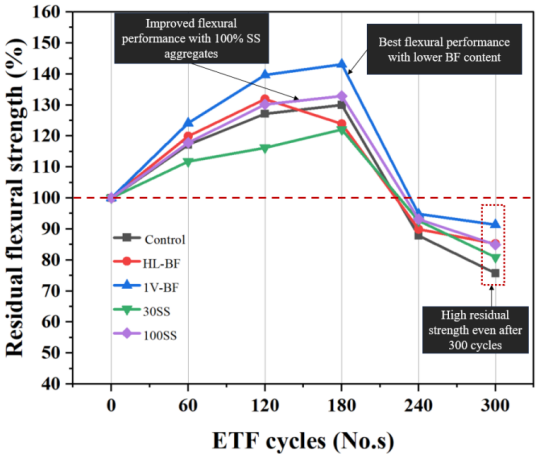

Fig. 7.5. Residual flexural strength of all mixes with ETF cycles

After 180 cycles, the amount of portlandite in the system may not be sufficient for continued formation of CSH and therefore can be considered as a point of decline due to pore coarsening and microcracking. Also, as demonstrated in the section 7.3.5.1, introduction of fibres increases the porosity into the matrix and BF has been found to form a poor bonding with the matrix. This fibre-matrix bond over repeated thermal exposure may deteriorate and cause a reduction in the bending capacity of the FRCC. Consequently, the mix 1V-BF demonstrated the best performance when exposed to ETF despite containing 1% lower fibre content. This mix may contain lower pore volume and enhancement in the pore structure with ETF level may have densified the matrix and enhanced the performance. Also, the availability of lower fibre content prevented the formation of weaker fibre-matrix zones and hence protected the FRCC from loss of flexural strength.

7.3.5 SEM analysis

7.3.5.1 General microstructure

The microstructure of control, 1V-BF, and 100SS were used to discover the behaviour of all the mixes used in the study. The microstructure of these mixes at ambient temperature has been shown in Fig. 7.6. The microstructure of all the mixes has abundant unreacted or partially reacted particles of FA (uFA).

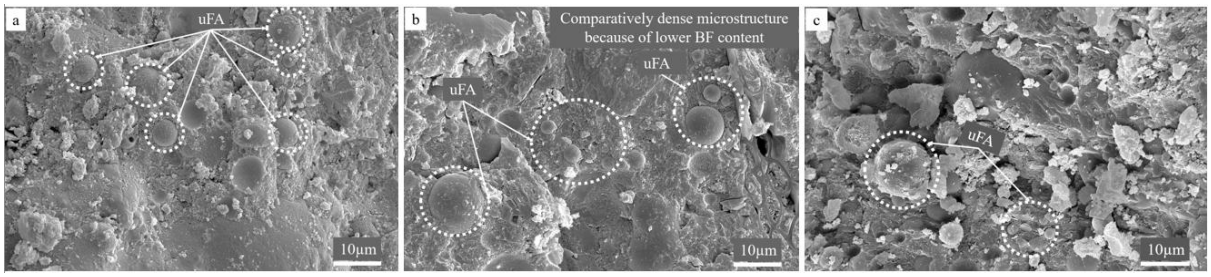

Fig. 7.6. Morphology of (a) control, (b) 1V-BF and (c) 100SS at ambient temperature

Upon closer examination of the control mix, it was found that the incorporation of BF in FRCC increased the porosity of the cementitious composite as demonstrated in Fig. 7.7. Consequently, reduction in BF content from 2% to 1% (by vol.) had contributed to the increase in the compactness of the microstructure which in turn improved the compressive performance of the 1V-BF mix.

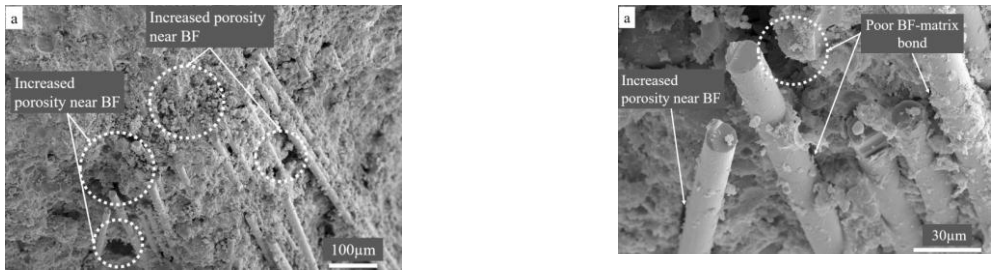

Fig. 7.7. Effect of BF (a) Increased porosity with incorporation of BF and (b) poor bond of BF in control mix

On exposure to ETF cycles, significant changes in the microstructure were observed. This can be identified from the microstructure of control, 1V-BF, and 100SS at 60, 180, and 300 cycles

as shown in Fig. 7.8. As can be seen from the figure, the microstructure of the paste phase progressively densifies in all the mixes with repeated thermal cycles. Also, the prevalence of uFAs reduces significantly with increased ETFs. In general, the rise in temperature accelerates the cement hydration and pozzolanic reaction of FA particles. Consequently, there is formation of additional CSH in the matrix which increased the compactness and hence, the strength of the composite.

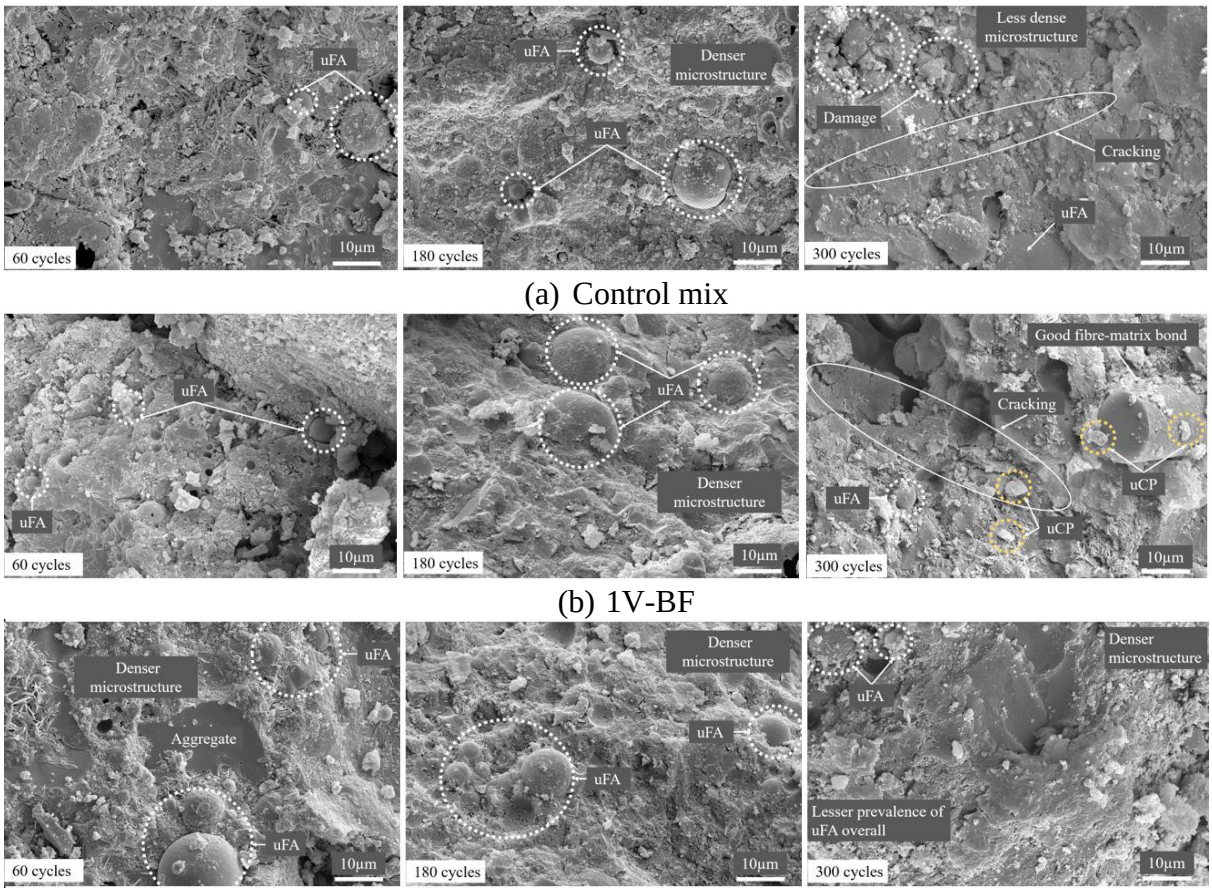

Fig. 7.8. Variation in the microstructure of (a) control mix, (b) 1V-BF and (c) 100SS at 60, 180, and 300 ETF cycles

In case of mixes exposed to 60 ETF cycles, microstructure had more well hydrated phases and lesser FA and unreacted cement particles as compared to the ambient temperature counterparts. Moreover, mix 100SS was found to be denser compared to other mixes at the same thermal exposure cycles. At 180 ETF cycles, matrix of all the mixes densified in all the mixes.

However, upon exposure to 300 ETF cycles, the microstructure of control mix and 1V-BF demonstrated signs of damage in terms of coarsening and internal microcracking. This caused a decline in compressive strength (w.r.t. 180 ETF cycles). However, the microstructure of 100SS continued to densify without any damage. The underlying reason for this improved performance is discussed in later sections.

From this section, it must be noted that all the mixes performed exceptionally well, retaining more than 100% of its compressive strength even after 300 ETF cycles because of continued pozzolanic reaction of slow reacting FA particles. These particles densify the matrix when exposed to ETF cycles as opposed to deterioration in case of ordinary concrete.

7.3.5.1 Effect of ETF on the ITZ

The ITZ properties of the RS aggregates in control and 1V-BF and SS aggregates in the 100SS mix without any thermal cycling is depicted in Fig. 7.9. The discontinuity and cracking between the RS and the paste phase is visible in the control and 1V-BF (Fig. 7.9 a-b). On the other hand, the mix 100SS demonstrated good bonding with the surrounding matrix at ambient temperature. This is because of rough surface texture, angular shape and similar chemical composition of SS aggregates.

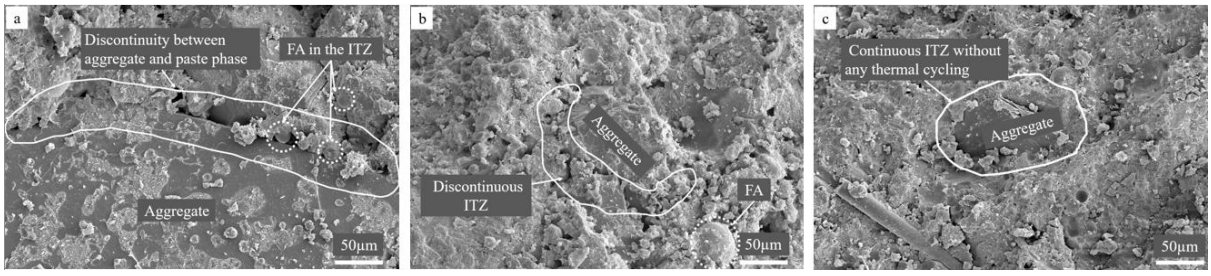

Fig. 7.9. ITZ between aggregate and matrix in mixes (a) control (b) 1V-BF (c) 100SS

The influence of repeated exposure to higher temperatures on the ITZ properties of control, 1V-BF, and 100SS has been further demonstrated in Fig. 7.10. The control mix with RS demonstrated an improvement in bonding when exposed to 60 ETF cycles. Similar

observations were noted for mix 1V-BF and 100SS. The enhancement in the bonding properties is because of the accelerated pozzolanic reaction of FA particles and hydration reaction of cement. The improvement in the bonding and reduction in porosity of the ITZ continued even at 180 cycles of thermal fatigue exposure. The mixes with RS demonstrated densest ITZ at this exposure condition.

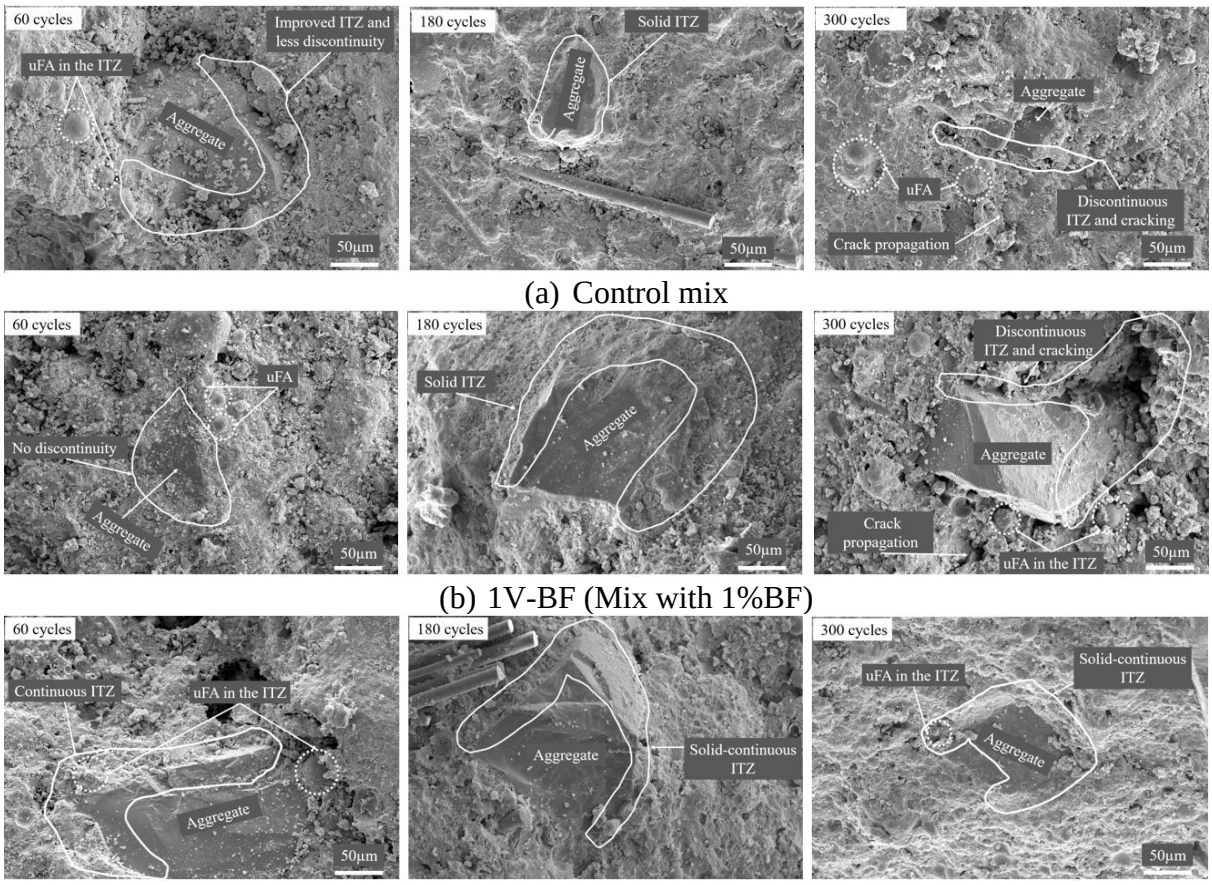

Fig. 7.10. Effect of TC on ITZ in (a) Control (b) 1V-BF and (c) 100SS at various temperature cycles.

At 300 ETF cycles, the ITZ around RS in both control and 1V-BF demonstrated cracking and discontinuity. This is further exacerbated when aggregates are nearby and cracks from individual ITZ form clusters as shown in Fig. 7.11. The cracking in the ITZ is initiated when the system becomes portlandite deficient for continued pozzolanic reaction. Consequently, a reduction in strength was observed at this exposure condition for both control and 1V-BF with respect to 180 ETF cycles. On the other hand, mix 100SS with SS aggregates demonstrated

further improvement in the bonding with the surrounding paste and improvement in ITZ properties. This is attributed to the similar chemical composition of SS aggregates with the cement which prevents the differential thermal expansion between aggregate and paste phase during ETF. Therefore, the mix 100SS demonstrates an upward trend for compressive strength even at 300 ETF cycles when all other mixes demonstrate a decline.

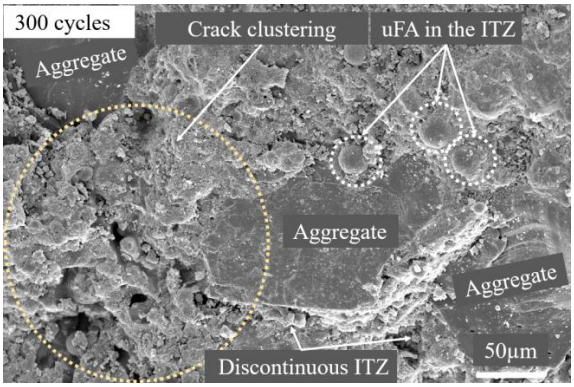

Fig. 7.11. Crack clustering due to differential thermal expansion in control mix after 300 cycles of ETF

7.3.6 DSC Analysis

DSC curves for control and 100SS at ambient temperature, and after 180 and 300 ETF cycles have been illustrated in Fig. 7.12. All the samples demonstrated an endothermic peak near 120-150°C, 450°C, and 750°C representing dehydration of free and physically bound water, dehydroxylation of portlandite, and decarbonation of calcium carbonate, respectively [103,173]. Furthermore, the DSC curves clearly indicate variations due to ETF. The intensity of initial endothermic peak between 120-150°C (suggesting removal of physically bound water) reduced in sample exposed to 180 ETF cycles. Subsequent exposure up to 300 cycles resulted in only a minor change in the endothermic peak intensity due to specimen drying.

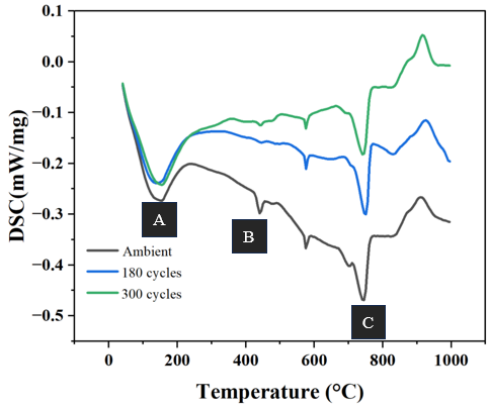

(a) Control

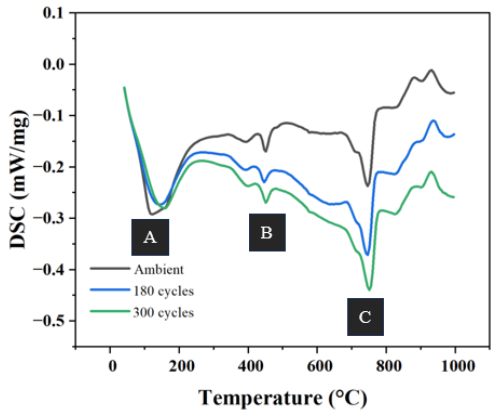

(b) 100SS

A- Dehydration, B- Dehydroxylation, C- Decarbonation

Fig. 7.12. Differential scanning calorimetry of (a) Control (b) 100SS

It should be noted that the significant energy change occurs in the temperature range of 400-500°C. A distinct endothermic peak at 450°C, associated with the dehydroxylation of portlandite, was observed in all samples at ambient temperature. Despite the use of high volumes of low calcium FA, portlandite was available in the system. Upon exposure 180 ETFs, the intensity of the peak corresponding to portlandite reduced in the control mix suggesting the occurrence of pozzolanic reaction. This supports the theory previously put forth with regards to continued strength increment as a result of accelerated reaction of unreacted particles (FA and cement) when exposed to ETF cycles. The intensity of this peak at 180 cycles was found to be very low, and no further pozzolanic reaction was possible for continued exposure to ETF. The reduction in the peak intensity of decarboxylation of calcite with increasing ETF cycles,

is also indicative of reduction in portlandite with increasing ETF cycles. Consequently, a decrement in strength in control mix was observed (w.r.t 180 cycles) when samples were exposed to 300 cycles.

In comparison, only a minor variation in the peak intensity was observed upon exposure to 180 ETF cycles in 100SS mix. Moreover, the peak intensity corresponding to dehydroxylation did not change even after 300 ETF cycles (w.r.t 180 cycles). Also, this peak intensity at 180 ETF cycles was much higher for 100SS as compared to that of control specimen. Contrary to the control mix, peaks associated with decarboxylation of calcite intensified with increasing ETF cycles. This indicates the reactivity of fine steel slag aggregates in the matrix which introduces the additional portlandite to the system. Subsequently, it reacts with the atmospheric CO_2 to form calcite (a strength providing compound) over time. This is in addition to the secondary CSH formation from pozzolanic reaction. With secondary CSH and additional calcite formation, a continual improvement in compressive strength is observed in 100SS.

Consequently, the strength of mix 100SS did not demonstrate a declining trend at any point throughout the study as opposed to that of the control mix. This clearly proves that incorporation of SS is not just beneficial from a sustainability standpoint, but also from thermal enhancement perspective.

7.3.7 MIP Analysis

Fig. 7.13 illustrates the pore size distribution of the control, 1V-BF, and 100SS specimens at ambient temperature. The pore sizes are differentiated into micropores (<100nm), mesopores (100-1000nm) and macropores (1000-100000nm).

It can be observed that the control specimen exhibited the greatest pore volume in the micropore range at ambient temperature. A 1% reduction in BF content in the 1V-BF mix positively influenced the pore structure, resulting in a noticeable enhancement over the control

mix. In the early part of mesopore range (100nm – 1000nm), the 1V-BF mix initially outperformed the control mix and then followed a similar trend as the pore size range increased. The 100SS mix (with 100% SS aggregates) demonstrated a performance comparable to 1V-BF in the micropore range, despite having a higher BF content. This could be because of the reactivity of SS fine aggregates combined with higher SP content of this mix. PCE based SP cause pore refinement and improve packing density through cement particle dispersion and water demand reduction [174,175].

In the mesopore range (100nm – 1000nm), the mixes 1V-BF and 100SS outperformed the control mixture. The 100SS mix had the lowest pore volume among the compared mixes up to 1000nm, but this increased in the initial part of the macropore range (1000nm – 10000nm). Nevertheless, the system achieved higher strength than the control mix due to the reduced pore volume in the micropore and mesopore ranges and improved ITZ (as previously demonstrated). All the mixes showed a similar performance in the later part of the macropore range (>10000nm).

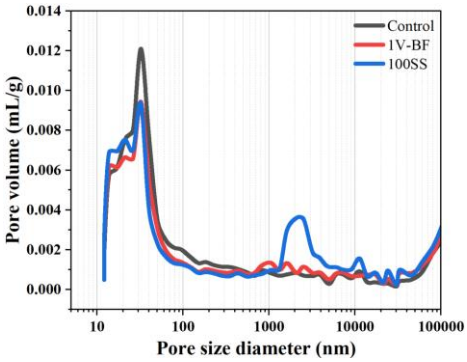

Fig. 7.13. Pore size distribution of (a) Control (b) 1V-BF and (c) 100SS without thermal cycling.

Fig. 7.14. demonstrates the effect of ETF on pore size distribution of the control, 1V-BF and 100SS. Following 180 ETF cycles, the control mix exhibited a significant decrease in pore volume in the initial part of the micropore region, which supports compressive strength

observations. The control mix after 300 ETF cycles exhibited refinement of pores in the initial part of the micropore range. Subsequently, an increase in pore volume across the micropore (comparatively larger micropores), mesopore, and macropore regions indicated deterioration. As a result, a decline in the compressive strength was observed after 300 cycles compared to samples exposed to 180 cycles.

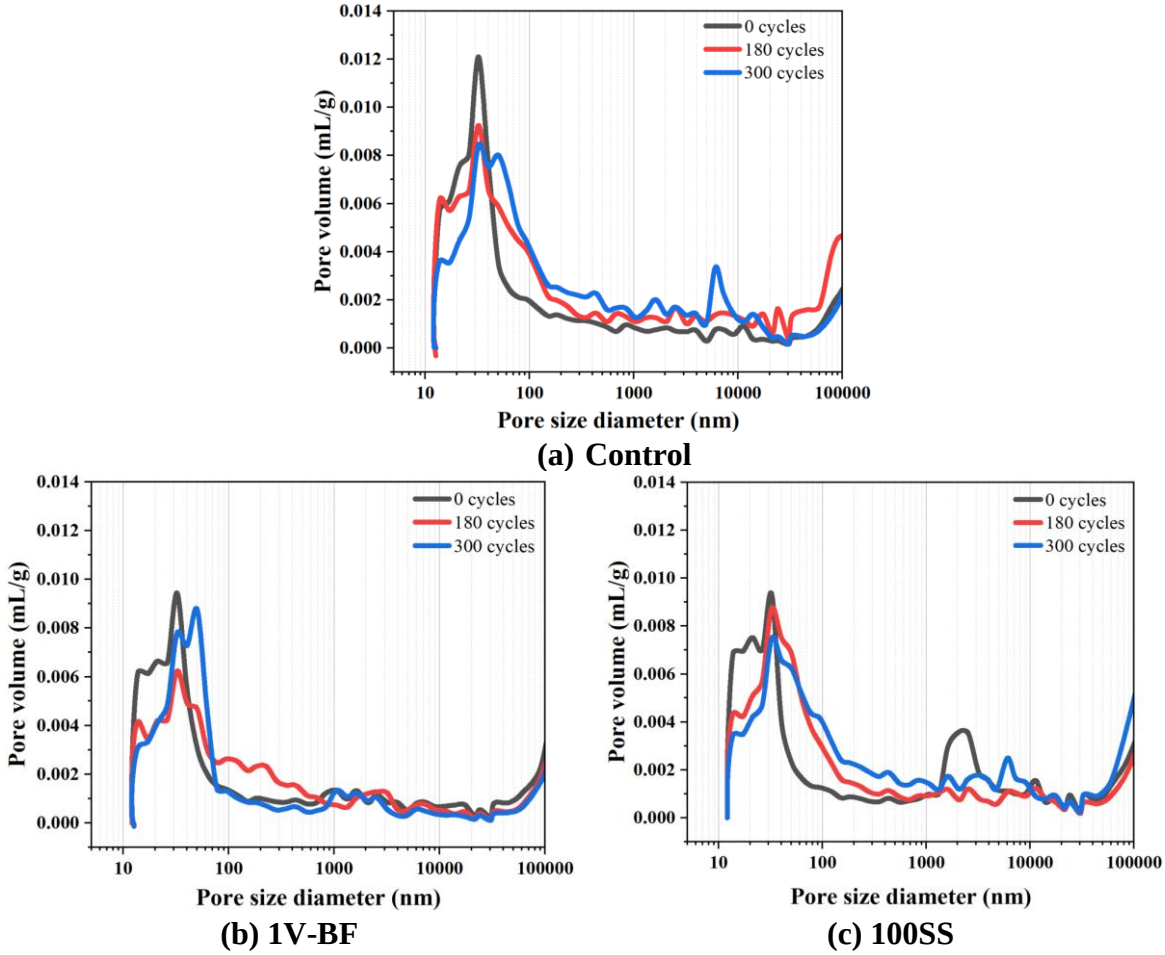

(a) Control

(b) 1V-BF

(c) 100SS

Fig. 7.14. Pore size distribution of (a) Control (b) 1V-BF and (c) 100SS after 0, 180, and 300 ETF cycles

For the 1V-BF mix, exposure to 180 cycles resulted in a significant decrease in pore volume in the micropore region. The reduction in macropores, combined with the decrease in micropore volume, led to an enhancement in strength of the composite. Upon exposure to 300 ETF cycles, a substantial increase in micropores was noted compared to the 180 cycles. However, the mesopores and macropores remained similar to those in the control mix. This sudden surge in micropores at 300 cycles is unique to the 1V-BF mix, given its denser microstructure compared

to the other mixes. Therefore, the increase in ETF cycles from 180 to 300 caused a more pronounced decline in compressive strength, as also evidenced in the general microstructure and ITZ of the composite.

In case of 100SS, exposure to 180 ETF cycles led to an increase in micropores, likely due to the pore refinement because of the development of a denser matrix and ITZ. In contrast, there was a notable decrease in macropores compared to the sample exposed to ambient temperature. This resulted in a gradual increase in strength after 180 ETF cycles. After 300 cycles, the specimen showed a marked reduction in micropores and macropores when compared to the specimen exposed to ambient temperature. Consequently, significant improvement in compressive strength was observed because of exposure to thermal cycles. This clearly demonstrates the pore refinement with incorporation HVFA and SS aggregates. A dense matrix caused a decline in strength initially; however, it recouped with continued hydration reaction of cement and FA.

7.4 Synopsis of underlying mechanisms

ETF may lead to increase in average pore diameter, differential thermal expansion, internal microcracking, surface cracking and strength loss in cement-based materials. Incorporating HVFA in the cementitious composite leads to ongoing formation of CSH and pore refinement under ETF conditions, which in turn improves strength, reduces porosity, and delays thermal crack formation. This is often aided by the presence of unreacted and partially reacted cement particles. However, after 180 ETF cycles, the system's portlandite may become insufficient for sustained pozzolanic and hydration reactions. To counter this, the use of SS fine aggregates is suggested, which shows enhanced reactivity under ETF conditions and supplies necessary portlandite. Moreover, these aggregates form a strong bond with the surrounding matrix due to their similar chemical composition and surface texture, as previously demonstrated.

Additionally, HVFA also reduces the coefficient of thermal expansion (CTE) of the mix because of a higher porosity and lower portlandite content. Shui et al. [176] demonstrated that CTE is a function of porosity and portlandite content. With higher internal porosity and lower portlandite content, a material with lower CTE can be achieved. The current system which already has a lower portlandite content becomes even more deficient upon acceleration of pozzolanic reaction under ETF conditions. Consequently, a match between CTE of the RS and that of the paste phase is established that delays the cracking of the general microstructure, ITZ, as well as the surface. Consequently, the HVFA based system has low probability of differential thermal expansion under environmental thermal fatigue which makes it more resistant to thermal cracks.

The HVFA-SS based system's resistance to thermal cracks is further complemented by the inclusion of fibres, which play a pivotal role in enhancing the FRCC's thermal endurance. The enhancement in tensile capacity protects it from internal microcracking and surface cracking that arise because of drying and differential thermal expansion. As discussed previously, incorporation of fibres can effectively enhance the tensile strength of the composite and control the occurrence of cracking. Additionally, the design choice to eliminate coarse aggregates plays a crucial role in this enhanced performance. The presence of larger coarse aggregates act as zones of defects as their larger size produces larger porous ITZ zones. Also, upon exposure to elevated temperature, the differential thermal expansion of these coarse aggregates initiates cracking at a larger scale which then progresses towards the paste phase of the concrete composite [32]. Therefore, concrete with coarse aggregates is more susceptible to thermal fatigue and experience a more rapid decline in compressive strength upon exposure to thermal cycles.

Overall, the addition of TPEs in the form of HVFA and SS fine aggregates and elimination of coarse aggregates significantly removed the issues related to ETF, such as internal

microcracking, differential thermal expansion, and porous ITZ. Additionally, incorporation of hybrid fibres led to an increase in the tensile strength of the composite and may have further helped in eliminating cracks at ETF temperatures.

7.5 Summary

The utility of TPE in the form of HVFA and SS for cement-based materials to resist ETF has been demonstrated. This has been validated by thorough investigation of mechanical performance and the results were supported by microstructural, DSC, and MIP analysis and the following conclusions have been derived:

- All five FRCC mixes exhibited thermal resistance with residual compressive strengths > 100% and excellent surface characteristics without any major cracks even after 300 ETF cycles. This confirmed the positive influence of HVFA and hybrid BF-PP system against ETF.
- The control mix retained compressive strengths of ~112%, ~114% and ~106% after 60, 180 and 300 ETF cycles respectively. On the other hand, 100SS retained ~104, ~106 and ~112% at 60, 180 and 300 ETF cycles respectively.
- Contrary to the available literature, a decrease in fibre content was found to be beneficial for the enhancement in residual flexural strength. The mix 1V-BF retained ~91% of its flexural strength after exposure to 300 ETF cycles as opposed to ~76% and 85% as in the case of control and 100SS respectively. As the ETF exposure increase, internal microcracking, pore coarsening and deterioration of fibre matrix bond causes a degradation in flexural strength. A reduction in fibre content reduces the overall porosity and potential loss in the bond between fibre and matrix.
- HVFA incorporation in FRCC introduces slow reacting particles which get activated upon exposure to elevated temperature in the presence of portlandite to form CSH. The reduction in portlandite content as observed through DSC suggests the continued

reaction of unreacted particles under ETF conditions. Consequently, an improvement in strength is observed in addition to delaying the formation of microcracks. MIP analysis also revealed the beneficial effect of incorporation of HVFA on reduction in pores of size <100nm.

- Densification of matrix was observed up to 180 ETF cycles as demonstrated using SEM micrographs. Thereafter, internal microcracking and coarsening was observed in mixes with RS. On the other hand, FRCC mixes with SS fine aggregates demonstrated further densification.
- The mixes with RS, became portlandite deficient after exposure to 180 ETF cycles, which reduces the extent of continued pozzolanic reaction. On the other hand, SS fine aggregates in the mix 100SS supplied portlandite which caused a continued improvement in the strength up to 300 ETF cycles.
- The advantage of using SS fine aggregates was also apparent by observation of ITZ using SEM. The SS fine aggregates form a strong bond with the surrounding matrix at ambient temperature and this bond observed to be improved with repeated ETF cycles.

Chapter 8

Performance of the developed FRCC against combined effect of ETF and aircraft operating fluids for airfield pavement application

8.1 Introduction

Chapter 7 focused on demonstrating the suitability of the developed FRCC against ETF. The testing replicated the severe case of temperature fluctuation over the service life of the structure. In general, ETF results in the problem of differential thermal expansion and contraction which may cause microcracks to form and propagate within concrete, leading to a reduction in its durability. The developed FRCC, however, showed a greater resistance to ETF with no major cracks and residual compressive strength greater than 100 percent even after 300 cycles. This chapter further extends the experimental investigation to a special case involving airfield pavements where the problem is exacerbated due to the continuous exposure to aircraft operating fluids.

Airfield pavements not only experience fatigue load, impact load, as well as shrinkage in addition to severe weather conditions, but they are also exposed to hydraulic oil, lubricating fluid, and air traffic fuel leaked from the aircrafts. This may lead to saponification, scaling, chipping, and strength loss of concrete [33,50,51]. Moreover, the penetration of these deleterious fluids through the cracking caused by ETF can potentially increase the rate of degradation and significantly reduce the service life of pavement. Consequently, material selection for the construction of airfield pavements must consider thermal and chemical resistance to enhance the service life of the pavements. However, the studies in this area are very scarce. Considering the immense potential of the developed FRCC against ETF, its durability against chemical attacks must be assessed to determine its potential as construction material for airfield pavements.

This chapter presents the first systematic investigation of the combined influence of ETF and aircraft fluids for pavement materials. The compressive and flexural performance of developed cementitious composites have been studied against the combined impact of the frequently used aircraft fluids and ETF between 20 and 60°C. The performance has been assessed after exposure to 60, 120, 180, 240 and 300 cycles and further analysed using SEM, DSC, and MIP analysis to provide deeper insights into the underlying mechanisms.

8.2 Materials and methods

8.2.1 Materials and mix proportions

This study utilized OPC, FA and SF as the binder material, RS and SS passing through 300µm sieve as fine aggregate and 12- and 18-mm long BF and 12 mm long PP fibres. The mix proportions have been provided in Table 8.1.

Table 8.1. Mix proportions used for the study.

Mix ID	**#Cement**	**FA**	**SF**	**RS**	**SS**	**w/b**	**SP**	**BF (#%Vol.)**	**PP (%Vol.)**
Control	522.5	838	71.5	573	0	0.24	4.87	2	0.11
HBF	522.5	838	71.5	573	0	0.24	6.56	**1%12+1%18**	0.11
BF1	522.5	838	71.5	573	0	0.24	03.50	**1**	0.11
SS30	522.5	838	71.5	401	172	0.24	8.75	2	0.11
SS100	522.5	838	71.5	0	573	0.24	14.22	2	0.11
* Values presented for binders, fine aggregate and SP are in kg/m^3									
HBF- Hybrid length BF, BF1-1% Vol. of BF, SS30-30% replacement of RS with steel slag, SS100- 100% replacement of RS with steel slag									

In addition to the above, the commonly used aircraft fluids in the form of Aeroshell fluid 31 (hydraulic fluid), Aeroshell Turbine Engine oil 500 (lubricating fluid), and Air traffic fuel were used to investigate their impact. These were purchased from Fledge Aero Private Ltd., Delhi. The lubricating oils contain esters of fatty acid, carboxylic acid, phosphate esters whereas the hydraulic oil contains alcohols, esters of fatty acid and phosphate esters. The jet fuel consists of long chain hydrocarbons and aromatic compounds.

8.2.2 Sample preparation and test methods

The mixing technique used for this study is described in Section 3.3. To evaluate the compressive strength of the composite, four cubes of side length 50 mm were cast for each mix at each combined temperature and fuel exposure level constituting a total of 120 cubes. Additionally, four cubes each were cast for control mix and SS100 for exposure to ETF alone which brings the total to 128 cubes. Also, for assessing the bending strength, three beams of dimensions 350×40×40 mm were cast or each mix and for each combined temperature and fuel exposure level constituting a total of 90 beams. The cubes and beams were demoulded one and a half day after casting and subjected to water curing for 28 days and air curing for another 28 days.

Following the 56-day curing period, the samples were transferred into an environmental chamber for exposure to ETF and aircraft fluids. The aircraft fluids were mixed in equal parts and poured on the samples at the start of each day. Then the chamber programmatically cycled between 20°C and 60°C at a ramp rate of 1°C per minute, including a hold period of two hours at each peak temperature. Each day, the samples underwent four ETF cycles. This has been further explained in Section 3.4.4.

The samples were then removed at intervals corresponding to every 60 combined cycles (CCs) of ETF and aircraft fluid application, to assess their mechanical performance and durability under these conditions. The compressive and bending strength tests were conducted to assess the mechanical performance as per the procedure outlined in Section 3.4.2. SEM, MIP and DSC tests were further carried out after the mechanical testing to get further insight into the core mechanism.

8.3 Results and Discussion

8.3.1 Surface characteristics

Fig. 8.1 demonstrates the variation in surface characteristics when exposed to 300 CCs as compared to the control specimens. The samples appeared darker in colour because of combined effect of aircraft fluids and heat. Except that, the developed mixes demonstrate excellent surface characteristics.

Control HBF BF1 SS30 SS100

(c) Without exposure

Control HBF BF1 SS30 SS100

(d) Exposure to 300 CC

Fig. 8.1. Surface characteristics of all the mixes before and after exposure to ETF

The samples exposed to ETF alone have the tendency to crack because thermal expansion and contraction and thermal mismatch between various constituents of the cementitious composites. The incorporation of BF in the matrix enhances the tensile strength of the composite that can resist the occurrence of cracks. This may also have been aided by the formation of secondary CSH from accelerated FA reaction at ETF temperatures. Furthermore, Shill et al. [33,50,177] suggested saponification can remove aggregates from the surface of the composite. No such damage to the surface was observed up to 300 CCs. This is because of advancement of pozzolanic reaction caused by exposure to ETF which densifies the matrix and reduces the available portlandite. Consequently, no surface degradation or scaling was observed in any of the mixes designed in the current study.

8.3.2 Compressive strength observations

Compressive strength of all the mixes with increasing CCs have been plotted as shown in Fig. 8.2. The control mix and HBF demonstrated similar compressive strengths of ~46 and ~43 MPa. However, decreasing BF volume by 1% in the mix BF1 led to a 12% increase in strength. Additionally, using SS aggregates (30% and 100% SS) improved compressive strength over the control mix.

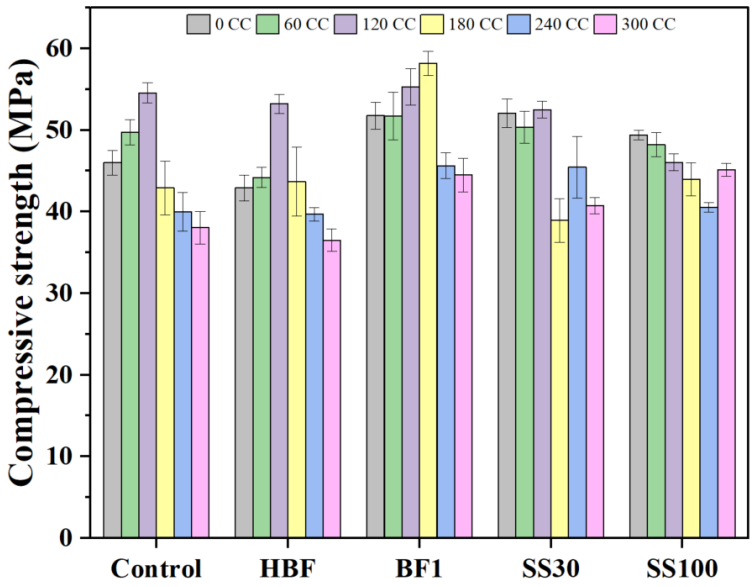

Fig. 8.2. Compressive strength of all mixes with increasing combined ETF and aircraft fluid cycles

Typically, the exposure to ETF alone has the potential to cause internal microcracking and damage to ITZ which leads to strength degradation. On the other hand, the aircraft fluids cause saponification as discussed previously. Up to 120 CCs, the mixes containing only RS demonstrated an improvement in compressive strength owing to the improved pozzolanic and hydration reactions at higher ETF temperatures. This is coupled with delayed reaction of aircraft fluids in calcium deficient cementitious composites. However, upon exposure to 180 CCs, the effect of aircraft fluids became apparent. Significant decline in compressive strengths were observed in all mixes at this exposure level. This is attributed to the reaction of calcite

with carboxylic acid to form calcium carboxylate salts, which reduces the aggregate matrix bond. After exposure to 180 CCs, a reduction in compressive strength (w.r.t 120 CCs) by 25% and 22% was observed for the control and HBF mixes, respectively. However, the mix BF1 demonstrated a continued improvement in strength till 180 CC. This mix contained lower fibre volume which perhaps reduced the porosity of the mix. Consequently, a reduced depth of penetration of aircraft fluids resulted in a higher strength retention at this exposure level.

On the other hand, the mixes with steel slag aggregates, namely, SS30 and SS100, exhibited a reduction in compressive strength immediately after 60 CCs owing to the presence calcium-rich SS aggregates. These aggregates undergo accelerated hydration at ETF temperatures and release additional portlandite in the system that reacts with carboxylic acid from the aircraft fluids to form soap and water. This in agreement with Arrhenius's law which suggests that an increase in temperature increases the reaction rate [178].

The formation of these soaps and salts reduces the elasticity and makes the cementitious composite weaker. The mix with 30% and 100% SS lost around 26% and 4% of its compressive strength (w.r.t 120 CCs) after exposure to 180 CCs.

In terms of failure pattern, the mixes exposed to 180 CCs, demonstrated a highly brittle failure by a single crack. This is evident from the failure pattern observed during the testing of the cubical specimens under compression as shown in Fig. 8.3. The damage pattern in sample not exposed to aircraft fluids exhibit failure by multiple cracking.

(a) Multiple cracking (b) Single crack

Fig. 8.3. Comparison of failure pattern: (a) samples not exposed to CCs and (b) samples exposed to 180 CCs

After exposure to 240 and 300 CCs, strength degradation was less severe than at 180 CCs because of the lesser prevalence of portlandite and calcium carbonate, which are crucial for the saponification. Interestingly, the mix SS100 demonstrated a minor improvement in compressive strength at 300 CCs. This may be because of the pozzolanic reaction of unreacted/partially reacted fly ash particles with the portlandite supplied from the SS aggregates from areas unaffected by the aircraft fluids. The degradation at this point is primarily through ETF. The increased porosity of the matrix through previous exposure to CCs also made the cementitious composite more resistant to ETF as observed through SEM images presented later in the chapter. After exposure to 300 CCs, the loss in strength because of combined effect of ETF and aircraft fluids was approximately 17, 15, 14, 22, and 9% in control, HBF, BF1, SS30 and SS100 specimens, respectively. As can be observed, the performance of FRCC with 100% SS aggregates is better at both 0 CCs (or at ambient temperature) and after exposure to 300 CCs.

8.3.3 Flexural strength

Fig. 8.4 provides the flexural strength of all the mixes up to 300 CCs. As can be observed, hybrid length basalt fibres increased the composite's flexural strength by ~7% possibly because of better bridging effects. On the other hand, reducing BF volume by 1% in the mix BF1 decreased flexural strength by ~19%. The mixes with 30% and 100% SS fine aggregate exhibited similar flexural strength to that of control mix at ambient temperature as shown in Fig. 8.4.

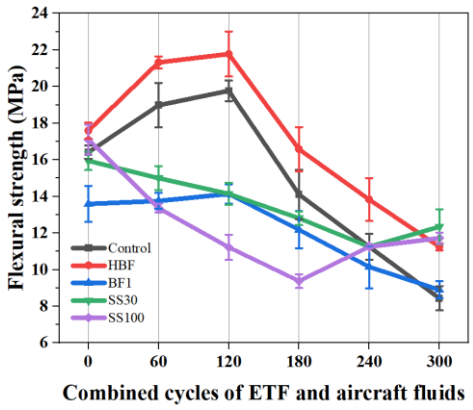

Fig. 8.4. Flexural strength variations of all mixes up to 300 CCs

The mixes with only RS demonstrated an improvement in flexural strength up to 120 CCs owing to the elevated temperature accelerated reaction of FA. The control mix and HBF gained strength ~15% and 21%, respectively over the flexural strengths achieved by the specimens at 0 CCs. The mix BF1 demonstrated a marginal increase in flexural strength. Upon exposing the control, HBF and BF1 mixes to 120 CCs, smaller increment in strengths of approximately 5, 3 and 3% respectively were observed.

After 180 CCs when sample is sufficiently saturated with aircraft fluids in areas with portlandite and calcite, deterioration was observed. All the mixes with RS demonstrated a flexural strength decline between 6-15% after 180 CCs with respect to 0 CCs. After exposure to 240 CCs, a further decline of 22-32% was observed in these mixes. The loss exhibited by the control, HBF, and 1BF was reported to be ~32, 22, and 25%, respectively. The mix HBF performed better than the control mix because of better anchorage of longer BF, while the mix BF1 performed better because of its lower porosity that reduces the ingress of deleterious aircraft fluids. After exposure to 300 CCs, the control mix lost ~49% of its flexural strength while the strength loss of HBF and BF1 was observed to be ~36% and ~35%, respectively.

The mixes SS30 and SS100 both demonstrated a decline in flexural strength immediately after exposure to the first 60 CCs as opposed to an increase in flexural strength as observed in mixes

with RS. This is because of the chemical attack from the aviation fluids on the calcium-rich matrix causing internal saponification. The decline in flexural strength of SS30 was found to be gradual, whereas the mix SS100 lost nearly 46% by 180 CCs. The strength decline for SS30 is continued till 240 CCs and then a reversal is observed at 300 CCs where a part of the flexural strength is recovered. This mix retained the maximum relative residual flexural strength of ~77% after exposure to 300 CCs. The mix SS100 demonstrated a strength redemption from 240 CCs and finally exhibited a higher relative residual flexural strength greater than that of the control mix.

Complete replacement of RS with SS aggregates may not be suggested for airfield pavements subjected to aviation fluids as significant early-stage strength loss is observed. On the other hand, a 30% replacement of RS with SS aggregates can be considered as it brings together positive effects of SS aggregates such as strong ITZ and possible participation in pozzolanic reaction in areas unaffected by aircraft fluids.

8.3.4 SEM analysis

8.3.4.1 General microstructural observations

Fig. 8.5 presents the microstructure of the control mix and SS100 for comparison. These two mixes are chosen given that their behaviour can be used to determine the underlying mechanisms of variations observed in the study. Both the mixes demonstrate abundant presence of uFA particles.

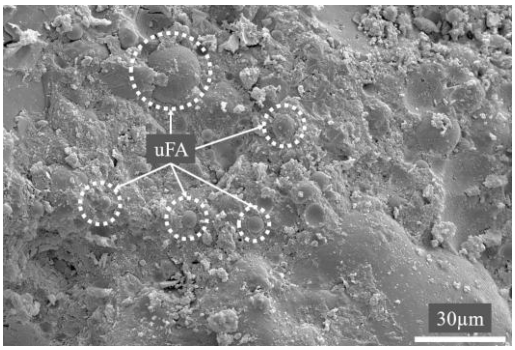

(a) Control

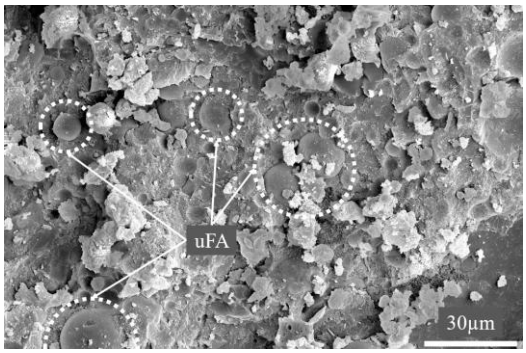

(b) SS100

Fig. 8.5. Microstructure demonstrating abundant unreacted FA content in (a) Control and (b) SS100

Fig. 8.6 further presents the microstructural variations of the control and SS100 when exposed to combined effect of aircraft fluids and ETF. After exposure to 60 CCs, the microstructure of control mix demonstrated an improvement in density while the microstructure of SS100 remained similar to the sample which was not exposed to the combined cycles. Consequently, the strength of the control mix increased by ~8% and the strength of SS100 remained approximately the same.

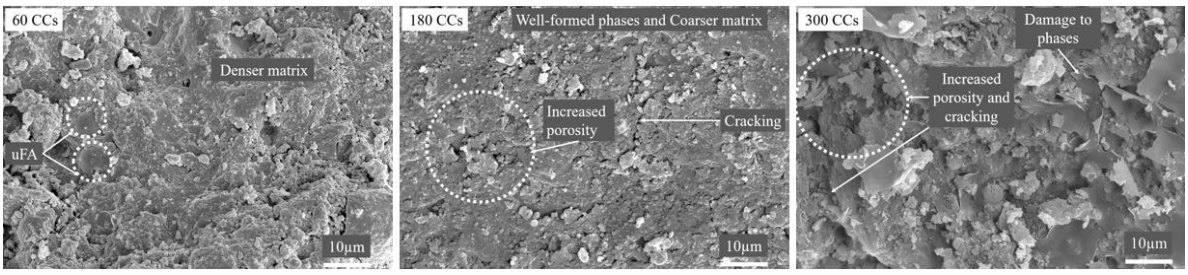

(a) Control mix at various exposure levels

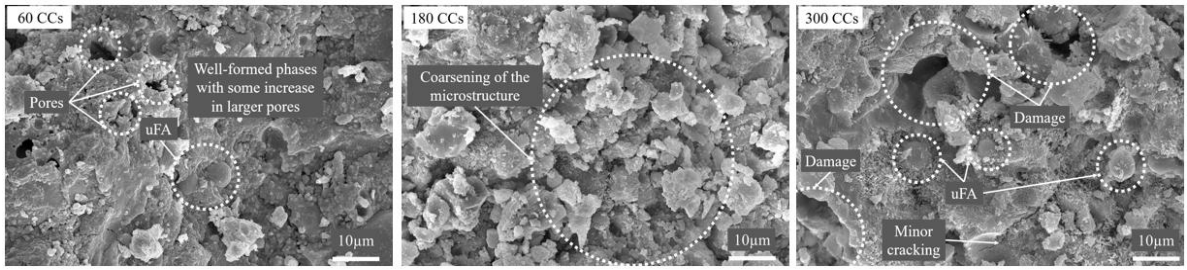

(b) SS100 mix at various exposure levels

Fig. 8.6. Microstructure of (a) Control and (b) SS100 at various exposure levels

After 180 CCs, the microstructure of the control mix began to demonstrate signs of damage with coarsening of the microstructure and increased porosity distributed unevenly throughout the microstructure as shown in Fig. 8.6. The adverse effects of aircraft fluids became apparent only after exposure to 180 CCs for mixes with RS alone. This delay in initiation of damage to the cementitious composite is because of positive effect of HVFA utilization. The unreacted FA particles initially densified the matrix upon exposure to ETF and delayed the percolation of aircraft fluids. Usually, ETF alone causes degradation of microstructure by cracking and pore coarsening which was delayed by the incorporation of TPE in the form of HVFA.

For the mix SS100 severe coarsening was observed in most regions and others demonstrated a formation of denser microstructure as demonstrated in Fig. 8.6 (b) and 8.7, respectively. This variability in behaviour may be attributed to the presence of conditions favourable for saponification in some regions of the samples.

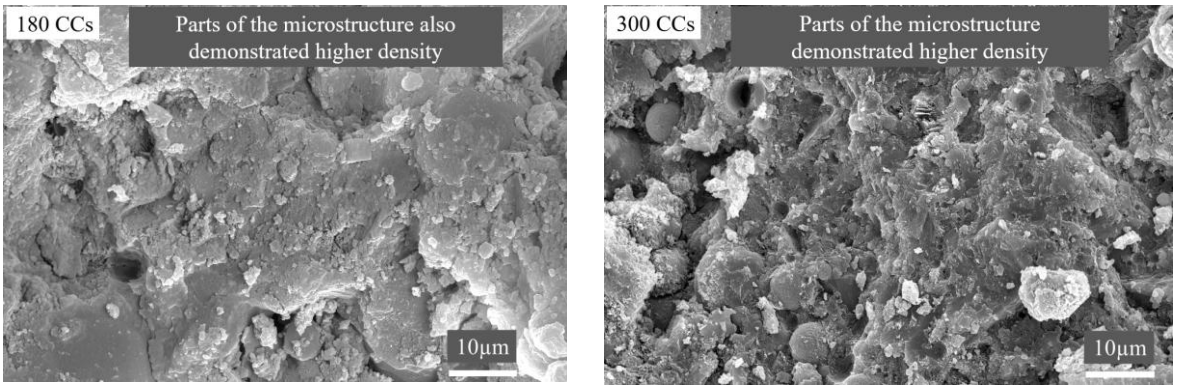

Fig. 8.7. Parts of microstructure with higher density in SS100 without exposure to aircraft fluids

After 300 CCs, the control mix exhibited a damaged microstructure with an increase in porous areas and cracking in addition to the clear signs of damage to the hydration phases. On the other hand, SS100 exhibited significantly enhanced density in comparison to that observed in case of the samples exposed to 180 CCs. This may be because of continued pozzolanic reaction from the parts not exposed to aircraft fluids. The presence of SS aggregates continually supplies the portlandite required for continued pozzolanic reaction which enhances the strength of the composite.

8.3.4.2 ITZ observations

The formation of calcium salts from the reaction of calcium carbonates with esters of fatty acid reduces the bonding between aggregate and paste phase. Therefore, a special focus on variation of ITZ behaviour with increasing combined cycles is essential and a comparison between RS and SS aggregates has been made in Fig. 8.8.

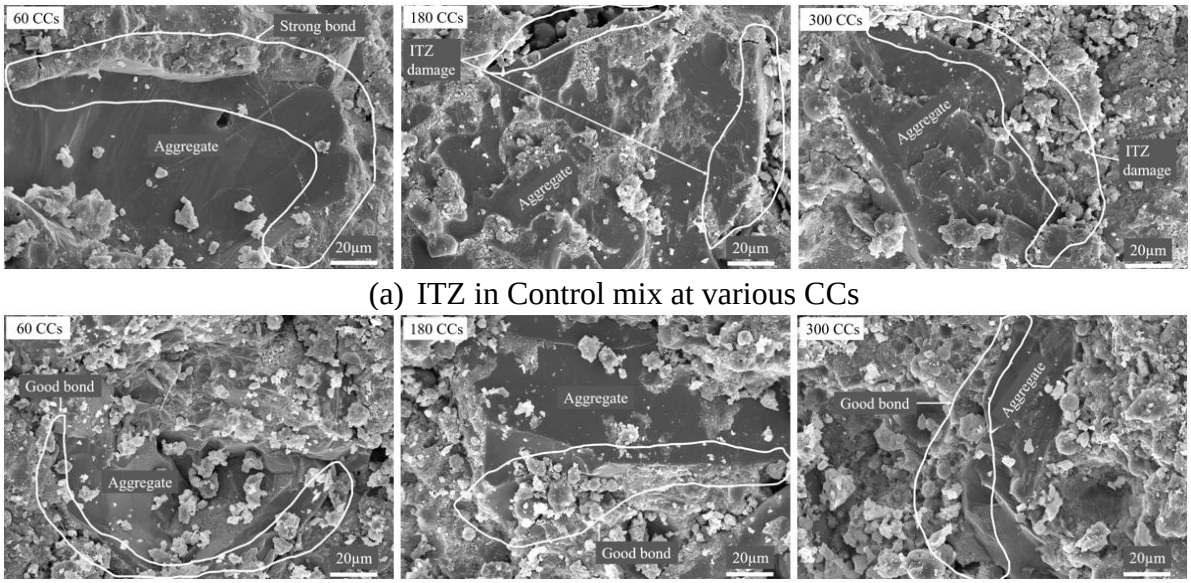

(a) ITZ in Control mix at various CCs

(b) ITZ in SS100 mix at various CCs

Fig. 8.8. Variation of ITZ observed in (a) Control mix and (b) SS100 at 60, 180, and 300 CCs

At 60 CCs, the ITZ of aggregates in control mix demonstrated a strong bond owing to accelerated pozzolanic reaction of uFA at higher temperatures of ETF. This also contributed to the enhancement of compressive strength of the composite. Again at 180 CCs, the effect of aircraft fluids was apparent and the bond between aggregate and cement paste deteriorates. This was exacerbated by differential thermal expansion of aggregate and cement paste. Consequently, this weakening of the ITZ contributed to a steep reduction in compressive strength as observed earlier. At 300 CCs, similar poor bond was observed between aggregate and paste phase.

On the contrary, the bond between SS aggregate and paste phase remained unaffected throughout, despite the calcium-rich products being the primary target of chemical attacks from the aircraft fluids. The strong interlocking of SS aggregates is because of its angular shape and rough texture in addition to the formation of hydration products on its surface when exposed to higher temperatures. Furthermore, the differential thermal expansion between SS aggregates and the paste phase is lesser provided they have similar chemical composition.

8.3.5 MIP analysis

Significant variation in porosity was observed through SEM analysis because of exposure to CCs. Therefore, to gain further insights into the porosity of the material and to ascertain the impact of both ETF and aircraft fluids, MIP analysis was conducted. Fig. 8.9 provides the information on pore size distribution of control and SS100 after exposure to various combined cycles.

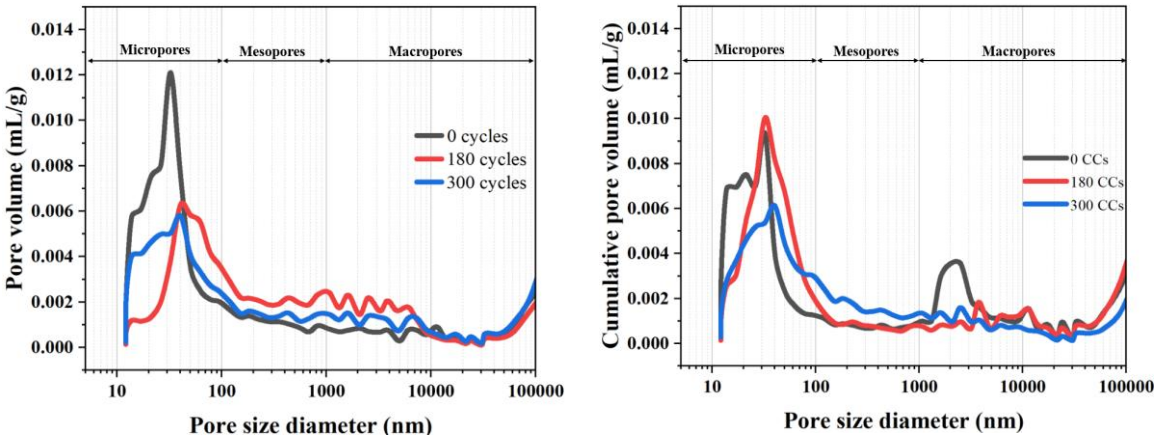

(a) Control (b) SS100

Fig. 8.9. MIP analysis of (a) Control and (b) SS100 after exposure to 0, 180 and 300 CCs

The effect of ETF on reduction of total pore volume is apparent in control mix. After exposure to 180 CCs, significant reduction in the early part of the micropore region is observed. Despite the reduction in smaller sized pores in micropore region, saponification-induced elasticity reduction can cause a decline in compressive strength of the composite. Also, pore coarsening can be observed in the micropore region from a visible shift of the curve towards right towards pores of higher diameter. Also, the curve for pore volume in the mesopore and macropore regions shifted up representing an increase in larger pores. These larger pores upon application of compressive load may have developed a failure plane that caused a brittle failure as shown in Fig. 8.3.

Consequently, a steep decline in compressive strength was observed despite reductions in total pore volume. Again, after exposure to 300 CCs, the micropore region coarsened with a visible

shift of the curve towards right. Also, in the mesopore and macropore region, higher volume of larger sized pores was observed.

For SS100, the application of 180 CCs, caused a significant increase in the pore volume and pore diameter in the micropore region. This was also observed through SEM where severe coarsening of microstructure was observed as demonstrated in Fig. 8.6. This caused a steep decline in compressive strength at 180 CCs. Interestingly, upon continual exposure to ETF and aircraft fluids up to 300 CCs, the significant reduction in total volume of micropores was observed. This is consistent with compressive strength observations and was perhaps due to the improvement caused by pozzolanic reaction of FA aided by the portlandite supplied by SS aggregates in regions not exposed to aircraft fluids. However, this was not sufficient to reduce the mesopores and macropores that continued to coarsen.

Pore coarsening along with saponification induced elasticity reduction can cause a brittle failure in the cementitious composite. Consequently, reduction in smaller sized pores may not always enhance the compressive strength of the composite.

8.3.6 DSC analysis

Fig. 8.10 provides DSC curves for control mix and SS100 after exposure to various exposure conditions. The application of ETF and aircraft fluids causes significant changes to the composition of the FRCC. In all the samples, endothermic peaks were observed near 120-150°C, 450°C, and 750°C. These peaks signify the dehydration of free and physically bound water, dehydroxylation of portlandite, and decarbonation of calcium carbonate, respectively [173,179].

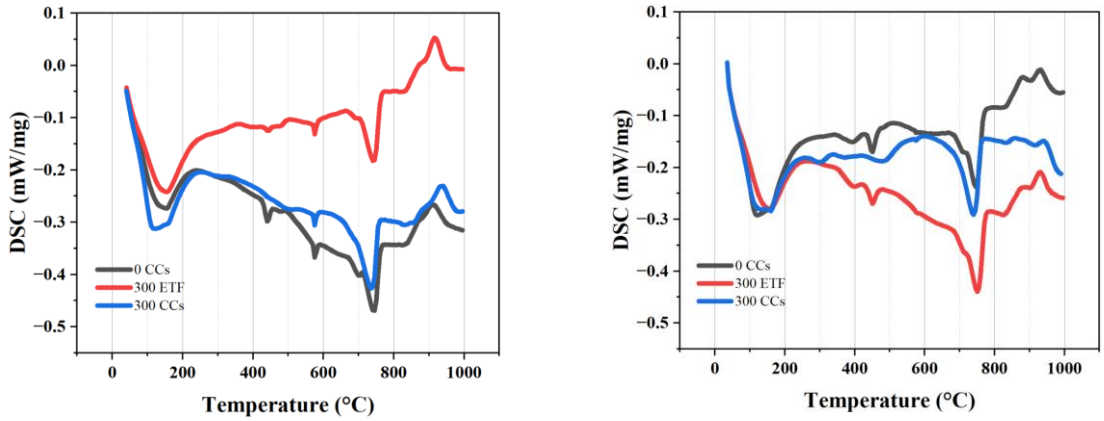

(a) Control (b) 100SS

Fig. 8.10. DSC curves for (a) Control and (b) SS100 after exposure to 0 CCs, 300 CCs and 300 ETF

In case of control mix, the endothermic peak corresponding to portlandite decomposition was absent after exposure to 300 CCs. The removal of portlandite from the system was because of accelerated pozzolanic reaction and saponification. Also, water is a by-product of saponification reaction as discussed earlier. Consequently, the peaks corresponding to dehydration exhibited an increasing energy indicating occurrence of saponification. On the other hand, clear reduction in energy for dehydration is observed in the sample subjected to 300 ETF. The consumption of calcium carbonate by esters of fatty acid to form calcium salts is evident from the reduction in endothermic peak at 300 CCs.

For SS100, it can be observed that portlandite is removed after exposure to 300 CCs. However, the portlandite existed in samples exposed to 300 ETF alone which is mainly contributed by SS aggregates (as this endothermic peak is missing from the control mix exposed to ETF). This portlandite made available by SS aggregates (from regions unaffected by aircraft fluids) improved the pore structure of the cementitious composite as demonstrated using MIP. A higher endothermic peak associated with decarboxylation was observed in case of SS100 subjected only to 300 ETF. The calcium carbonate was consumed by the formation of calcium salts when exposed to combined ETF and aircraft fluids.

8.4 Discussion on the Damage mechanism

The percolation of aviation fluids, the concentration of calcium compounds (namely hydroxide and carbonates), and the exposure temperature critically influence the deterioration of airfield pavements. Moreover, subjecting the surface of airfield pavement to repeated abrasion and impact from aircraft operations also generates FOD. The accumulation of soap on the pavement surface poses a grave risk to the safety of both aircraft and passengers.

The current study proved that systems with reduced concentrations of calcium hydroxide and calcium carbonates are less susceptible to soap formation, thus are more apt for airfield pavement construction. Moreover, the exclusion of coarse aggregates might be considered to improve the integrity of the material due to a homogenous ITZ. The study further demonstrated that when HVFA is utilized as TPE in FRCC, the detrimental effects of aircraft fluids are not immediately evident. This is attributed to the swift consumption of accessible portlandite, particularly near the surface, leading to a consequent densification of the microstructure. Additionally, a reduction in portlandite content decreases the coefficient of thermal expansion of the system, thereby reducing uncoordinated deformation within the cementitious composite, which delays microcracking [47,176].

The ETF, typically detrimental to cementitious composites, has been observed to beneficially delay the penetration of deleterious fluids for the adopted material system. However, once sufficient aircraft fluids infiltrate the sample because of repeated application and encounter regions containing calcium carbonate and/or calcium hydroxide, a process of saponification ensues, rendering the FRCC brittle and deteriorating the bond between the aggregate and the paste phase. Despite the reduction of smaller pores in the micropore region, the saponification-induced decrease in elasticity can lead to lower compressive strength in the composite. This can also be aided by an increase in larger sized pores which could form a failure plane under compressive stresses. Also, the utilization of hybrid BF-PP fibres have proven to be

exceedingly beneficial in mitigating cracking, while also enhancing the flexural strength of the composite [19,20].

The design choice to eliminate larger coarse aggregates is also beneficial. Coarse aggregates with larger sizes tend to have a more porous and weaker interfacial transition zone (ITZ), making them prone to dislodgement [42]. Once dislodged, these aggregates contribute to foreign object debris on pavements, posing a serious risk to aircraft safety and occupant well-being. Additionally, the cracking caused by the differential thermal expansion between the coarse aggregates and the matrix is more pronounced [32].

Therefore, a composite with HVFA, low content of SS fine aggregate with a design choice of elimination of coarse aggregates can be a good combination for the development of construction material suitable for airfield pavement.

8.5 Summary

This chapter focussed on the combined effects of ETF and aircraft fluids on the HVFA based cementitious composite. Macro properties in terms of compressive and flexural strengths were investigated at various exposure levels up to 300 CCs and the damage mechanism was uncovered using SEM, DSC, and MIP. The following conclusions can be derived.

- Compressive strength of the mixes with RS, initially increased up to 120 CCs. An increase of ~18, ~23 and ~6 % was observed in the control mix, HBF and BF1 respectively. A steep decline in compressive strength was observed after exposure to 180 CCs. Compressive strength continued to decline at a slower rate for 240 and 300 CCs.
- The mixes with SS fine aggregates demonstrated immediate decline in compressive strength after exposure to 60 CCs. This was because of the calcium-rich SS that release portlandite at ETF temperatures. The microstructure coarsened significantly after exposure

to 180 CCs. A higher strength was observed when exposed to 300 CCs proving the positive effect of utilization of SS aggregates.

- HVFA as TPE effectively delays the loss in flexural strength up to 120 CCs.
- Both fibre hybridization and fibre volume reduction were found to be effective strategies for reducing the extent of flexural strength deterioration.
- Utilization of SS aggregates reduces the flexural strength initially and is then redeemed with increasing CCs.
- The microstructure of the FRCC demonstrated varied characteristics with some parts demonstrating an improvement in density while others demonstrating porous structures suggesting that the combined exposure to ETF and aircraft fluids induces diverse effect. MIP analysis further revealed the impact of incorporation of HVFA. The pore volume of the control mix in the micropore region reduced upon exposure to 180 CCs and 300 CCs, however, an increase in larger sized pores in mesopore and macropore region was observed. Contrarily, in case of SS100, a steep rise in pore volume in the initial micropore range was observed. Interestingly, after exposure to 300 CCs, a decline in pore volume of initial part of micropore range was observed. This indicates that the SS aggregates which were not affected by aircraft fluids supplied portlandite for continued pozzolanic and hydration reactions. At the same time, pore volume in mesopore and macropore region increased.

Overall, the HVFA-based cementitious composites are less vulnerable to attacks from aircraft fluids considering the carboxylic acid, phosphoric acid, and esters of fatty acids all require calcium hydroxide and calcium carbonate for soap formation. Replacement of cement with low calcium fly ash in high quantities reduces both these compounds that are necessary for deterioration. Upon exposure to ETF, the reactivity of FA particles is enhanced and pozzolanic reaction starts to deplete the available portlandite. Therefore, the HVFA-system can delay and reduce the extent of saponification. Consequently, a better performance can be achieved with

low calcium systems in airfield pavement that are exposed to aviation fluid damage. A complete replacement of RS with SS aggregates is not suggestible given the rapid decline in both compressive and flexural strengths. A lower replacement level of 30% should be considered which yields better results in comparison.

Chapter 9
Conclusions and Future scope

This thesis presents a comprehensive study on the development of fibre-reinforced cementitious composites with enhanced thermal endurance by leveraging the properties of high-volume fly ash, steel slag aggregates and hybrid basalt-polypropylene fibres. The primary aim was to contribute to the advancement of sustainable construction materials by optimizing their performance under various conditions, including high temperatures and environmental thermal fatigue. The research encapsulates a series of systematic investigations involving exposure to high temperatures up to 800°C, cyclic exposure to sub-elevated temperatures in the form of environmental thermal fatigue and long-term durability evaluations. A special case of airfield pavement was also considered in addition to ETF, to assess the durability of the material against chemical attacks from the leaked aircraft fluids. The key findings of this study are provided below.

9.1 Key findings

9.1.1 Utilization of HVFA and hybrid Basalt-Polypropylene Fibres for development of thermally enhanced FRCC

- Mixes 50FA (50% cement replaced by fly ash) and R60FA (60% cement replaced by fly ash with reduced silica fume w.r.t control) retained good strength at 600°C and at 800°C, they showed 46% and 38% strength retention.
- Increase in the HVFA dosage reduced the mass loss of the composite. The HVFA system is especially advantageous at higher temperatures because of reduced portlandite and calcite content.
- The compatible matrix and hybrid fibre combination prevented surface cracking, indicating high temperature resilience. PP fibres mitigated pore pressure and prevented spalling by melting, while basalt fibres preserved specimen integrity.

The mix R60FA was chosen as control mix for subsequent studies because of optimal performance in terms of thermal endurance and sustainability.

9.1.2 Enhancement of the fire performance of developed FRCC with additional utilization of steel slag aggregates

The best performing mix from the previous chapter was used as the base mix and effect of variations in terms of basalt fibre length (12 and 18 mm) and content (2% and 1% by vol.) and steel slag aggregate content as a replacement of river sand (30% and 100%) was studied.

- Incorporating steel slag fine aggregates not only presented a sustainable solution but also delivered significant advantages by improving the ITZ properties through surface reactions and interlocking mechanisms. Similar enhanced performance was observed even in the case of mix with 30% of river sand replaced by steel slag fine aggregates.
- Importantly, both 12BF18 and 100SS demonstrated a residual compressive strength ~56 and ~55% respectively at 800°C, which is a marked improvement over the base mix whose residual strength was ~38% at the same temperature level.

Three of the four mixes outperformed the mix derived from the previous chapter in terms of relative residual compressive strength at all temperature levels. These mixes were further used in the subsequent studies.

9.1.3 Long term durability performance of the developed eco-friendly FRCC

The previous chapter established that excellent thermal performance can be achieved as a result of utilization of high-volume fly ash and steel slag aggregate. In continuation to this, further investigations in terms of long term compressive and flexural strength performance, chloride ion penetration resistance, water absorption, dimensional stability were essential to establish it as a valid construction material.

- Significant improvements in compressive strength over time was noticed because of pozzolanic reaction of fly ash which enhances the overall density of the microstructure and the ITZ around aggregates. This was important considering complex interactions between various constituents did not cause any adverse impact on the long-term compressive strength.
- The developed composite posed as an excellent material for applications requiring high chloride ion penetration resistance.
- Incorporating SS aggregates into cementitious composites repurposes a hazardous material without negatively impacting the mechanical properties. Minor increases in water absorption and electrical charge in RCPT tests was noted.
- No dimensional instability was observed with the incorporation of SS aggregates.

Overall, this chapter demonstrated that the mixes developed satisfies the generally expected mechanical and durability criteria.

9.1.4 Performance of the developed FRCC against Environmental Thermal Fatigue

In this study, the material was checked against 300 ETF cycles between 20 and 60°C to estimate the general trend of material performance.

- All the mixes retained compressive strengths > 100% even after 300 cycles of environmental thermal fatigue.
- Densification of matrix was observed up to 180 ETF cycles as demonstrated using SEM micrographs. Thereafter, internal microcracking and minor coarsening was observed in mixes with RS. On the other hand, FRCC mixes with SS aggregates demonstrated further densification because of continued pozzolanic reaction from the portlandite supplied by the aggregates.

- The thermal cycles have the potential to cause a bond loss between paste phase and the fibre. Consequently, the optimum basalt fibre content was suggested to be 1% (by vol.)

This chapter demonstrated that the theories previously established about strength enhancement and homogenization of the mix work even in case of repeated low temperature thermal cycles.

9.1.5 Performance of the developed FRCC against Environmental Thermal Fatigue and aircraft operating fluids

This chapter further extends the application of the developed material in airfield pavements by assessing its suitability under the combined action of ETF (300 thermal cycles between 20 and 60°C) and chemical attack from leaked aircraft fluids.

- The strength enhancement action of high-volume fly ash delayed the strength deterioration up to 120 cycles. When sufficient aircraft fluids percolate through the system, saponification ensues. This caused coarsening of the pore structure and reduction in elasticity of the composite.
- Mix with 100% steel slag aggregates exhibited steep decline in compressive strength up to 180 cycles. Thereafter, the strength remained comparable to the control specimens.
- The deleterious effect of aircraft fluids on flexural strength was even more pronounced. This was especially true for mixes with steel slag aggregates.
- Overall, cementitious composites based on HVFA were found more resistant to damage from aircraft fluids, as substances like carboxylic acid, phosphoric acid, and esters of fatty acid require calcium hydroxide and calcium carbonate to form soap. However, completely substituting RS with SS aggregates is not recommended for this application due to significant declines in both compressive and flexural strengths. Instead, a lower

replacement level of 30% could be considered, as it provides better results in comparison.

9.2 Proposed hypothesis

The inherent slow reacting property of fly ash can be utilized to enhance the thermal endurance of the cementitious composites across all the temperature ranges considered in the study including cyclic exposure to sub elevated temperatures. Increase in temperature accelerates the pozzolanic reaction of these slow reacting particles to form strength providing CSH. Furthermore, between 400-600°C, formation of tobermorite which is 2-3 times stronger than CSH is observed and is highly beneficial for strength retention. Consequently, normalized relative residual compressive strength greater than 100% can be achieved by incorporating high-volume fly ash in FRCC mixes.

One of the key features of high-volume fly ash mixes is its characteristic portlandite deficiency as large volumes of cement is replaced by low calcium fly ash. Consequently, the amount of calcite formed in the matrix is also reduced. During exposure to high temperatures up to 800°C, dehydroxylation of portlandite and decarbonation of calcite are among the primary mechanisms responsible for the mass loss. Additionally, the available portlandite is consumed during pozzolanic reaction at high temperatures. Consequently, significant reduction in the mass loss can be expected by replacing high volumes of cement by class-F fly ash.

A low portlandite system is also highly useful in reducing the internal microcracking caused by the differential thermal expansion between paste phase and the aggregate. Reducing the portlandite is a good strategy to reduce the coefficient of thermal expansion of the paste phase which effectively establishes a match with the aggregate phase. Consequently, when exposed to elevated temperatures, aggregate debonding and associated cracking can be avoided or delayed.

The low portlandite content of the HVFA system has also been found useful in the special case of airfield pavements where combined effect of environmental thermal fatigue and leaked aircraft fluids were studied. Aircraft fluids contain carboxylic acid and esters of fatty acids which react with calcium hydroxide and calcium carbonate to form calcium carboxylate salts which are known as soaps. In a low portlandite system, this reaction cannot continue for longer duration which reduces the extent of degradation generally observed in ordinary concrete.

Further enhancements in thermal performance can be achieved by incorporating steel slag fine aggregates as they have the potential the homogenize the whole cementitious composite and reduce the extent of degradation at elevated temperatures. The chemical composition of steel slag is similar to that of OPC which reduces the uncoordinated expansion between aggregate and cement phase when exposed to elevated temperatures. The differential thermal expansion in addition to generating cracks in the composite causes the loss of bond between aggregate and cement phase. In case of steel slag fine aggregates, a strong interlocking can be established at ambient temperature because of its angular shape and porous surface. Furthermore, these aggregates retain a strong bond with the surrounding matrix up to 800°C because of the hydration reactions on the surface of the aggregates in addition to its shape and surface morphology. These aggregates also maintain excellent bond with the surrounding matrix even in the case of repeated thermal cycles during environmental thermal fatigue. Furthermore, their active participation in pozzolanic reaction by supplying necessary portlandite helps retain higher compressive strength.

9.3 Limitations and future scope

This study was dedicated to developing a construction material with superior thermal resistance, with a focus on understanding how the chemical makeup of paste and aggregate ingredients influences phase changes. Each section of the thesis acknowledges specific limitations.

- In chapters 4 and 5, exploring the impact of high temperatures on the tensile properties of cementitious composites can be a valuable contribution to existing literature, particularly noting the limited research on the ductility of basalt fibre-reinforced cementitious composites.
- One of the key observations from chapter 6 is the high chloride ion penetration resistance (determined using RCPT) of the developed cementitious composite. This can further be explored using salt ponding test, accelerated chloride migration test, resistance to sulphate resistance to abrasion etc to assess its suitability for offshore structures.
- The bond behaviour of basalt fibres with the surrounding matrix plays a crucial role in both ambient and high temperature mechanical performance of the cementitious composite. In chapter 6 and 7, it was observed that the basalt fibres do not form a very strong bond with the surrounding matrix, and this worsens when exposed to repeated thermal cycles. Therefore, further research in the field of surface modification of basalt fibres can effectively enhance the mechanical properties of cementitious composites.
- In chapter 8, it was determined that the steel slag fine aggregates in raw form are not ideal for airfield pavement conditions. Stabilization of steel slag aggregates using carbonation or water treatment can effectively mitigate the ill effects and improve the sustainability of the composite. Also, the 100SS mix exposed to 300CCs, a significant decline in flexural strength was observed. However, the compressive strength showed a less pronounced reduction. This may be due to the susceptibility of BF to acidic conditions (caused by carboxylic acid from aircraft fluids), which degrade its mechanical properties. Therefore, it is recommended to study the effects of aircraft fluids on various fibers to identify the most suitable fiber for this application.

  The observations in this study are empirical and may change if there are significant variations in the properties of the materials. HVFA based cementitious composites have

previously been investigated for their performance at elevated temperatures and literature provides varying results. However, all the available literature equivocally suggests an improvement in thermal properties (up to 600°C) and chloride resistance, despite the inherent varying nature of FA. Also, the observations concerning SS fine aggregates are specifically relevant to their untreated form where the chemical composition has not been altered. Therefore, further studies pertaining to the effect of variation in chemical composition, physical properties on thermal and durability properties of cementitious composites are essential.

Overall, the developed cementitious composites exhibited good thermal resistance and durability which makes them suitable for general construction purposes. With further testing at a structural scale and with appropriate thermal loading, this material could potentially be applied in high-rise buildings, where fire safety is a critical requirement. Its strong resistance to ETF also suggests suitability for large surfaces exposed to fluctuating temperatures and environmental conditions, such as bridge decks, where continuous temperature variations and water splashing are common. Also, with its high chloride resistance, it can be used for construction of structures near seashore.

References

[1] A. Kunche, B. Mielczarek, Application of system dynamic modelling for evaluation of co2 emissions and expenditure for captive power generation scenarios in the cement industry, Energies (Basel) 14 (2021). https://doi.org/10.3390/en14113115.

[2] C. Gunasekara, M. Sandanayake, Z. Zhou, D.W. Law, S. Setunge, Effect of nano-silica addition into high volume fly ash–hydrated lime blended concrete, Constr Build Mater 253 (2020). https://doi.org/10.1016/j.conbuildmat.2020.119205.

[3] C. Meyer, The greening of the concrete industry, Cem Concr Compos 31 (2009) 601–605. https://doi.org/10.1016/j.cemconcomp.2008.12.010.

[4] A.M. Rashad, An exploratory study on high-volume fly ash concrete incorporating silica fume subjected to thermal loads, J Clean Prod 87 (2015) 735–744. https://doi.org/10.1016/j.jclepro.2014.09.018.

[5] G.K. Park, H.J. Yim, Evaluation of Fire-Damaged Concrete: An Experimental Analysis based on Destructive and Nondestructive Methods, Int J Concr Struct Mater 11 (2017) 447–457. https://doi.org/10.1007/s40069-017-0211-x.

[6] V. Kodur, Properties of concrete at elevated temperatures, ISRN Civil Engineering 2014 (2014). https://doi.org/10.1155/2014/468510.

[7] M. Sandanayake, Y. Bouras, R. Haigh, Z. Vrcelj, Current sustainable trends of using waste materials in concrete—a decade review, Sustainability 12 (2020) 1–38. https://doi.org/10.3390/su12229622.

[8] É. Lublóy, K. Kopecskó, G.L. Balázs, Á. Restás, I.M. Szilágyi, Improved fire resistance by using Portland-pozzolana or Portland-fly ash cements, J Therm Anal Calorim 129 (2017) 925–936. https://doi.org/10.1007/s10973-017-6245-0.

[9] C.D. Atiş, O. Karahan, Properties of steel fiber reinforced fly ash concrete, Constr Build Mater 23 (2009) 392–399. https://doi.org/10.1016/j.conbuildmat.2007.11.002.

[10] A.K. Saha, Effect of class F fly ash on the durability properties of concrete, Sustainable Environment Research 28 (2018) 25–31. https://doi.org/10.1016/j.serj.2017.09.001.

[11] A.M. Rashad, A brief on high-volume Class F fly ash as cement replacement – A guide for Civil Engineer, International Journal of Sustainable Built Environment 4 (2015) 278–306. https://doi.org/10.1016/j.ijsbe.2015.10.002.

[12] C. Herath, C. Gunasekara, D.W. Law, S. Setunge, Performance of high volume fly ash concrete incorporating additives: A systematic literature review, Constr Build Mater 258 (2020). https://doi.org/10.1016/j.conbuildmat.2020.120606.

[13] P.R. de Matos, M. Foiato, L.R. Prudêncio, Ecological, fresh state and long-term mechanical properties of high-volume fly ash high-performance self-compacting concrete, Constr Build Mater 203 (2019) 282–293. https://doi.org/10.1016/j.conbuildmat.2019.01.074.

[14] J. Vargas, A. Halog, Effective carbon emission reductions from using upgraded fly ash in the cement industry, J Clean Prod 103 (2015) 948–959. https://doi.org/10.1016/j.jclepro.2015.04.136.

[15] M. Ondova, N. Stevulova, A. Estokova, The study of the properties of fly ash based concrete composites with various chemical admixtures, Procedia Eng 42 (2012) 1863–1872. https://doi.org/10.1016/j.proeng.2012.07.582.

[16] S. Du, Y. Ge, X. Shi, A targeted approach of employing nano-materials in high-volume fly ash concrete, Cem Concr Compos 104 (2019) 103390. https://doi.org/10.1016/j.cemconcomp.2019.103390.

[17] M. Heikal, Effect of temperature on the physico-mechanical and mineralogical properties of Homra pozzolanic cement pastes, Cem Concr Res 30 (2000) 1835–1839.

[18] M. Heikal, H. El-Didamony, T.M. Sokkary, I.A. Ahmed, Behavior of composite cement pastes containing microsilica and fly ash at elevated temperature, Constr Build Mater 38 (2013) 1180–1190. https://doi.org/10.1016/j.conbuildmat.2012.09.069.

[19] E.S. Rentier, L.H. Cammeraat, The environmental impacts of river sand mining, Science of the Total Environment 838 (2022) 155877. https://doi.org/10.1016/j.scitotenv.2022.155877.

[20] M. Dan Gavriletea, Environmental impacts of sand exploitation. Analysis of sand market, Sustainability 9 (2017). https://doi.org/10.3390/su9071118.

[21] J.T. Kolawole, A.J. Babafemi, S.C. Paul, A. du Plessis, Performance of concrete containing Nigerian electric arc furnace steel slag aggregate towards sustainable production, Sustainable Materials and Technologies 25 (2020) e00174. https://doi.org/10.1016/j.susmat.2020.e00174.

[22] X. Liang, C. Wu, Y. Su, Z. Chen, Z. Li, Development of ultra-high performance concrete with high fire resistance, Constr Build Mater 179 (2018) 400–412. https://doi.org/10.1016/j.conbuildmat.2018.05.241.

[23] P. Ter Teo, S.K. Zakaria, S.Z. Salleh, M.A.A. Taib, N.M. Sharif, A.A. Seman, J.J. Mohamed, M. Yusoff, A.H. Yusoff, M. Mohamad, M.N. Masri, S. Mamat, Assessment of electric arc furnace (EAF) steel slag waste's recycling options into value added green products: A review, Metals (Basel) 10 (2020) 1–21. https://doi.org/10.3390/met10101347.

[24] S. Rawat, C.K. Lee, Y.X. Zhang, Performance of fibre-reinforced cementitious composites at elevated temperatures : A review, Constr Build Mater 292 (2021) 123382. https://doi.org/10.1016/j.conbuildmat.2021.123382.

[25] Y. Li, K.H. Tan, E.H. Yang, Synergistic effects of hybrid polypropylene and steel fibers on explosive spalling prevention of ultra-high performance concrete at elevated temperature, Cem Concr Compos 96 (2019) 174–181. https://doi.org/10.1016/j.cemconcomp.2018.11.009.

[26] S. Rawat, R. Narula, N. Upasani, G. Muthukumar, A relook on dosage of basalt chopped fibres and its influence on characteristics of concrete, Lecture Notes in Civil Engineering 35 (2020) 87–96. https://doi.org/10.1007/978-981-13-7480-7_7.

[27] H. Jamshaid, R. Mishra, A green material from rock: basalt fiber – a review, Journal of the Textile Institute 107 (2016) 923–937. https://doi.org/10.1080/00405000.2015.1071940.

[28] A. Tangirala, S. Rawat, M. Lahoti, Performance of ternary blended Basalt-Polypropylene fibre reinforced cementitious composite at elevated temperatures, in: SiF 2022– The 12th International Conference on Structures in Fire, 2022: pp. 457–465.

[29] M. Xu, S. Song, L. Feng, J. Zhou, H. Li, V.C. Li, Development of basalt fiber engineered cementitious composites and its mechanical properties, Constr Build Mater 266 (2021). https://doi.org/10.1016/j.conbuildmat.2020.121173.

[30] M.T. Afzal, R.A. Khushnood, W. Ahmed, An Experimental Investigation on Assessment of Residual Mechanical Performance of Basalt Fiber Reinforced High Strength Concrete at Elevated, Fire Technol 58 (2022) 3067–3090. https://doi.org/10.1007/s10694-022-01279-2.

[31] Z. Li, H. Shang, S. Xiao, L. Yang, Z. Li, Effect of thermal fatigue on mechanical properties and microstructure of concrete in constant ambient humidity, Constr Build Mater 368 (2023). https://doi.org/10.1016/j.conbuildmat.2023.130367.

[32] M. An, H. Huang, Y. Wang, G. Zhao, Effect of thermal cycling on the properties of high-performance concrete: Microstructure and mechanism, Constr Build Mater 243 (2020). https://doi.org/10.1016/j.conbuildmat.2020.118310.

[33] S.K. Shill, S. Al-Deen, M. Ashraf, Concrete durability issues due to temperature effects and aviation oil spillage at military airbase – A comprehensive review, Constr Build Mater 160 (2018) 240–251. https://doi.org/10.1016/j.conbuildmat.2017.11.025.

[34] A. Korten, V. Wetzig, Spalling of concrete - Influence of porosity and specimen size and its critical factors regarding safety, in: MATEC Web of Conferences, EDP Sciences, 2013. https://doi.org/10.1051/matecconf/20130601010.

[35] A.C.Y. Yuen, T.B.Y. Chen, A. Li, I.M. De Cachinho Cordeiro, L. Liu, H. Liu, A.L.P. Lo, Q.N. Chan, G.H. Yeoh, Evaluating the fire risk associated with cladding panels: An overview of fire incidents, policies, and future perspective in fire standards, Fire Mater 45 (2021) 663–689. https://doi.org/10.1002/fam.2973.

[36] Q. Ma, R. Guo, Z. Zhao, Z. Lin, K. He, Mechanical properties of concrete at high temperature-A review, Constr Build Mater 93 (2015) 371–383. https://doi.org/10.1016/j.conbuildmat.2015.05.131.

[37] C. Alonso, L. Fernandez, Dehydration and rehydration processes of cement paste exposed to high temperature environments, J Mater Sci 39 (2004) 3015–3024.

[38] G. Wang, C. Zhang, B. Zhang, Q. Li, Z. Shui, Study on the high-temperature behavior and rehydration characteristics of hardened cement paste, Fire Mater 39 (2015) 741–750. https://doi.org/10.1002/fam.2269.

[39] M.K. Dash, S.K. Patro, P.K. Acharya, M. Dash, Impact of elevated temperature on strength and micro-structural properties of concrete containing water-cooled ferrochrome slag as fine aggregate, Constr Build Mater 323 (2022) 126542. https://doi.org/10.1016/j.conbuildmat.2022.126542.

[40] L. Alarcon-Ruiz, G. Platret, E. Massieu, A. Ehrlacher, The use of thermal analysis in assessing the effect of temperature on a cement paste, Cem Concr Res 35 (2005) 609–613. https://doi.org/10.1016/j.cemconres.2004.06.015.

[41] I. Halikia, L. Zoumpoulakis, E. Christodoulou, D. Prattis, Kinetic study of the thermal decomposition of calcium carbonate by isothermal methods of analysis, The European Journal of Mineral Processing and Environmental Protection 1 (2001) 89–102.

[42] A. Elsharief, M.D. Cohen, J. Olek, Influence of aggregate size, water cement ratio and age on the microstructure of the interfacial transition zone, Cem Concr Res 33 (2003) 1837–1849. https://doi.org/10.1016/S0008-8846(03)00205-9.

[43] L. Stelzner, B. Powierza, T. Oesch, R. Dlugosch, F. Weise, Thermally-induced moisture transport in high-performance concrete studied by X-ray-CT and 1H-NMR, Constr Build Mater 224 (2019) 600–609. https://doi.org/10.1016/j.conbuildmat.2019.07.065.

[44] S. Sinaie, A. Heidarpour, X.L. Zhao, A micro-mechanical parametric study on the strength degradation of concrete due to temperature exposure using the discrete element method, Int J Solids Struct 88–89 (2016) 165–177. https://doi.org/10.1016/j.ijsolstr.2016.03.009.

[45] H. Zeng, W. Li, M. Jin, J. Zhang, Y. Ma, C. Lu, J. Liu, Deterioration of performances and structures of cement pastes under the action of thermal cycling fatigue, Int J Fatigue 165 (2022). https://doi.org/10.1016/j.ijfatigue.2022.107181.

[46] X. Chen, D. Shi, S. Guo, Experimental Study on Damage Evaluation, Pore Structure and Impact Tensile Behavior of 10-Year-Old Concrete Cores After Exposure to High Temperatures, Int J Concr Struct Mater 14 (2020). https://doi.org/10.1186/s40069-020-0393-5.

[47] H. Huang, M. An, Y. Wang, Z. Yu, W. Ji, Effect of environmental thermal fatigue on concrete performance based on mesostructural and microstructural analyses, Constr Build Mater 207 (2019) 450–462. https://doi.org/10.1016/j.conbuildmat.2019.02.072.

[48] G. White, Comparing the cost of rigid and flexible aircraft pavements using a parametric whole of life cost analysis, Infrastructures (Basel) 6 (2021). https://doi.org/10.3390/infrastructures6080117.

[49] H. Ma, Z. Zhang, Paving an engineered cementitious composite (ECC) overlay on concrete airfield pavement for reflective cracking resistance, Constr Build Mater 252 (2020). https://doi.org/10.1016/j.conbuildmat.2020.119048.

[50] S. Kumer Shill, S. Al-Deen, M. Ashraf, Saponification and scaling in ordinary concrete exposed to hydrocarbon fluids and high temperature at military airbases, Constr Build Mater 215 (2019) 765–776. https://doi.org/10.1016/j.conbuildmat.2019.04.215.

[51] S.K. Shill, S. Al-Deen, M. Ashraf, M.M. Hossain, Residual properties of conventional concrete repetitively exposed to high thermal shocks and hydrocarbon fluids, Constr Build Mater 252 (2020). https://doi.org/10.1016/j.conbuildmat.2020.119072.

[52] M.M. Hossain, S. Al-Deen, M.K. Hassan, S.K. Shill, M.A. Kader, W. Hutchison, Mechanical and thermal properties of hybrid fibre-reinforced concrete exposed to recurrent high temperature and aviation oil, Materials 14 (2021). https://doi.org/10.3390/ma14112725.

[53] S. Kumer, Cementitious Composites to Mitigate Surface Scaling of Concrete at Military Airbases, 2020. https://doi.org/10.26190/unsworks/22109.

[54] H. Wang, C. Thakkar, X. Chen, S. Murrel, Life-cycle assessment of airport pavement design alternatives for energy and environmental impacts, J Clean Prod 133 (2016) 163–171. https://doi.org/10.1016/j.jclepro.2016.05.090.

[55] C. Fu, M. Chen, R. Guo, R. Qi, Green-Engineered Cementitious Composite Production with High-Strength Synthetic Fiber and Aggregate Replacement, Materials 15 (2022). https://doi.org/10.3390/ma15093047.

[56] V. Pantić, S. Šupić, M. Vučinić-Vasić, T. Nemeš, M. Malešev, I. Lukić, V. Radonjanin, Effects of Grinding Methods and Water-to-Binder Ratio on the Properties of Cement Mortars Blended with Biomass Ash and Ceramic Powder, Materials 16 (2023). https://doi.org/10.3390/ma16062443.

[57] S. Wu, K.A. Moges, P. Vashistha, S. Pyo, Sustainable cementitious composites with 30% porosity and a compressive strength of 30 MPa, Journal of Materials Research and Technology 25 (2023) 5494–5505. https://doi.org/10.1016/j.jmrt.2023.07.036.

[58] R.M. Andrew, Global CO2 emissions from cement production, 1928-2018, Earth Syst Sci Data 11 (2019) 1675–1710. https://doi.org/10.5194/essd-11-1675-2019.

[59] Y. Zhou, W. Guo, S. Zheng, F. Xing, M. Guo, Z. Zhu, Development of Sustainable Engineered Cementitious Composites by Incorporating Local Recycled Fine Aggregate, Polymers (Basel) 15 (2023). https://doi.org/10.3390/polym15122701.

[60] L. Li, M. Khan, X. Jiang, P. Shakor, Y. Zhang, Sustainable Fiber Reinforced Cementitious Composites for Construction and Building Materials, Frontiers Media SA, 2023. https://doi.org/10.3389/978-2-8325-3055-9.

[61] A.M. Onaizi, G.F. Huseien, N.H.A. Shukor Lim, W.C. Tang, M. Alhassan, M. Samadi, Effective Microorganisms and Glass Nanopowders from Waste Bottle Inclusion on Early Strength and Microstructure Properties of High-Volume Fly-Ash-Based Concrete, Biomimetics 7 (2022). https://doi.org/10.3390/biomimetics7040190.

[62] M.P. Mokal, R. Mandal, S. Nayak, S.K. Panda, Efficacy of high-volume fly ash and slag on the physicomechanical, durability, and analytical characteristics of high-strength mass concrete, Journal of Building Engineering 76 (2023). https://doi.org/10.1016/j.jobe.2023.107295.

[63] A. Georgiou, N. Chousidis, I. Ioannou, Self-Compacting Cementitious Composites with Heavy Fuel Fly Ash Replacement, Construction Materials 2 (2022) 276–296. https://doi.org/10.3390/constrmater2040018.

[64] G.F. Huseien, Z. Kubba, A.M. Mhaya, N.H. Malik, J. Mirza, Impact Resistance Enhancement of Sustainable Geopolymer Composites Using High Volume Tile Ceramic Wastes, Journal of Composites Science 7 (2023). https://doi.org/10.3390/jcs7020073.

[65] M. Asabonga, B. Cecilia, M.C. Mpundu, N.M.D. Vincent, The physical and environmental impacts of sand mining, Transactions of the Royal Society of South Africa 72 (2017) 1–5. https://doi.org/10.1080/0035919X.2016.1209701.

[66] W.L. Filho, J. Hunt, A. Lingos, J. Platje, L.W. Vieira, M. Will, M.D. Gavriletea, The unsustainable use of sand: Reporting on a global problem, Sustainability (Switzerland) 13 (2021). https://doi.org/10.3390/su13063356.

[67] S.K. Singh, P. Vashistha, R. Chandra, A.K. Rai, Study on leaching of electric arc furnace (EAF) slag for its sustainable applications as construction material, Process Safety and Environmental Protection 148 (2021) 1315–1326. https://doi.org/10.1016/j.psep.2021.01.039.

[68] R.I. Iacobescu, D. Koumpouri, Y. Pontikes, R. Saban, G.N. Angelopoulos, Valorisation of electric arc furnace steel slag as raw material for low energy belite cements, J Hazard Mater 196 (2011) 287–294. https://doi.org/10.1016/j.jhazmat.2011.09.024.

[69] F. Maghool, A. Arulrajah, Y.J. Du, S. Horpibulsuk, A. Chinkulkijniwat, Environmental impacts of utilizing waste steel slag aggregates as recycled road construction materials, Clean Technol Environ Policy 19 (2017) 949–958. https://doi.org/10.1007/s10098-016-1289-6.

[70] M.D. Yehualaw, D. Fantahun, S.A. Endale, S. Getahun, D.-H. Vo, Investigation on Utilizing of Steel Slag as a Partial Replacement of Natural River Sand as a Fine Aggregate in Concrete Production, in: Green Energy and Technology , 2023: pp. 143–165. https://doi.org/10.1007/978-3-031-33610-2_8.

[71] H.L. Dinh, J. Liu, D.E.L. Ong, J.H. Doh, A sustainable solution to excessive river sand mining by utilizing by-products in concrete manufacturing: A state-of-the-art review, Cleaner Materials 6 (2022). https://doi.org/10.1016/j.clema.2022.100140.

[72] T. Vaddeboina, G. Rama krishna, P. Kumar Balguri, Effect of steel slag on the properties of self compacting concrete, Mater Today Proc 62 (2022) 3011–3014. https://doi.org/10.1016/j.matpr.2022.02.645.

[73] X. Yu, Z. Tao, T.Y. Song, Z. Pan, Performance of concrete made with steel slag and waste glass, Constr Build Mater 114 (2016) 737–746. https://doi.org/10.1016/j.conbuildmat.2016.03.217.

[74] A. Adesina, Performance of cementitious composites reinforced with chopped basalt fibres – An overview, Constr Build Mater 266 (2021). https://doi.org/10.1016/j.conbuildmat.2020.120970.

[75] M. Inman, E.R. Thorhallsson, K. Azrague, A Mechanical and Environmental Assessment and Comparison of Basalt Fibre Reinforced Polymer (BFRP) Rebar and Steel Rebar in Concrete Beams, Energy Procedia 111 (2017) 31–40. https://doi.org/10.1016/j.egypro.2017.03.005.

[76] A. Alaskar, A. Albidah, A.S. Alqarni, R. Alyousef, H. Mohammadhosseini, Performance evaluation of high-strength concrete reinforced with basalt fibers exposed to elevated temperatures, Journal of Building Engineering 35 (2021). https://doi.org/10.1016/j.jobe.2020.102108.

[77] J. Sim, C. Park, D.Y. Moon, Characteristics of basalt fiber as a strengthening material for concrete structures, Compos B Eng 36 (2005) 504–512. https://doi.org/10.1016/j.compositesb.2005.02.002.

[78] P. Matar, J.J. Assaad, Concurrent effects of recycled aggregates and polypropylene fibers on workability and key strength properties of self-consolidating concrete, Constr Build Mater 199 (2019) 492–500. https://doi.org/10.1016/j.conbuildmat.2018.12.091.

[79] Y. Ling, P. Zhang, J. Wang, Y. Chen, Effect of PVA fiber on mechanical properties of cementitious composite with and without nano-SiO2, Constr Build Mater 229 (2019). https://doi.org/10.1016/j.conbuildmat.2019.117068.

[80] R. Siddique, Properties of concrete incorporating high volumes of class F fly ash and san fibers, Cem Concr Res 34 (2004) 37–42. https://doi.org/10.1016/S0008-8846(03)00192-3.

[81] F.U.A. Shaikh, S.W.M. Supit, Mechanical and durability properties of high volume fly ash (HVFA) concrete containing calcium carbonate (CaCO3) nanoparticles, Constr Build Mater 70 (2014) 309–321. https://doi.org/10.1016/j.conbuildmat.2014.07.099.

[82] A. Durán-Herrera, C.A. Juárez, P. Valdez, D.P. Bentz, Evaluation of sustainable high-volume fly ash concretes, Cem Concr Compos 33 (2011) 39–45. https://doi.org/10.1016/j.cemconcomp.2010.09.020.

[83] Y. Li, B. Wu, R. Wang, Critical review and gap analysis on the use of high-volume fly ash as a substitute constituent in concrete, Constr Build Mater 341 (2022). https://doi.org/10.1016/j.conbuildmat.2022.127889.

[84] D. Bhuvaneswari, V. Revathi, K. Thiyagu, Effect of addition of NaOH on compressive strength of high volume fly ash concrete, International Journal of Earth Sciences and Engineering 7 (2014) 2614–2619. https://doi.org/10.33736/jcest.5081.2023.

[85] S. Du, Q. Zhao, X. Shi, High-Volume Fly Ash-Based Cementitious Composites as Sustainable Materials: An Overview of Recent Advances, Advances in Civil Engineering 2021 (2021). https://doi.org/10.1155/2021/4976169.

[86] C. Herath, C. Gunasekara, D.W. Law, S. Setunge, Long term mechanical performance of nano-engineered high volume fly ash concrete, Journal of Building Engineering 43 (2021). https://doi.org/10.1016/j.jobe.2021.103168.

[87] R. Siddique, Wear Resistance of High-Volume Fly Ash Concrete, n.d. http://ljs.academicdirect.org.

[88] B.J. Kim, G.W. Lee, Y.C. Choi, Hydration and Mechanical Properties of High-Volume Fly Ash Concrete with Nano-Silica and Silica Fume, Materials 15 (2022). https://doi.org/10.3390/ma15196599.

[89] C.S. Poon, L. Lam, Y.L. Wong, A study on high strength concrete prepared with large volumes of low calcium fly ash, Cem Concr Res 30 (2000) 447–455.

[90] J.H. Filho, ; M H F Medeiros, ; E Pereira, ; P Helene, M. Asce, G.C. Isaia, High-Volume Fly Ash Concrete with and without Hydrated Lime: Chloride Diffusion Coefficient from Accelerated Test, 2013.

[91] M. Şahmaran, I.Ö. Yaman, M. Tokyay, Transport and mechanical properties of self consolidating concrete with high volume fly ash, Cem Concr Compos 31 (2009) 99–106. https://doi.org/10.1016/j.cemconcomp.2008.12.003.

[92] T. Cheewaket, C. Jaturapitakkul, W. Chalee, Long term performance of chloride binding capacity in fly ash concrete in a marine environment, Constr Build Mater 24 (2010) 1352–1357. https://doi.org/10.1016/j.conbuildmat.2009.12.039.

[93] H. Hirao, K. Yamada, H. Takahashi, H. Zibara, Chloride Binding of Cement Estimated by Binding Isotherms of Hydrates, Journal of Advanced Concrete Technology 3 (2005) 77–84.

[94] ASTM C 1202-07, Standard test method for electrical indication of concrete's ability to resist chloride ion penetration, ASTM International, West Conshohocken, PA., 2007.

[95] H. Yadav, S. Kumar, B. Rai, Durability and fire resistance of high-performance fiber reinforced concrete with fly ash, Journal of Structural Integrity and Maintenance (2023). https://doi.org/10.1080/24705314.2023.2262249.

[96] S. Bernstein, K.T. Fehr, The formation of 1.13 nm tobermorite under hydrothermal conditions: 1. the influence of quartz grain size within the system CaO-SiO 2-D 2O, Progress in Crystal Growth and Characterization of Materials 58 (2012) 84–91. https://doi.org/10.1016/j.pcrysgrow.2012.02.006.

[97] J.A. Gard, J.W. Howison, H.F.W. Taylor, Synthetic compounds related to tobermorite: an electron-microscope, X-ray, and dehydration study, Https://Doi.Org/10.1680/Macr.1959.11.33.151 11 (2015) 151–158. https://doi.org/10.1680/MACR.1959.11.33.151.

[98] P. Paradiso, R.L. Santos, R.B. Horta, J.N.C. Lopes, P.J. Ferreira, R. Colaço, Formation of nanocrystalline tobermorite in calcium silicate binders with low C/S ratio, Acta Mater 152 (2018) 7–15. https://doi.org/10.1016/j.actamat.2018.04.006.

[99] M. Chen, L. Lu, S. Wang, P. Zhao, W. Zhang, S. Zhang, Investigation on the formation of tobermorite in calcium silicate board and its influence factors under autoclaved curing, Constr Build Mater 143 (2017) 280–288. https://doi.org/10.1016/j.conbuildmat.2017.03.143.

[100] M.S. Khan, H. Abbas, Effect of elevated temperature on the behavior of high volume fly ash concrete, KSCE Journal of Civil Engineering 19 (2015) 1825–1831. https://doi.org/10.1007/s12205-014-1092-z.

[101] M.S. Khan, M. Shariq, S. Akhtar, A. Masood, Performance of high-volume fly ash concrete after exposure to elevated temperature, Journal of the Australian Ceramic Society 56 (2020) 781–794. https://doi.org/10.1007/s41779-019-00396-6.

[102] S. Donatello, C. Kuenzel, A. Palomo, A. Fernández-Jiménez, High temperature resistance of a very high volume fly ash cement paste, Cem Concr Compos 45 (2014) 234–242. https://doi.org/10.1016/j.cemconcomp.2013.09.010.

[103] R.K. Ibrahim, R. Hamid, M.R. Taha, Fire resistance of high-volume fly ash mortars with nanosilica addition, Constr Build Mater 36 (2012) 779–786. https://doi.org/10.1016/j.conbuildmat.2012.05.028.

[104] D. Glosser, P. Suraneni, O.B. Isgor, W.J. Weiss, Estimating reaction kinetics of cementitious pastes containing fly ash, Cem Concr Compos 112 (2020). https://doi.org/10.1016/j.cemconcomp.2020.103655.

[105] G.V.P. Bhagath Singh, K.V.L. Subramaniam, Influence of temperature and added lime on the glassy phase dissolution in low-calcium fly ash binary blend, Journal of Advanced Concrete Technology 14 (2016) 614–624. https://doi.org/10.3151/jact.14.614.

[106] T. Oey, Y.H. Hsiao, E.C. La Plante, B. Wang, I. Pignatelli, M. Bauchy, G. Sant, Rate controls on silicate dissolution in cementitious environments, RILEM Technical Letters 2 (2017) 67–73. https://doi.org/10.21809/rilemtechlett.2017.35.

[107] X. Ji, K. Takasu, H. Suyama, H. Koyamada, The Effects of Curing Temperature on CH-Based Fly Ash Composites, Materials 16 (2023). https://doi.org/10.3390/ma16072645.

[108] S.H. Kang, H. Kang, N. Lee, Y.H. Kwon, J. Moon, Development of cementless ultra-high performance fly ash composite (UHPFC) using nucleated pozzolanic reaction of low Ca fly ash, Cem Concr Compos 132 (2022). https://doi.org/10.1016/j.cemconcomp.2022.104650.

[109] J. Fernández, M.J. Renedo, Hydrothermal reaction of fly ash/hydrated lime: Characterization of the reaction products, Chem Eng Commun 193 (2006) 1253–1262. https://doi.org/10.1080/00986440500440199.

[110] E. Haustein, A. Kuryłowicz-Cudowska, Effect of Particle Size of Fly Ash Microspheres (FAMs) on the Selected Properties of Concrete, Minerals 12 (2022). https://doi.org/10.3390/min12070847.

[111] W.T. Lin, Reactive ultra-fine fly ash as an additive for cement-based materials, Mater Today Commun 25 (2020). https://doi.org/10.1016/j.mtcomm.2020.101466.

[112] I. Arribas, A. Santamaría, E. Ruiz, V. Ortega-López, J.M. Manso, Electric arc furnace slag and its use in hydraulic concrete, Constr Build Mater 90 (2015) 68–79. https://doi.org/10.1016/j.conbuildmat.2015.05.003.

[113] G. Adegoloye, A. Beaucour, S. Ortola, A. Noumowé, Concretes made of EAF slag and AOD slag aggregates from stainless steel process : Mechanical properties and durability, Constr Build Mater 76 (2015) 313–321. https://doi.org/10.1016/j.conbuildmat.2014.12.007.

[114] A.M. Rashad, Behavior of steel slag aggregate in mortar and concrete - A comprehensive overview, Journal of Building Engineering 53 (2022). https://doi.org/10.1016/j.jobe.2022.104536.

[115] W. Ten Kuo, C.Y. Shu, Effect of particle size and curing temperature on expansion reaction in electric arc furnace oxidizing slag aggregate concrete, Constr Build Mater 94 (2015) 488–493. https://doi.org/10.1016/j.conbuildmat.2015.07.019.

[116] V. Ducman, A. Mladenovič, The potential use of steel slag in refractory concrete, Mater Charact 62 (2011) 716–723. https://doi.org/10.1016/j.matchar.2011.04.016.

[117] S. Diener, L. Andreas, I. Herrmann, H. Ecke, A. Lagerkvist, Accelerated carbonation of steel slags in a landfill cover construction, Waste Management 30 (2010) 132–139. https://doi.org/10.1016/j.wasman.2009.08.007.

[118] M. Frías, J.T. San-José, I. Vegas, Steel slag aggregate in concrete: The effect of ageing on potentially expansive compounds, Materiales de Construccion 60 (2010) 33–46. https://doi.org/10.3989/mc.2019.45007.

[119] W.J.J. Huijgen, R.N.J. Comans, Carbonation of steel slag for CO2 sequestration: Leaching of products and reaction mechanisms, Environ Sci Technol 40 (2006) 2790–2796. https://doi.org/10.1021/es052534b.

[120] N. Kabay, Abrasion resistance and fracture energy of concretes with basalt fiber, Constr Build Mater 50 (2014) 95–101. https://doi.org/10.1016/j.conbuildmat.2013.09.040.

[121] C. Jiang, K. Fan, F. Wu, D. Chen, Experimental study on the mechanical properties and microstructure of chopped basalt fibre reinforced concrete, Mater Des 58 (2014) 187–193. https://doi.org/10.1016/j.matdes.2014.01.056.

[122] Y. Zheng, P. Zhang, Y. Cai, Z. Jin, E. Moshtagh, Cracking resistance and mechanical properties of basalt fibers reinforced cement-stabilized macadam, Compos B Eng 165 (2019) 312–334. https://doi.org/10.1016/j.compositesb.2018.11.115.

[123] H. Chen, C. Xie, C. Fu, J. Liu, X. Wei, D. Wu, Orthogonal analysis on mechanical properties of basalt-polypropylene fiber mortar, Materials 13 (2020) 1–16. https://doi.org/10.3390/ma13132937.

[124] Y. Yao, B. Wang, Y. Zhuge, Z. Huang, Properties of hybrid basalt-polypropylene fiber reinforced mortar at different temperatures, Constr Build Mater 346 (2022) 128433. https://doi.org/10.1016/j.conbuildmat.2022.128433.

[125] Q. Su, J. Xu, Durability and mechanical properties of rubber concrete incorporating basalt and polypropylene fibers: Experimental evaluation at elevated temperatures, Constr Build Mater 368 (2023). https://doi.org/10.1016/j.conbuildmat.2023.130445.

[126] V. Kočí, E. Vejmelková, D. Koňáková, V. Pommer, S. Grzeszczyk, A. Matuszek-Chmurowska, A. Mordak, R. Černý, Basic physical, mechanical, thermal and hygric properties of reactive powder concrete with basalt and polypropylene fibers after high-temperature exposure, Constr Build Mater 374 (2023). https://doi.org/10.1016/j.conbuildmat.2023.130922.

[127] K.H. Mo, Z.P. Loh, C.G. Tan, U.J. Alengaram, S.P. Yap, Behaviour of fibre-reinforced cementitious composite containing high-volume fly ash at elevated temperatures, Sadhana - Academy Proceedings in Engineering Sciences 43 (2018) 1–8. https://doi.org/10.1007/s12046-018-0937-4.

[128] X. Li, Y. Bao, L. Wu, Q. Yan, H. Ma, G. Chen, H. Zhang, Thermal and mechanical properties of high-performance fiber-reinforced cementitious composites after exposure to high temperatures, Constr Build Mater 157 (2017) 829–838. https://doi.org/10.1016/j.conbuildmat.2017.09.125.

[129] A.M. Rashad, An investigation of high-volume fly ash concrete blended with slag subjected to elevated temperatures, J Clean Prod 93 (2015) 47–55. https://doi.org/10.1016/j.jclepro.2015.01.031.

[130] ASTM C618. Standard specification for coal fly ash and raw or calcined natural pozzolan for use in concrete. American society for testing and materials, West Conshohocken, PA, USA, 2003.

[131] ASTM C 1437-07: Standard Test Method for Flow of Hydraulic Cement Mortar, 100 Barr Harbor Drive, West Conshohocken, PA 19428-2959, United States, 2007.

[132] ASTM C39/C39M-18a, Standard Test Method for Compressive Strength of Cylindrical Concrete Specimens, 2021.

[133] ASTM C348-21,Standard Test Method for Flexural Strength of Hydraulic-Cement Mortars, ASTM International, 100 Barr Harbor Drive, PO Box C700, West Conshohocken, PA 19428-2959. United States, n.d. https://doi.org/10.1520/C0348-19.

[134] A. Lau, M. Anson, Effect of high temperatures on high performance steel fibre reinforced concrete, Cem Concr Res 36 (2006) 1698–1707. https://doi.org/10.1016/j.cemconres.2006.03.024.

[135] R.H. Haddad, R.J. Al-Saleh, N.M. Al-Akhras, Effect of elevated temperature on bond between steel reinforcement and fiber reinforced concrete, Fire Saf J 43 (2008) 334–343. https://doi.org/10.1016/j.firesaf.2007.11.002.

[136] Y. Fu, L. Li, Study on mechanism of thermal spalling in concrete exposed to elevated temperatures, Materials and Structures/Materiaux et Constructions 44 (2011) 361–376. https://doi.org/10.1617/s11527-010-9632-6.

[137] A. Maanser, A. Benouis, N. Ferhoune, Effect of high temperature on strength and mass loss of admixtured concretes, Constr Build Mater 166 (2018) 916–921. https://doi.org/10.1016/j.conbuildmat.2018.01.181.

[138] J. Xiao, H. Falkner, On residual strength of high-performance concrete with and without polypropylene fibres at elevated temperatures, Fire Saf J 41 (2006) 115–121. https://doi.org/10.1016/j.firesaf.2005.11.004.

[139] A. Nadeem, S.A. Memon, T.Y. Lo, The performance of Fly ash and Metakaolin concrete at elevated temperatures, Constr Build Mater 62 (2014) 67–76. https://doi.org/10.1016/j.conbuildmat.2014.02.073.

[140] S. Mindess, Resistance of concrete to destructive agencies, 5th ed., Elsevier Ltd., 2019. https://doi.org/10.1016/B978-0-08-100773-0.00006-X.

[141] M. Şahmaran, E. Özbay, H.E. Yücel, M. Lachemi, V.C. Li, Effect of Fly Ash and PVA Fiber on Microstructural Damage and Residual Properties of Engineered Cementitious Composites Exposed to High Temperatures, Journal of Materials in Civil Engineering 23 (2011) 1735–1745. https://doi.org/10.1061/(asce)mt.1943-5533.0000335.

[142] Y.B. Ahn, J.G. Jang, H.K. Lee, Mechanical properties of lightweight concrete made with coal ashes after exposure to elevated temperatures, Cem Concr Compos 72 (2016) 27–38. https://doi.org/10.1016/j.cemconcomp.2016.05.028.

[143] F.U.A. Shaikh, S.W.M. Supit, Compressive strength and durability properties of high volume fly ash (HVFA) concretes containing ultrafine fly ash (UFFA), Constr Build Mater 82 (2015) 192–205. https://doi.org/10.1016/j.conbuildmat.2015.02.068.

[144] J. Sun, X. Shen, G. Tan, J.E. Tanner, Compressive strength and hydration characteristics of high-volume fly ash concrete prepared from fly ash, J Therm Anal Calorim 136 (2019) 565–580. https://doi.org/10.1007/s10973-018-7578-z.

[145] T.M. Borhan, C.G. Bailey, Modelling basalt fibre reinforced glass concrete slabs at ambient and elevated temperatures, Materials and Structures/Materiaux et Constructions 47 (2014) 999–1009. https://doi.org/10.1617/s11527-013-0109-2.

[146] A.M. Rashad, Y. Bai, P.A.M. Basheer, N.C. Collier, N.B. Milestone, Chemical and mechanical stability of sodium sulfate activated slag after exposure to elevated temperature, Cem Concr Res 42 (2012) 333–343. https://doi.org/10.1016/j.cemconres.2011.10.007.

[147] S. Donatello, C. Kuenzel, A. Palomo, A. Fernández-Jiménez, High temperature resistance of a very high volume fly ash cement paste, Cem Concr Compos 45 (2014) 234–242. https://doi.org/10.1016/j.cemconcomp.2013.09.010.

[148] Q. Song, M.Z. Guo, T.C. Ling, A review of elevated-temperature properties of alternative binders: Supplementary cementitious materials and alkali-activated materials, Constr Build Mater 341 (2022) 127894. https://doi.org/10.1016/j.conbuildmat.2022.127894.

[149] M.D.S. Magalhães, R.D. Toledo Filho, E.D.M.R. Fairbairn, Thermal stability of PVA fiber strain hardening cement-based composites, Constr Build Mater 94 (2015) 437–447. https://doi.org/10.1016/j.conbuildmat.2015.07.039.

[150] M.S. Khan, M. Shariq, Performance of high-volume fly ash concrete after exposure to elevated temperature, Journal of Australian Ceramic Society (2019).

[151] G.F. Peng, S.Y.N. Chan, M. Anson, Chemical kinetics of C-S-H decomposition in hardened cement paste subjected to elevated temperatures up to 800°C, Advances in Cement Research 13 (2001) 47–52. https://doi.org/10.1680/adcr.2001.13.2.47.

[152] M.R. Irshidat, M.H. Al-Saleh, Thermal performance and fire resistance of nanoclay modified cementitious materials, Constr Build Mater 159 (2018) 213–219. https://doi.org/10.1016/j.conbuildmat.2017.10.127.

[153] O.E. Babalola, P.O. Awoyera, D.H. Le, L.M. Bendezú Romero, A review of residual strength properties of normal and high strength concrete exposed to elevated temperatures: Impact of materials modification on behaviour of concrete composite, Constr Build Mater 296 (2021). https://doi.org/10.1016/j.conbuildmat.2021.123448.

[154] X.Y. Wang, Effect of fly ash on properties evolution of cement based materials, Constr Build Mater 69 (2014) 32–40. https://doi.org/10.1016/j.conbuildmat.2014.07.029.

[155] X. Wei, H. Zhu, G. Li, C. Zhang, L. Xiao, Properties of high volume fly ash concrete compensated by metakaolin or silica fume, Journal Wuhan University of Technology, Materials Science Edition 22 (2007) 728–732. https://doi.org/10.1007/s11595-006-4728-0.

[156] M. Sahmaran, M. Lachemi, V.C. Li, Sahmaran_Assessing-the-Mechanical-Properties-and-Microstructure-of-Fire-Damaged-Engineered-Cementitious-Composites, ACI Mater J 107 (2010) 297–304.

[157] S. Aydin, B. Baradan, Effect of pumice and fly ash incorporation on high temperature resistance of cement based mortars, Cem Concr Res 37 (2007) 988–995. https://doi.org/10.1016/j.cemconres.2007.02.005.

[158] H. Qasrawi, F. Shalabi, I. Asi, Use of low CaO unprocessed steel slag in concrete as fine aggregate, Constr Build Mater 23 (2009) 1118–1125. https://doi.org/10.1016/j.conbuildmat.2008.06.003.

[159] I. Hager, Colour Change in Heated Concrete, Fire Technol 50 (2014) 945–958. https://doi.org/10.1007/s10694-012-0320-7.

[160] N.R. Short, J.A. Purkiss, S.E. Guise, Assessment of fire damaged concrete using colour image analysis, 2001.

[161] L. Lei, L. Zhang, Synthesis and performance of a non-air entraining polycarboxylate superplasticizer, Cem Concr Res 159 (2022). https://doi.org/10.1016/j.cemconres.2022.106853.

[162] M. Khan, M. Cao, Effect of hybrid basalt fibre length and content on properties of cementitious composites, Magazine of Concrete Research 73 (2021) 487–498. https://doi.org/10.1680/jmacr.19.00226.

[163] X. Wang, J. He, A.S. Mosallam, C. Li, H. Xin, The Effects of Fiber Length and Volume on Material Properties and Crack Resistance of Basalt Fiber Reinforced Concrete (BFRC), Advances in Materials Science and Engineering 2019 (2019). https://doi.org/10.1155/2019/7520549.

[164] W. Jing, J. Jiang, S. Ding, P. Duan, Hydration and microstructure of steel slag as cementitious material and fine aggregate in mortar, Molecules 25 (2020). https://doi.org/10.3390/molecules25194456.

[165] E. Grabias-Blicharz, W. Franus, A critical review on mechanochemical processing of fly ash and fly ash-derived materials, Science of the Total Environment 860 (2023). https://doi.org/10.1016/j.scitotenv.2022.160529.

[166] L. Coppola, A. Buoso, D. Coffetti, P. Kara, S. Lorenzi, Electric arc furnace granulated slag for sustainable concrete, Constr Build Mater 123 (2016) 115–119. https://doi.org/10.1016/j.conbuildmat.2016.06.142.

[167] L. Lam, Y.L. Wong, C.S. Poon, Degree of hydration and gel/space ratio of high-volume fly ash/cement systems, Cem Concr Res 30 (2000) 747–756. https://doi.org/10.1016/S0008-8846(00)00213-1.

[168] B. Pacewska, I. Wilińska, Usage of supplementary cementitious materials: advantages and limitations: Part I. C–S–H, C–A–S–H and other products formed in different binding mixtures, J Therm Anal Calorim 142 (2020) 371–393. https://doi.org/10.1007/s10973-020-09907-1.

[169] J.T. Kolawole, A.J. Babafemi, S.C. Paul, A. du Plessis, Performance of concrete containing Nigerian electric arc furnace steel slag aggregate towards sustainable production, Sustainable Materials and Technologies 25 (2020). https://doi.org/10.1016/j.susmat.2020.e00174.

[170] E.R. Teixeira, A. Camões, F.G. Branco, Synergetic effect of biomass fly ash on improvement of high-volume coal fly ash concrete properties, Constr Build Mater 314 (2022). https://doi.org/10.1016/j.conbuildmat.2021.125680.

[171] C. Pellegrino, P. Cavagnis, F. Faleschini, K. Brunelli, Properties of concretes with black/oxidizing electric arc furnace slag aggregate, Cem Concr Compos 37 (2013) 232–240. https://doi.org/10.1016/j.cemconcomp.2012.09.001.

[172] J. Fernández, M.J. Renedo, A. Pesquera, J.A. Irabien, Kinetic study of the hydrothermal reaction of fly ash with Ca(OH 2 in the preparation of desulfurant sorbents, Chem Eng Commun 189 (2002) 310–321. https://doi.org/10.1080/00986440212083.

[173] M.T. Palou, E. Kuzielová, M. Žemlička, J. Tkácz, J. Másilko, Insights into the hydration of Portland cement under hydrothermal curing, J Therm Anal Calorim 138 (2019) 4155–4165. https://doi.org/10.1007/s10973-019-08542-9.

[174] H. Huang, C. Qian, F. Zhao, J. Qu, J. Guo, M. Danzinger, Improvement on microstructure of concrete by polycarboxylate superplasticizer (PCE) and its influence on durability of concrete, Constr Build Mater 110 (2016) 293–299. https://doi.org/10.1016/j.conbuildmat.2016.02.041.

[175] B. Ma, H. Qi, H. Tan, Y. Su, X. Li, X. Liu, C. Li, T. Zhang, Effect of aliphatic-based superplasticizer on rheological performance of cement paste plasticized by polycarboxylate superplasticizer, Constr Build Mater 233 (2020). https://doi.org/10.1016/j.conbuildmat.2019.117181.

[176] Z.H. Shui, R. Zhang, W. Chen, D.X. Xuan, Effects of mineral admixtures on the thermal expansion properties of hardened cement paste, Constr Build Mater 24 (2010) 1761–1767. https://doi.org/10.1016/j.conbuildmat.2010.02.012.

[177] S.K. Shill, S. Al-Deen, M. Ashraf, M.A. Elahi, M. Subhani, W. Hutchison, A comparative study on the performance of cementitious composites resilient to airfield conditions, Constr Build Mater 282 (2021). https://doi.org/10.1016/j.conbuildmat.2021.122709.

[178] N. Nasuha, S. Ismail, B.H. Hameed, Activated electric arc furnace slag as an efficient and reusable heterogeneous Fenton-like catalyst for the degradation of Reactive Black 5, J Taiwan Inst Chem Eng 67 (2016) 235–243. https://doi.org/10.1016/j.jtice.2016.07.023.

[179] R.K. Ibrahim, R. Hamid, M.R. Taha, Fire resistance of high-volume fly ash mortars with nanosilica addition, Constr Build Mater 36 (2012) 779–786. https://doi.org/10.1016/j.conbuildmat.2012.05.028.

List of publications

Journals

- A. Tangirala, S. Rawat, M. Lahoti, High volume fly ash and basalt-polypropylene fibres as performance enhancers of novel fire-resistant fibre reinforced cementitious composites, Journal of Building Engineering, 78, (2023). https://doi.org/10.1016/j.jobe.2023.107586.
- A. Tangirala, S. Rawat, M. Lahoti, A Year-Long Study of Eco-Friendly Fibre Reinforced Cementitious Composites with High Volume Fly Ash and Industrial Waste Aggregates, Innovative Infrastructure Solutions, 9(5), 179 (2024). https://doi.org/10.1007/s41062-024-01495-5.
- A. Tangirala, S. Rawat, M. Lahoti, Enhancing the Resistance of Cementitious Composites to Environmental Thermal Fatigue Using High-Volume Fly Ash and Steel Slag, Journal of Building Engineering, 94, (2024). https://doi.org/10.1016/j.jobe.2024.109905.
- A. Tangirala, S. Rawat, M. Lahoti, Resilient Runways: Effects of Aircraft Operating Fluids and Environmental Thermal Fatigue on Fly Ash and Steel Slag based Cementitious Composites, Scientific Reports, 14(1), 12745 (2024). https://doi.org/10.1038/s41598-024-63558-y.

Conference

- A. Tangirala, S. Rawat, M. Lahoti, Performance of ternary blended Basalt-Polypropylene fibre reinforced cementitious composite at elevated temperatures, in: SiF 2022– The 12th International Conference on Structures in Fire, 2022: pp. 457–465.

Research work under consideration

- A. Tangirala, S. Rawat, K.H. Tan, M. Lahoti, Enhanced Thermal Performance of Fibre Reinforced Green Cementitious Composite with High-Volume Fly Ash and Steel Slag Aggregates, Journal of Materials in Civil Engineering **(Review submitted**).

Biography of the candidate

Aniruddha Tangirala is pursuing his Ph.D. in the Civil Engineering Department at the Birla Institute of Technology & Science (BITS) in Pilani, Rajasthan. He holds a Bachelor of Engineering in Civil Engineering from Visvesvaraya Technological University and a Master of Engineering in Structural Engineering from BITS Pilani.

His research is focused on the development of thermally stable fiber-reinforced cementitious composites that have potential applications in construction, roadways, and energy sectors. During his doctoral studies, Aniruddha has effectively utilized techniques such as Scanning Electron Microscopy (SEM), Thermogravimetric Analysis (TGA), Differential Scanning Calorimetry (DSC), and Mercury Intrusion Porosimetry (MIP) to investigate the degradation processes these materials undergo under various conditions and has developed strategies to mitigate such damage.

His work has been acknowledged through publications in a prestigious journals and presentation at an esteemed conference. Additionally, his papers from this thesis are under review in notable publications.

Biography of the supervisor

Dr. Mukund Lahoti serves as an Assistant Professor in the Department of Civil Engineering at Birla Institute of Technology & Science (BITS), Pilani. He is a distinguished researcher in the realm of alternative construction materials, notably contributing to the development of geopolymers that are tailored for a range of applications, including the creation of fire-resistant and ductile composites.

His academic credentials include completing both his undergraduate and postgraduate studies at BITS Pilani, followed by a Ph.D. from Nanyang Technological University (NTU), Singapore. With six years of tenure as an Assistant Professor at BITS Pilani, Dr. Lahoti has been instrumental in teaching a variety of courses. At the undergraduate level, he covers Civil Engineering Materials, Pavement Material Characterisation, Construction Planning and Technology, and at the master's level, he delves into Advanced Concrete Technology.

Dr. Lahoti's commitment to the advancement of civil engineering is evident from his active involvement in collaborative research projects and his scholarly works, which have been widely recognized and cited within the academic community. Through his research, Dr. Lahoti not only enriches academic discussions but also lays the groundwork for innovative practices in civil engineering and construction material technologies.